CO2 Langgak

by Fiki Hidayat

skkmigas spr langgak

A COMPREHENSIVE STUDY OF CO2 ENHANCED OIL RECOVERY IN THE LANGGAK FIELD

Dr.Eng, Muslim
Prof. Ir. Asep Kurnia Permadi, Ph.D, IPU,
Mohammad Yasin Abdulfatah, MT
Ivan Efriza, M.Eng
Dimas Hadi Prabowo, MT
Fiki Hidayat, M.Eng
Novia Rita, MT

PRESS

A Comprehensive Study of CO_2 Enhanced Oil Recovery in the Langgak Field

Dr.-Eng, Muslim, Prof. Ir. Asep Kurnia Permadi, Ph.D, IPU, Mohammad Yasin Abdulfatah, MT, Ivan Efriza, M.Eng, Dimas Hadi Prabowo, MT, Fiki Hidayat, M.Eng, Novia Rita, MT

Publisher:

UNIVERSITAS ISLAM RIAU

A Comprehensive Study of CO_2 Enhanced Oil Recovery in the Langgak Field

Author: Dr.-Eng, Muslim, Prof. Ir. Asep Kurnia Permadi, Ph.D, IPU, Mohammad Yasin Abdulfatah, MT, Ivan Efriza, M.Eng, Dimas Hadi Prabowo, MT, Fiki Hidayat, M.Eng, Novia Rita, MT

ISBN: 978-623-6598-10-8

Editor: Prof. Wisup Bae, Prof. Radzuan Junin

Copy Editing: Dr.-Eng, Adi Novriansyah

Publisher: Universitas Islam Riau (UIR) Press

Redaction:

Gedung Kantor Bersama Universitas Islam Riau

Jl. Kaharuddin Nasution No. 113

Marpoyan 28284, Pekanbaru, Riau, Indonesia

Telp: (0761) 674674

Fax: (0761) 674834

Email: uirpress@uir.ac.id

First Printing, March 2021

PREFACE

Alhamdulillah, praise to Allah Subhanahu Wa ta'ala for all the guidance and blessings He has given upon completing this book. This book is based on the laboratory and field research on Langgak Field, operated by SPR Langgak as one of Province-Owned Oil Company. This book is written to be a guideline and to add knowledge related to enhanced oil recovery (EOR) activity, particularly CO_2 Injection. The authors are aware that the information about EOR activity in Indonesia is still limited, so with the presence of this book, we hope it can be made as a reference, not only for students but also for engineers and other researchers who would like to carry out or perform EOR project using CO_2 Injection.

The authors realize that there are some flaws in the completion of this book. Nonetheless, the authors believe this book will serve as a foundation for other CO_2 EOR projects in Indonesia and improve the readers' understanding of CO_2 Injection activity. Special thanks are given to the Director of PT. SPR Langgak, Mr Ikin Faizal, who gave us excellent support in the making of this book.

Pekanbaru, March 2021

The Authors

TABLE OF CONTENTS

LIST OF FIGURES

LIST OF TABLE

SUMMARY

Alternative or renewable energy is a long way from achieving the durability, efficiency, and feasibility of hydrocarbon fuels (Bennett, 2008). Several engines require fuel with a very high calorific value to tolerate energy losses attributed to heat and noise to operate efficiently. Alternative organic-based fuel sources such as ethanol affect world food supplies (University of Groningen, 2004), and renewable energy sources that generate either electricity or hydrogen infringe on rural development and produce significant risks (DOE, 2006). Therefore, world energy forecasts for alternative or renewable energy sources are negligible for the next three decades (IEA, 2008; IEA, 2010).

Enhanced Oil Recovery (EOR) has been trying to solve it. EOR is the technique or process where the physicochemical (physical and chemical) properties of the rock are changed to enhance hydrocarbon recovery. The properties of the reservoir fluid system affected by the EOR process are chemical, biochemical, density, miscibility, interfacial tension (IFT)/surface tension (ST), viscosity, and thermal. EOR often is called tertiary recovery if it is performed after waterflooding.

The screening criteria of EOR selection used for this report are adapted from Taber based on previous CO_2 huff and puff injection project at Meruap; Screening Criteria Revisited – Part 1 and Part 2 for Introduction to Screening Criteria and Enhanced Recovery Field Projects by Taber, and Screening Criteria for CO_2 Huff and Puff Operations. The screening provides the best method based on certain parameters. Despite those reservoir parameters, there must have been something urgent also to be considered in enhance oil recovery, such as economic evaluation and availability of chemical used and previous reflection projects. Therefore, it shows that CO_2 injection Huff and Puff can be considered a method based on overall concern.

A study on the laboratory to determine Minimum Miscibility Pressure of CO_2 to reservoir fluid in Langgak Field has been conducted in Sejong University, South Korea.

According to Swelling Experiment, the MMP of Langgak Field is in the range of 2400 – 2600 psia. An extension study was conducted using EoS and 1-D Slimtube simulation to determine the MMP of Langgak Field. The results of both simulation studies are 1612.5 psia and 1538 psia, respectively.

Simulation study results on CO_2 Huff and Puff injection performance implementing to Langgak Field are represented by using a single well simulation model that can lift additional oil about 15 MSTB for one well (LGK-24) in 547 days of implementation.

CHAPTER I
INTRODUCTON

1.1 Enhanced Oil Recovery

The term Improved Oil Recovery (IOR) has been used increasingly instead of the traditional EOR, or the more restrictive “tertiary recovery.” Most petroleum engineers understand the meaning of all the words and phrases, but our technical communications are improved if we use the terms with their intended technical meanings. Successful enhanced recovery projects are being conducted as tertiary, secondary, and even enhanced primary operations. The terms should continue to be used with their evolved historic meanings. Tertiary should not be used as a synonym for EOR because some EOR methods work quite well as either secondary or tertiary projects (e.g. CO_2 flooding), while others, such as steam or polymer flooding, are most effective as enhanced secondary operations. EOR simply means that something other than plain water or brine is being injected into the reservoir. We use the terms “enhanced secondary” or tertiary when necessary for clarity. Others may use the phrase Advanced Secondary Recovery (ASR) for EOR in the secondary mode. Engineers should consider this improved (enhanced or advanced) secondary option much more often in the future.

Alternative or renewable energy is a long way from achieving the durability, efficiency and feasibility of hydrocarbon fuels (Bennett, 2008). To operate efficiently, several types of engines require a fuel with a very high calorific value in order to tolerate energy losses attributed to heat and noise. Alternative organic-based fuel sources such as ethanol effect world food supplies (University of Groningen, 2004), and renewable energy sources that generate either electricity or hydrogen infringe on rural development and produce significant risks (DOE, 2006). Therefore, world energy forecasts for alternative or renewable energy sources are negligible for the next three decades (IEA, 2008; IEA, 2010).

EOR utilizes unconventional hydrocarbon recovery methods that target the approximately two-thirds of oil volume remaining in reservoirs after conventional recovery methods have been exhausted (Green and Wilhite,1998). Applying EOR provides operators with several advantages. EOR application does not require a substantial capital investment because existing infrastructures can be used to develop depleted hydrocarbon fields. The potential to tap into reserves from giant oil fields without any discovery or drilling completion risks is beneficial. EOR has the potential to secure the world's needed energy supply for several decades. An additional benefit is that this method deals with a proven energy source that is highly efficient and familiar to the refining, petrochemical and transportation industries.

Enhanced oil production is critical today when many analysts are predicting that the world has already reached its peak production and that the demand for oil continues to grow faster than the supply. Only 22 billion of the 649 billion barrels of oil remaining in reservoirs in the United States (US) are recoverable by conventional means. However, EOR methods offer the prospect of recovering as much as 200 billion barrels of oil from existing US reservoirs, a quantity of oil equivalent to the cumulative oil production to date (DOE, 2005). In the early 1980s, many researchers investigated EOR because oil prices were rising unabated, and a dramatic need arose to extract oil from depleted reservoirs. During this time, most major oil companies operated research centers and funded major programs to develop new technologies. These programs resulted in the production of more than 20,000 bbl/day as a result of chemical EOR in the US alone. However, oil prices collapsed in 1986 and hovered around $20 per barrel from 1986 to 2003. Most operators, concerned about the lower price of oil, simply did not invest in either new EOR technologies or new ideas to extract incremental oil from existing reservoirs. However, oil prices recently have reached new highs of $60 to even $140 per barrel, and many analysts believe that oil prices may stabilize above $100 per barrel. In this new price environment and under conditions of increasing worldwide oil demand, few discoveries of new fields, and the rapid maturation of fields worldwide, EOR technologies have drawn increased interest.

Crude oil is found in underground porous sandstone and carbonate rock formations. In the primary stage of oil recovery, the oil is displaced from the reservoir into the wellbore (production well) and up to the surface under its own reservoir energy, such as gas drive, water drive, or gravity drainage. In the second stage, an external fluid, such as water or gas, is injected into the reservoir through injection wells located in the rock that have fluid communication with production wells. The purpose of secondary oil recovery is to maintain reservoir pressure and displace hydrocarbons towards the wellbore. The most common secondary recovery technique is water flooding (Craig, 1971). Once the secondary oil recovery process has been exhausted, about two-thirds of the original oil in place (OOIP) is left behind due to both microscopic and macroscopic factors. EOR methods aim to recover the remaining OOIP (Green and Wilhite, 1998). Microscopic factors include the various effects of oil-water interfacial tension (IFT) and rock-fluid interaction (wettability) that give rise to oil in pores and crevices; this oil cannot be dislodged under even large applied pressures (Stegemeier, 1977; Slattery, 1974). The reservoir pore size may be as small as 0.1 µm or less; therefore, it is not surprising that IFT influences oil mobilization. The oil left behind after a sweep is called residual oil saturation, expressed as S_{or}.

Macroscopic factors include reservoir stratification, with some strata showing varying degrees of permeability. Thus, the displacing fluid travels through the high permeability zones, leaving oil in the low-permeability zones unswept (Bai and colleagues 2007a; Bai and colleagues 2007b). Even in a uniformly permeable reservoir, uniform displacement can break down when the displacing fluid is less viscous than the crude, a situation known as adverse mobility ratio. In places, the less viscous fluid penetrates the oil, a situation known as viscous fingering. Another important reason why oil remains unswept is the negative capillary force in oil-wet formations; this force impedes water imbibition into pore spaces in the reservoir rock. This situation often occurs in carbonate reservoirs, more than 80% of which are said to be oil wet. Other factors, such as areal heterogeneity, permeability anisotropy, and well patterns, also leave some oil unswept by water. The unswept oil is called remaining oil, and its corresponding saturation is called remaining oil saturation. Oil recovery is the product of displacement efficiency (*ED*) and sweep efficiency (*ES*). EOR methods focus on increasing either displacement efficiency by reducing residual oil saturation in swept regions or sweep efficiency by displacing the remaining oil in unswept regions. Residual oil saturation is a function of the capillary number, which is the ratio of viscous force to capillary force. Typically, the capillary number for water flooding is confined to below 10-6, usually to 10-7. The capillary number increases during effective EOR by three magnitudes to about 10-3 to 10-4. The capillary number can be reduced significantly by either lowering the IFT or altering the rock's wettability to create a more water-wet surface. Although the capillary number also can be reduced by increasing the viscous forces, the reservoir fracture gradient and pressure drops across the wells are limiting factors in this method (Green and Wilhite, 1998). Oil in unswept regions can be recovered by (1) increasing the viscosity of the displacing fluid, (2) reducing oil viscosity, (3) modifying permeability, and/or (4) altering wettability.

The variety of EOR methods provides flexibility in applying them to oil fields with different petrologies and for different stages of oil and gas production. Applying EOR to developed fields offers the advantage of utilizing existing infrastructures. However, as reservoirs are unique in terms of their characterization and properties, each EOR method can serve as a candidate to reservoirs with a specific range of rock and fluid properties. EOR can be applied in the first stage of oilfield development in cases such as thermal flooding for heavy oil reservoirs in which natural reservoir forces are inadequate to induce the flow of oil to producing wells. EOR also has been adopted in the second stage to further augment production rates by promoting oil flow and to realize favorable recovery conditions, such as hydrocarbon flooding. Additionally, EOR methods often are used in the tertiary stage in cases in which oil fields have high water cut and low oil production rates. Therefore, EOR has the potential to reclassify unrecoverable and contingent reserves in amounts exceeding the quantity of oil currently produced. Oil is predicted to dominate the world's energy supply for the next three decades. The development of technologies that enhance oil recovery from existing oil fields would supply the world's energy needs for several decades. Therefore, it is more important than ever to understand lessons learned from past EOR applications and to develop new technologies and methods. Variety of EOR methods is shown on Figure I-1.

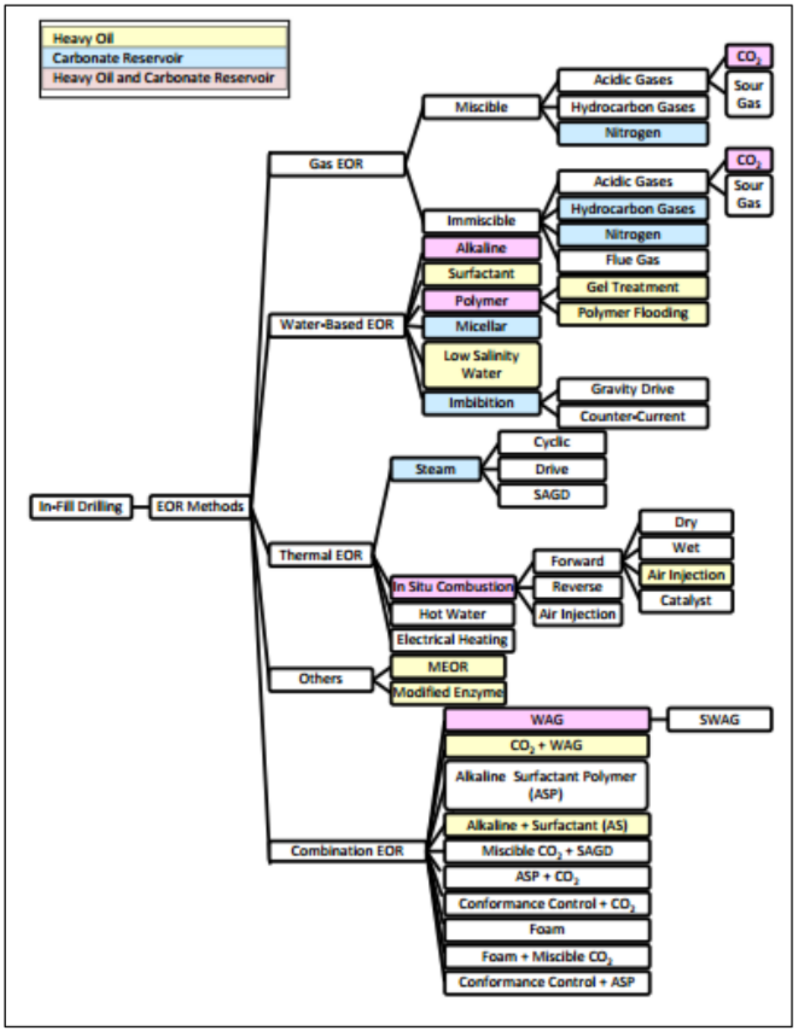

*Figure I-1. Worldwide EOR Project Subcategories**

*Adopted from *Updated EOR screening criteria and modeling the impacts of water salinity changes on oil recovery*, Alasadani Ahmad (2012)

Table I-1 lists more than 20 EOR methods that experienced intensive laboratory and, in most cases, significant field testing.

*Table I-1. Current and Past EOR Methods**

Method	Table Number (in Ref. 16)
Gas (and Hydrocarbon Solvent) Methods	
"Inert" gas injection	
Nitrogen injection	1
Flue-gas injection	1
Hydrocarbon-gas (and liquid) injection	2
High-pressure gasdrive	
Enriched-gasdrive	
Miscible solvent (LPG or propane) flooding	
CO_2 flooding	3
Improved Waterflooding Methods	
Alcohol-miscible solvent flooding	
Micellar/polymer (surfactant) flooding	4
Low IFT waterflooding	
Alkaline flooding	4
ASP flooding	4
Polymer flooding	5
Gels for water shutoff	
Microbial injection	
Thermal Methods	
In-situ combustion	6
Standard forward combustion	
Wet combustion	
02-enriched combustion	
Reverse combustion	
Steam and hot-water injection	7
Hot-waterflooding	
Steam stimulation	
Steamflooding	
Surface mining and extraction	—

**Adopted from *EOR Screening Criteria Revisited-Part 1: Introduction to Screening Criteria and Enhanced Recovery Field Projects,* Taber et al (1997)

The methods use about 15 different substances (or specific mixtures) that must be purchased and injected into the reservoir, always at costs somewhat greater than for the injection of water. Experience shows that the best profits come only from those methods where several barrels of fluid (liquid or gas at reservoir pressure) can be injected per barrel of incremental oil produced. This limits the main methods to either water (including heated, as steam, or as a dilute chemical solution) or one of the inexpensive gases. For some methods (e.g., micellar/polymer) there have been some technical successes but relatively few economic successes. These methods are included in our screening criteria because they are still being studied and applied in the field. If oil prices rise significantly, there is hope that these methods might become more profitable.

This paper provides screening criteria for the eight methods that are either the most important or still have some promise. These "current" EOR or IOR methods include the three gas (nitrogen, hydrocarbon, C02), three water [micellar/polymer plus alkaline/surfactant/polymer (ASP); polymer flooding; gel treatments] and the three thermal/ mechanical (combustion, steam, surface mining) methods.

A convenient way to show these methods is to arrange them by oil gravity as shown in Figure I-2.

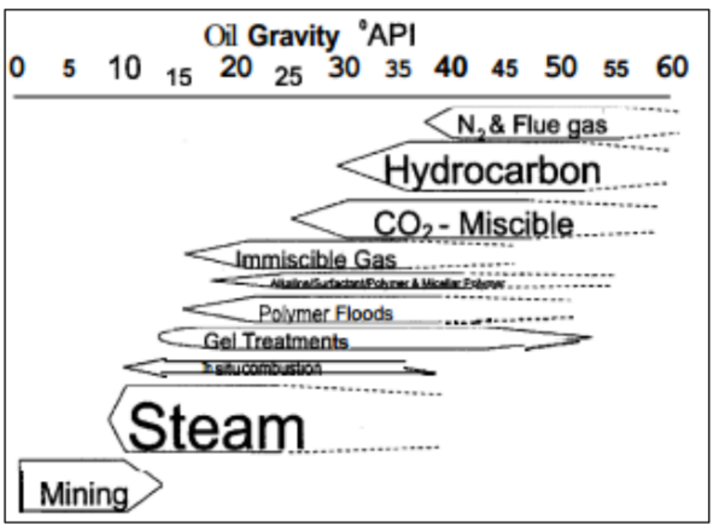

Figure I-2. Oil Gravity range of oil that is most effective for EOR methods. Relative production (BID) is shown by size of type.

*Adopted from *EOR Screening Criteria Revisited-Part 1: Introduction to Screening Criteria and Enhanced Recovery Field Projects,* Taber et al (1997)

This "at-a-glance" display also provides approximate oil gravity ranges for the field projects now under way. The size of the type in Figure I-2 is intended to show the relative importance of each of the EOR methods in terms of current incremental oil production.

Gas EOR is subcategorized as immiscible or miscible flooding using carbon dioxide and nitrogen gases, as well as water-alternating hydrocarbon gas (WAG) flooding. In the case of immiscible gas flooding, the gas is injected below its critical pressure, thereby enhancing the macroscopic displacement efficiency by increasing reservoir pressure and causing oil to swell. By contrast, miscible gas flooding involves injecting gas at a pressure high enough to achieve miscibility with the oil. Oil gravity is inversely proportional to the minimum miscibility pressure, whereas heavy gases have lower miscibility pressures. The injected gas solution achieves miscibility with the oil through single or multiple contacts (Ghomian and colleagues 2008). These contacts considerably reduce the IFT in the miscible zone; thus, the residual oil saturation decreases, and oil is mobilized. Additionally, when the miscible gas "evaporates" in oil (Vahidi and Zargar, 2007), the oil viscosity decreases, and the oil swells. The increase in viscous forces improves the macroscopic displacement efficiency. The improvement in both microscopic and macroscopic displacement efficiencies serves as evidence of the ability of miscible gas flooding generally to achieve greater effectiveness than immiscible flooding (Vahidi and Zargar, 2007).

Thermal EOR methods include steam, combustion, and hot water flooding, all three of which elevate the temperature inside the reservoir to reduce oil viscosity. In addition, oil swelling and an increased reservoir pressure resulting from high temperatures create favorable oil recovery conditions. Therefore, thermal EOR improves both the macroscopic and microscopic displacement efficiencies by reducing viscous forces and by reducing IFT, especially during steam distillation, respectively (Cadelle and colleagues 1981).

Chemical EOR methods inject chemicals, such as soluble polymers, cross-linked polymers, surfactants, alkalines and their combinations. Chemical EOR can improve either microscopic or macroscopic efficiency, or both. Polymers are added to water during flooding to achieve favorable mobility ratios in the displacing front. The displacing water becomes more viscous as the under-riding water is mitigated, thus improving the macroscopic displacement efficiency (Chang and colleagues 2006). Surfactants are added to the water during flooding to improve the microscopic displacement efficiency by generating an emulsion between the oil and water interface. This emulsion significantly reduces the IFT and mobilizes the oil (Krumrine and colleagues 1982). Surfactants also improve the microscopic displacement efficiency by reducing the capillary force, which decreases the oil contact angle. Alkaline interacts with some acid oils to generate surfactants, which reduce the IFT proportionally based on the pH value (Smith, J.E., 1993). Therefore, alkaline is added to the water to minimize the use of surfactants and reduce the capillary force. Polymer-based gels are used during conformance control to block high-permeability zones, diverting the displacing medium to areas where oil has not been swept (Bai and colleagues 2004). Microbes can be utilized to improve oil recovery. Microbial EOR generates gases under reservoir conditions, thus improving the macroscopic displacement efficiency by increasing reservoir pressure and decreasing oil viscosity. The macroscopic displacement efficiency also may improve when the absolute permeability increases due to acidic dissolution; alternatively, microbes could block high-permeability zones, thereby improving sweep efficiency. Microbes can generate bio-surfactants that could reduce the IFT and favorably alter wettability. Wettability also could be altered favorably by some microbes that decrease the population of sulfate-reducing bacteria (Dietrichm and colleagues 1996). However, microbial EOR is difficult to control. Furthermore, the adsorption of surfactants to the reservoir rock and the biodegradation of surfactants adversely impact the performance of microbial EOR (Gray and colleagues 2008).

1.2 EOR Database Analysis

EOR projects are better represented through dataset distribution. The number of EOR projects (datasets) should be evaluated to indicate where EOR projects are concentrated for each reservoir range. Extreme minimum and maximum values could adversely impact the EOR criteria, even when averages are established; therefore, box charts are used to illustrate the reservoir property distributions for the main EOR methods. The generated figures represent the range in which the majority of EOR projects are located plotted against selected reservoir properties. The minimum and maximum values for each reservoir property are identified.

Five EOR methods were selected to ensure an adequate number of data-sets. Legends include the minimum and maximum range and the average value; more significantly, the number of projects for each value was determined from the minimum to maximum API range. Subsequently, the highest percentage concentration of project clusters within the reservoir property range was established. The project clusters and the reservoir property dataset distributions are more indicative of EOR selection criteria than the minimum, maximum and average values, similar to the data-set distribution of reservoir properties reported in EOR projects.

Enhanced production, rather than project count, is used as an EOR selection criterion to establish key reservoir properties and their corresponding ranges. Two new approaches are proposed to identify candidate reservoirs for EOR methods. The first criterion correlates reservoir properties with enhanced production, and the second criterion correlates the number of data-set distributions.

The first step in analyzing the data stored in the EOR project database is to construct a profile of worldwide EOR projects. The EOR projects are classified into four main categories, namely, thermal, gas, chemical and microbial methods. The worldwide use of each of these main categories is shown in Figure I-3.

The main EOR categories are then subcategorized, as shown in Figure I-4, to provide a further breakdown of worldwide EOR projects.

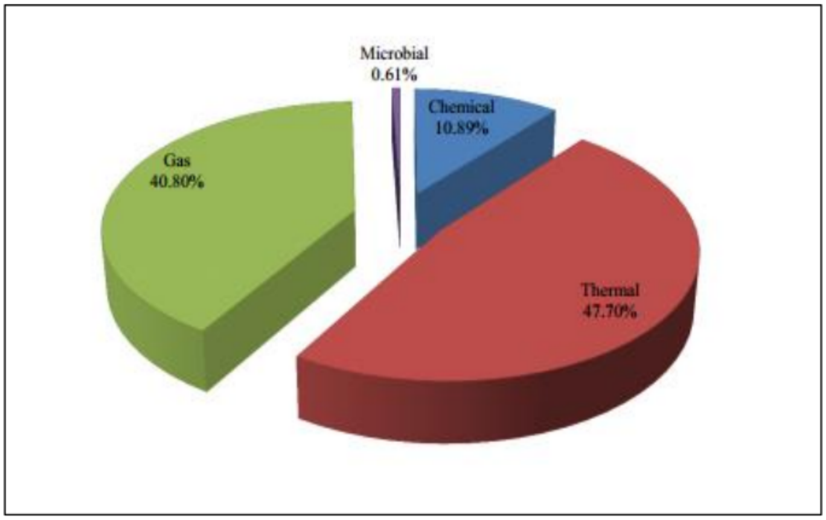

*Figure I-3. Worldwide EOR Project**

*Adopted from *Updated EOR screening criteria and modeling the impacts of water salinity changes on oil recovery*, Alasadani Ahmad (2012)

Figure I-4 indicates that thermal methods are the leading methods used worldwide for EOR projects, followed by gas methods. More specifically, steam flooding is the leading thermal EOR method, followed by miscible gas injection in the gas method category, as shown in Figure I-4. While thermal EOR continues to dominate (Figure I-3), the adoption of miscible flooding methods has increased gas EOR projects to 41 % (Figure I-4), and since 2006, gas EOR methods in the United States (US) have accounted for the majority of enhanced oil production at 53% (Koottungal, L., 2008). The second step is to represent each country's share of EOR projects and to break down the EOR methods implemented by each corresponding country.

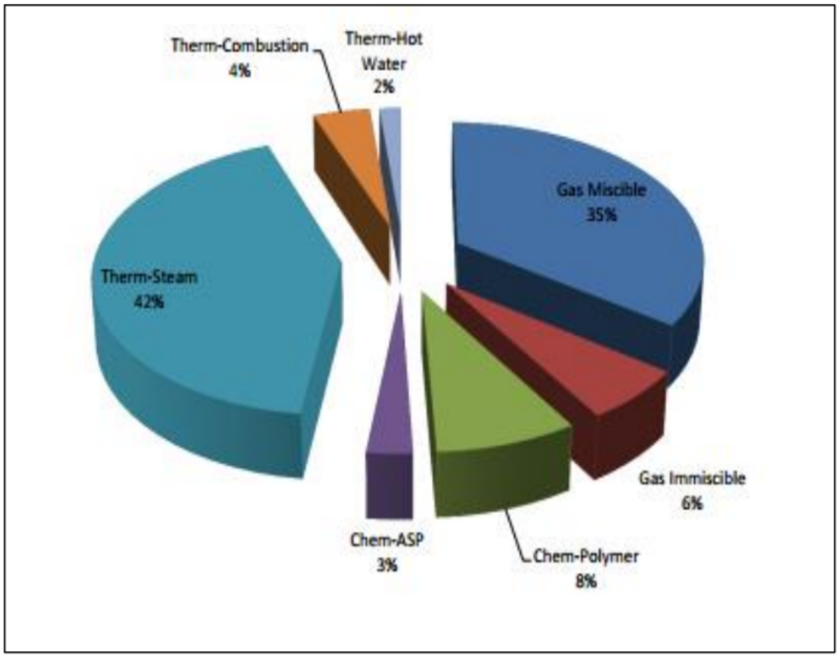

*Figure I-4. Worldwide EOR Project Subcategories**

*Adopted from *Updated EOR screening criteria and modeling the impacts of water salinity changes on oil recovery*, Alasadani Ahmad (2012)

Based on data, the US, Canada and China lead the world in EOR project implementation. The US and Venezuela conduct the majority of steam-flooding EOR projects. Miscible flooding is led by the US and Canada, while China leads the world in chemical EOR projects. To further examine worldwide EOR project implementation trends, the numbers of EOR projects implemented, as well as enhanced oil production and crude oil prices, are cross-plotted, as shown in Figure I-5. To establish a baseline, Figure I-5 includes only EOR projects reported in 2010; the enhanced production rates that year should not be considered as the initial production rate.

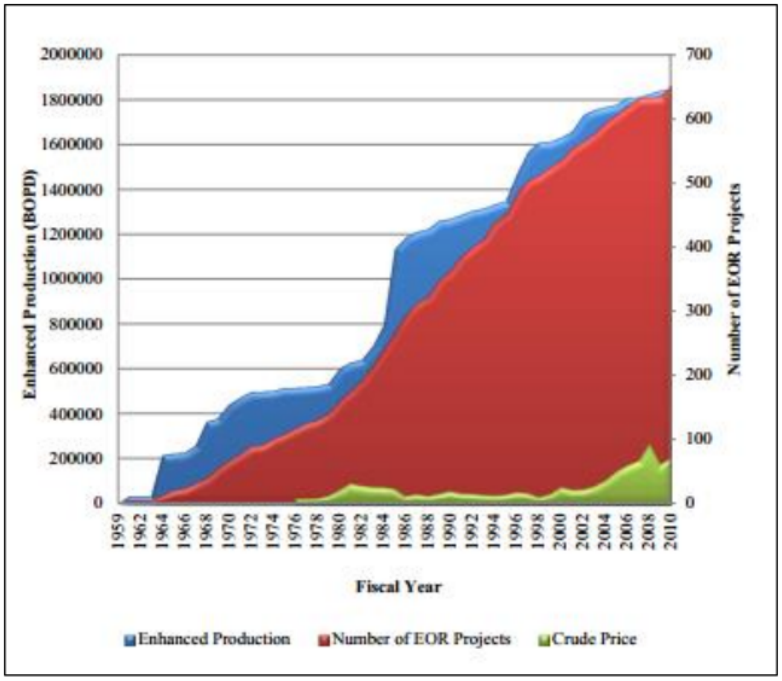

*Figure I-5. EOR Projects and Enhanced Production Trends**

*Adopted from *Updated EOR screening criteria and modeling the impacts of water salinity changes on oil recovery*, Alasadani Ahmad (2012)

The number of EOR projects has increased dramatically since 1959 when the first project was undertaken, most notably during the early 1980s and late 1990s (Figure I-5). Despite increasing enhanced production rates and oil prices, the number of EOR projects remained relatively constant from 2006 through 2010 (Figure I-5), a pattern that could be attributed to incomplete reporting of EOR projects.

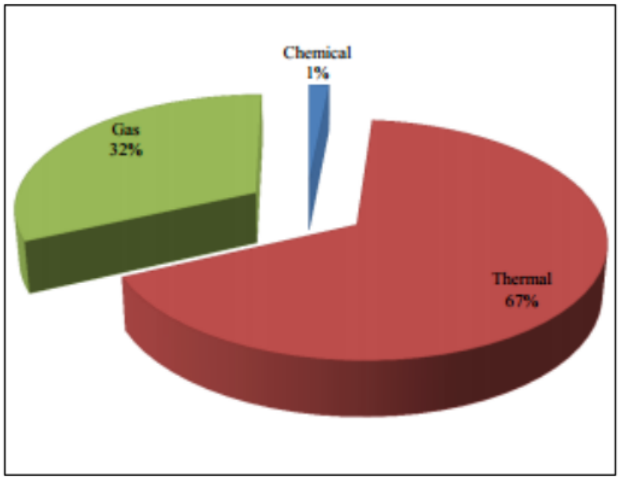

*Figure I-6. Worldwide Enhanced Production Share**

*Adopted from *Updated EOR screening criteria and modeling the impacts of water salinity changes on oil recovery*, Alasadani Ahmad (2012)

Thermal EOR accounts for the majority of EOR (Figure I-6); however, because EOR can be applied as a primary, secondary, or tertiary recovery stage, a new illustration is required to demonstrate the recovery stage of the main EOR methods. This is achieved by cross-plotting start and end oil saturations and enhanced production against the main EOR methods (Figure I-7).

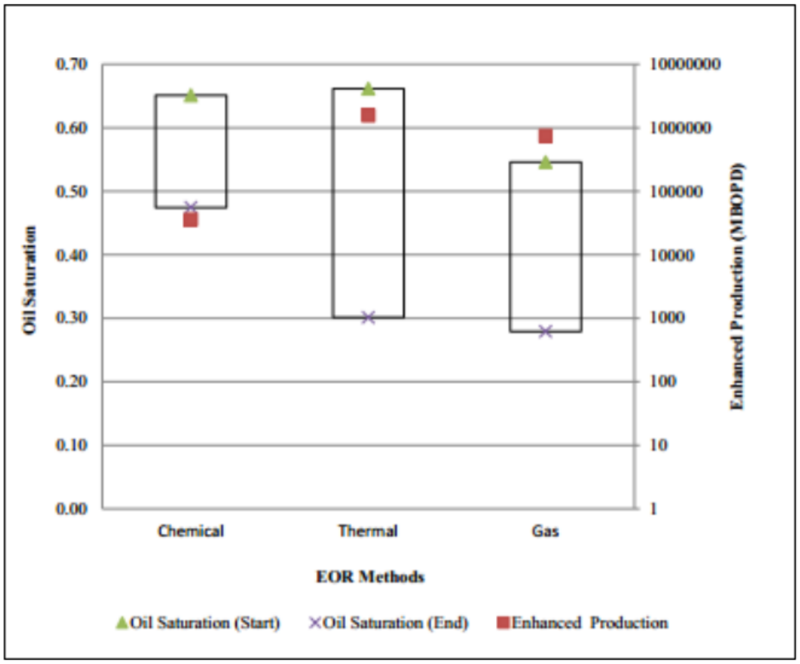

*Figure I-7. Oil Saturations and Enhanced Production Distribution**

*Adopted from *Updated EOR screening criteria and modeling the impacts of water salinity changes on oil recovery*, Alasadani Ahmad (2012)

It is evident from Figure I-7 that thermal EOR is applied over a wide range of oil saturation levels because it is used also in the primary and secondary oil recovery stages in heavy and medium-gravity oil recovery, respectively. Similarly, gas EOR also is used as a secondary recovery method; thus, a wider oil saturation range is observed in gas than in chemical EOR. Chemical EOR usually is employed after water flooding is well underway. Figure I-7 illustrates the benefits of initiating chemical EOR at the start of secondary recovery to improve overall recovery efficiency

The third step in analyzing the EOR database is to link reservoir formations with EOR methods. The possible importance of permeability for the aforementioned EOR methods is highlighted. To verify this observation, the range of reservoir properties for the selected EOR methods is illustrated in Figure I-8 and Figure I-9.

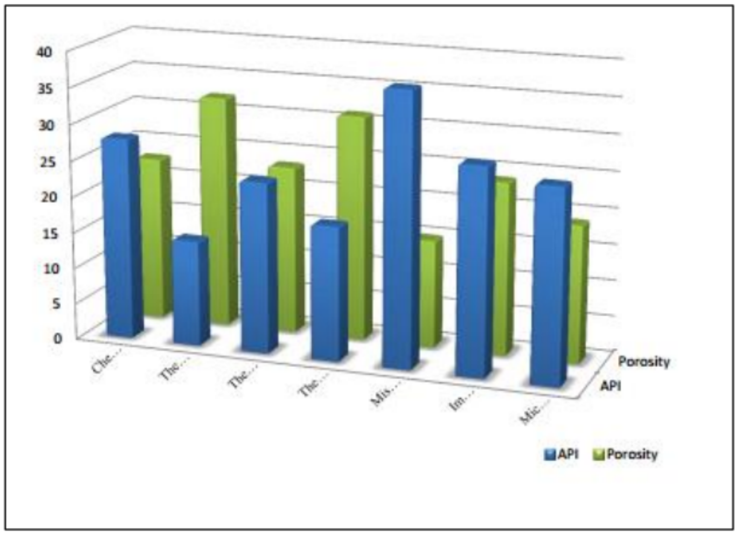

*Figure I-8. EOR Methods versus Selected Average Fluid and Reservoir Properties**

*Adopted from *Updated EOR screening criteria and modeling the impacts of water salinity changes on oil recovery*, Alasadani Ahmad (2012)

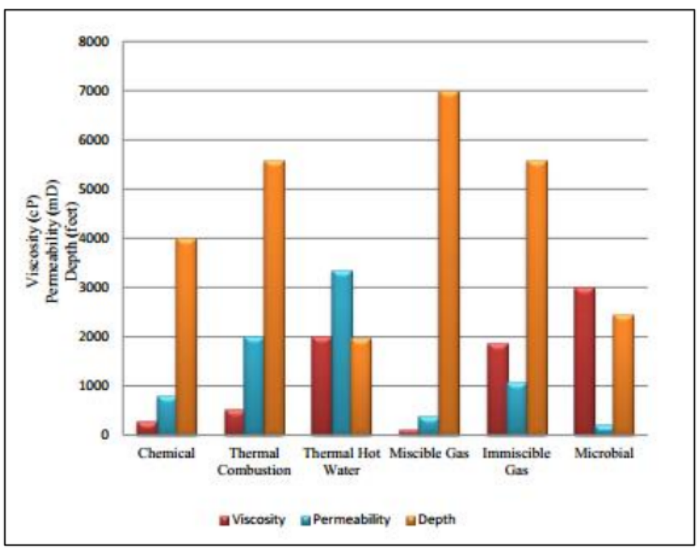

*Figure I-9. EOR Methods – Selected Average Fluid and Reservoir Properties**

*Adopted from *Updated EOR screening criteria and modeling the impacts of water salinity changes on oil recovery*, Alasadani Ahmad (2012)

It is concluded that EOR methods can be functions of one or more reservoir properties. For example, sandstone reservoirs, which are typically characterized by high permeability, rely almost exclusively on thermal steam, immiscible gas and chemical polymer methods. Similarly, API gravity and depth are functions of miscible gas flooding; this is to ensure that the minimum miscibility pressure (MMP) is achievable and that the MMP does not fracture the formation.

Crude oil development and production in oil reservoirs can include up to three distinct phases: primary, secondary, and tertiary (or enhanced) recovery. During primary recovery, the natural pressure of the reservoir or gravity drive oil into the wellbore, combined with artificial lift techniques (such as pumps) which bring the oil to the surface. But only about 10 percent of a reservoir's original oil in place is typically produced during primary recovery. Secondary recovery techniques extend a field's productive life generally by injecting water or gas to displace oil and drive it to a production wellbore, resulting in the recovery of 20 to 40 percent of the original oil in place .

Three major categories of EOR have been found to be commercially successful to varying degrees especially in U.S. oil fields:

- Thermal recovery, which involves the introduction of heat such as the injection of steam to lower the viscosity, or thin, the heavy viscous oil, and improve its ability to flow through the reservoir. Thermal techniques account for over 40 percent of U.S. EOR production, primarily in California.
- Gas injection, which uses gases such as natural gas, nitrogen, or carbon dioxide (CO_2) that expand in a reservoir to push additional oil to a production wellbore, or other gases that dissolve in the oil to lower its viscosity and improves its flow rate. Gas injection accounts for nearly 60 percent of EOR production in the United States.
- Chemical injection, which can involve the use of long-chained molecules called polymers to increase the effectiveness of waterfloods, or the use of detergent-like surfactants to help lower the surface tension that often

prevents oil droplets from moving through a reservoir. Chemical techniques account for about one percent of U.S. EOR production.

Each of these techniques has been hampered by its relatively high cost and, in some cases, by the unpredictability of its effectiveness.

In the U.S., there are about 114 active commercial CO2 injection projects that together inject over 2 billion cubic feet of CO2 and produce over 280,000 BOPD (April 19, 2010, Oil and Gas Journal).

1.3 CO2 Injection Offers Considerable Potential Benefits

The EOR technique that is attracting the newest market interest is CO2-EOR. First tried in 1972 in Scurry County, Texas, CO2 injection has been used successfully throughout the Permian Basin of West Texas and eastern New Mexico, and is now being pursued to a limited extent in Kansas, Mississippi, Wyoming, Oklahoma, Colorado, Utah, Montana, Alaska, and Pennsylvania.

Until recently, most of the CO2 used for EOR has come from naturally-occurring reservoirs. But new technologies are being developed to produce CO2 from industrial applications such as natural gas processing, fertilizer, ethanol, and hydrogen plants in locations where naturally occurring reservoirs are not available. One demonstration at the Dakota Gasification Company's plant in Beulah, North Dakota is producing CO2 and delivering it by a 204-mile pipeline to the Weyburn oil field in Saskatchewan, Canada. Encana, the field's operator, is injecting the CO2 to extend the field's productive life, hoping to add another 25 years and as much as 130 million barrels of oil that might otherwise have been abandoned.

1.4 Next Generation CO2 Enhanced Oil Recovery

DOE’s R&D program is moving into new areas, researching novel techniques that could significantly improve the economic performance and expand the applicability of CO2 injection to a broader group of reservoirs; expanding the technique out of the Permian Basin of West Texas and Eastern New Mexico into basins much closer to the major sources of man-made CO2. Next generation CO2-EOR has the potential to produce over 60 billion barrels of oil, using new techniques including injection of much larger volumes of CO2, innovative flood design to deliver CO2 to un-swept areas of a reservoir, and improved mobility control of the injected CO2.

In September 2010, DOE competitively selected seven Next Generation CO2 EOR research projects. Four projects are developing techniques for mobility control of the injected CO2. Novel foams and gels have the potential to prevent the highly-mobile CO2 from channeling through high-permeability areas of a reservoir, leaving un-swept, unproductive areas of the reservoir. The four projects are:

- Improved Mobility Control in CO2 Enhanced Oil Recovery using SPI Gels (Impact Technologies, LLC)
- Engineered Nanoparticle-Stabilized CO2 Foams to Improve Volumetric Sweep of CO2 EOR Processes (U. Texas - Austin)
- Novel CO2 Foam Concepts and Injection Schemes for Improving CO2 Sweep Efficiency in Sandstone and Carbonate Hydrocarbon Formations (U. Texas - Austin)
- Nanoparticle-Stabilized CO2 Foam for CO2-EOR Application (New Mexico Institute of Mining and Technology)

One project is investigating the potential for oil production by CO2 injection into the residual oil zone:

- "Next Generation" CO2-EOR Technologies To Optimize the Residual Oil Zone CO2 Flood At The Goldsmith Landreth Unit, Ector County, Texas (U. Texas – Permian Basin)

Two projects are developing simulation and modeling tools for CO2 EOR:

- Real Time Semi-Autonomous Geophysical Data Acquisition and Processing System to Monitor Flood Performance (Sky Research, Inc.)
- CO2-EOR and Sequestration Planning Software (NITEC LLC)

Although most of today's CO2 EOR projects involve large-scale continuous injection of CO2 solvent, there is increasing interest in cyclic CO2 injection into single wells. Typically, the rapid injection of CO2 (or CO2/hydrocarbon blends) is followed by a shut- in period. The well is then returned to production and the response monitored. In reservoirs with poor interwell communication, this single-well approach may afford the only means of recovering tertiary oil by a CO2 process. In reservoirs where interwell communication is not a problem, CO2 huff 'n' puff offers a fast, inexpensive alternative to traditional EOR methods.

The engineer faced with designing a CO2 huff 'n' puff project can find only a limited amount of prior experience in the literature. Laboratory studies in two different 14°API [0.97-g/cm3] crudes have indicated that CO2 huff 'n' puff will recover oil. The addition of nitrogen or methane as contaminants to the CO2 is not desirable because it reduces oil recovery. The optimum number of cycles is reported to be two or three, judging from field experience in Arkansas.

1.5 Opportunity of CO2 Injection in Indonesia

Looking at the facts above, CO2 injection has been developed and applied in many reservoirs especially in U.S. oil reservoirs. So does in Indonesia. CO2 injection was started to be developed and applied as pilot project and research development. Most of the fields in Indonesia have been categorized as mature field and its production phase are mostly in primary recovery. Oil production has declined steadily with decreasing rate of approximately 12% per year (Annual Report, BPMigas, 2011). Some oil companies tried to improve oil production by using secondary recovery method and Enhance Oil Recovery (EOR) method.

The potential to increase production through EOR is huge (A. Muslim, 2013). Based on annual reserve in 2011, the remaining reserve is s49.5 billion barrel which can be extracted by conducting EOR activity (Annual Report, BPMigas, 2011).if this activity succeeds on converting 7 to 13 % of the existing resource, it may lead to additional reserve of 6.24 billion barrel (A. Muslim 2013).

Based on that report also, steam flood has contributed 177,180 BOPD production or 19.7% of national production. Steam flood normally applied to heavy crude oil and shallow reservoir. Yet, in Indonesia most crude oil is light (more than 25^{o} API) and some of the reservoir depths are located more than 2,500 ft. furthermore, for light oil and reservoir more than 2,500 ft candidates as CO2-EOR based on Taber screening criteria that was firstly established in 1997 (A.Muslim, 2013).

From the facts and research above shows that CO2 injection has been applicable in Indonesia. Accordingly, this pilot project is meant to try and prove that CO2 injection is one of the best and most applicable methods in Indonesia.

CHAPTER II
FIELD OVERVIEW

2.1 Location

Figure 2-1. Langgak Field location

This field is located in Kampar District, Rokan Hulu, Riau. This field has area of 79.65 km2 and can be reached 135 km from Pekanbaru. The detail of the field location can be seen at the picture as follows.

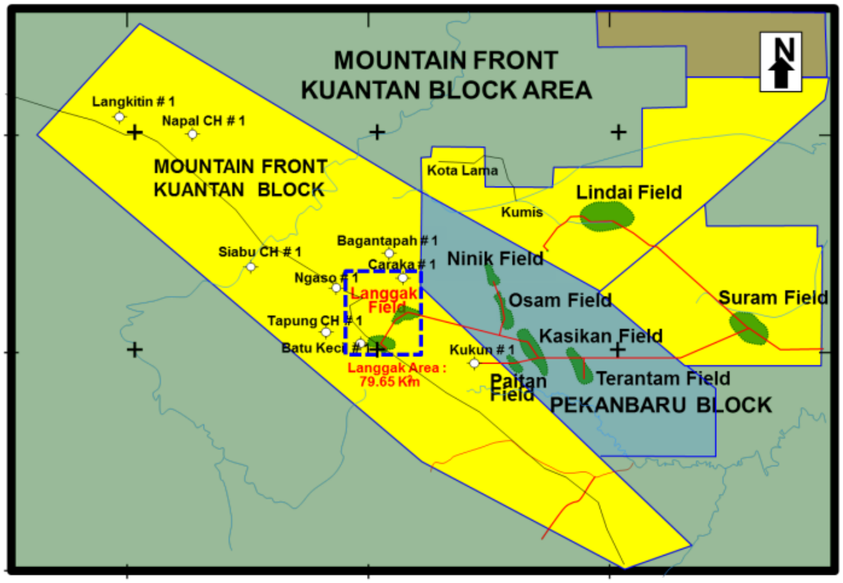

Figure 2-2. The detail of Langgak Field location

2.2 Field History

Langgak Field was discovered in 1975 and developed by CPI more than 40 years until April 2010. There are 33 wells including 6 PA wells that have already been drilled. Afterward, PT SPRL took the opportunity to replace CPI as oil company operator of this field to the present. For four years operation, there were 5 infill wells that have already been drilled. Now, there are 27 active wells which are 26 producer wells, and a water-well.

Langgak field had been drilled since 1979. It has 51.94 MMBO with current recovery factor of 27.2%. Until December 2017 current cumulative production was 14.1 MMBO with estimate primary recovery was 33.7% and remaining reserve was 3.40 MMBO. By those things, this EOR method can improve the recovery up to 20-25% (10-12 MMBO additional reserve) in return.

2.3 Reservoir Overview

a. Fluid Properties:

Langgak Oil:

Table 2-1. Reservoir and fluid Properties

Langgak Oil	
Gravity	30.8 API
Viscosity	14 cp
GOR	3. SCF/STB
Pour point	105-110 F
Pb	113 psi
Langgak Water	
Salinity	500-1000 ppm
Viscosity	0.52 cp
Density	1.003
Langgak Rock	
Porosity	26%
Permability	500 mD
Langgak Reservoir	
Avg depth	1100-1300 ft
Drive mechanism	Bottom drive mechanism
Pressure	530 psi
Temperature	136

CHAPTER III
EOR METHOD SELECTION

3.1 Screening Criteria

Screening criteria for Enhanced Oil Recovery (EOR) have evolved through the years to help the petroleum engineer make decision on what method should be taken. In 1997 based on "*EOR Screening Criteria Revisited-Part 1: Introduction to Screening Criteria and Enhanced Recovery Field Projects*", the most widely used screening criteria appeared in the 1976 and 1984 Natl. Petroleum Council (NPC) reports. Computer technology has improved the application of screening criteria through the use of artificial intelligence techniques. EOR Screening technique primarily based on a combination of the reservoir and oil characteristics of successful projects plus our understanding of the optimum conditions needed for good oil displacement by the different EOR fluids. One goal is to provide realistic parameters that can be used in the newer computer-assisted tools for reservoir management.

Taber et al. published the first EOR selection criteria in 1982; these criteria were updated in 1996 in a paper that became the most widely cited Society of Petroleum Engineers (SPE) paper. The EOR selection criteria categorize EOR methods into gas, chemical and thermal and are based on a range of reservoir properties listed for each of these methods. This range is based on reported EOR projects and surveys. The publication also includes the limitations of each EOR method based on the prevailing technologies at the time the paper was written. Much has changed since the EOR selection criteria were published in 1996. Firstly, numerous EOR projects have been implemented since 1996, out of which several new EOR categories and subcategories have been introduced. Additionally, technological advances have surpassed some of EOR's previous limitations. Furthermore, the EOR selection criteria were based on a range of reservoir properties without considering incremental recovery or the project's distribution scale. Despite the implementation of over 600 EOR projects since 1959 (*The Oil and Gas Journal*, 1998-2008), the use of EOR remains limited worldwide. The development and implementation of any recovery methodology, especially on a field-wide scale, requires confidence in its efficacy. Establishing such confidence requires an in-depth analysis of EOR projects that would provide updated and more concise EOR selection criteria.

Enhanced oil recovery (EOR) technologies can augment the production of hydrocarbons and therefore are key in achieving the ultimate goal of increasing recovery volumes, which is critical given the world's predicted energy needs and current supply. A review of the existing EOR criteria is presented here, revealing the need for updated criteria because of their datedness and their emphasis on minimum and maximum average values that do not represent a sound basis for the selection of candidate reservoirs for EOR. Updated criteria that provide a more representative understanding of selection values are necessary if EOR technologies are to be implemented to their full potential.

3.2 Oil/Reservoir Characteristics of Successful Projects

Figure III-1 shows the depth of most of the EOR projects inside U.S. It shows the general trend, ranging from the many steam projects for the heavy oils at shallow depths in California to very deep projects for the lightest oils that can be miscibly displaced by dry gas or nitrogen at high pressures. The water-based methods use oils in the mid-gravity range, while the CO_2 projects cover a fairly broad range of oil gravities between 30 and 45^o API. Figure III-1 confirms that all CO_2-miscible projects are at depths greater than 2,000 ft.

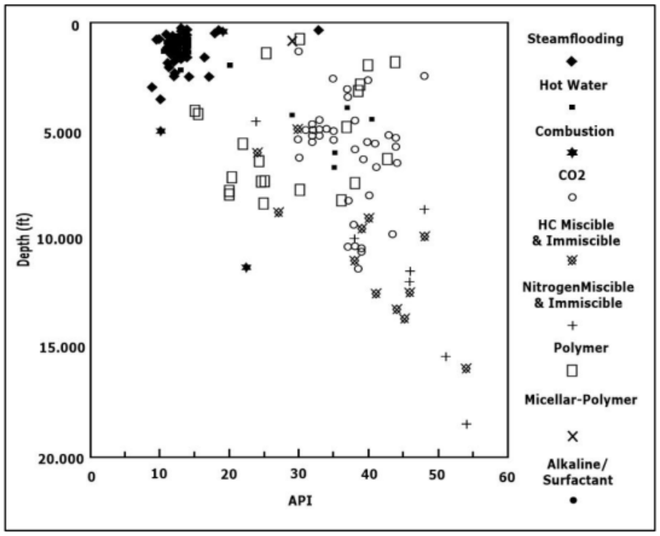

*Figure 3-1 . Depth of producing oil gravity of producing EOR projects in the U.S.**

*Adopted from *EOR Screening Criteria Revisited-Part 1: Introduction to Screening Criteria and Enhanced Recovery Field Projects,* Taber et al (1997)

Figure III-2 the non-U.S. world distribution of projects is similar, but that there are more hydrocarbon and fewer projects than in the U.S.

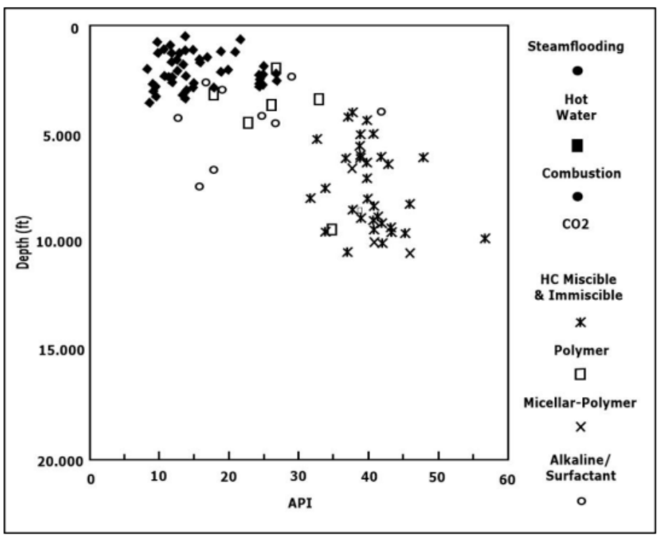

*Figure 3-2 . Depth of producing oil gravity of producing EOR projects outside the U.S.**

*Adopted from *EOR Screening Criteria Revisited-Part 1: Introduction to Screening Criteria and Enhanced Recovery Field Projects,* Taber et al (1997)

The incremental oil production from each EOR project is shown in Figure III-3 and Figure III-4. His dominance of steamflooding stands out clearly in these figures. Not only are there far more steamfloods, but the oil produced by steamflooding far exceeds that from all the other methods combined. Note that the largest EOR projects (in terms of oil production) are steamfloods, with the "off-scale'' (Figure III-4) Duri steamflood in Indonesia producing more than twice as much oil (245,000 B/D) as any other project in the world.

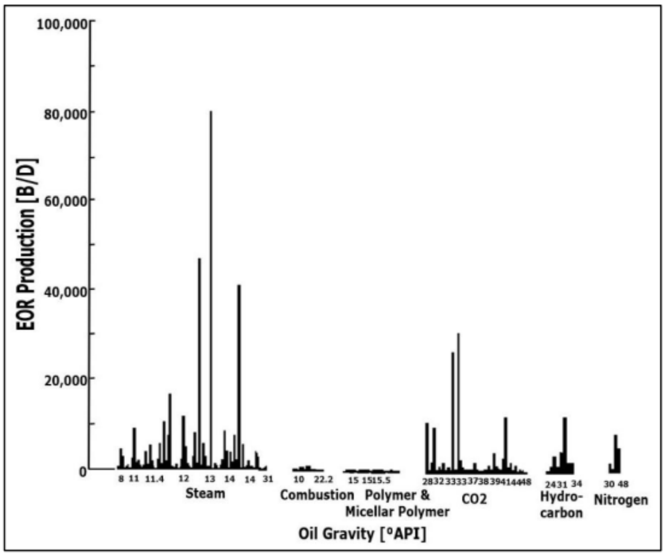

*Figure 3-3. EOR production vs. oil gravity in the U.S.**

*Adopted from *EOR Screening Criteria Revisited-Part 1: Introduction to Screening Criteria and Enhanced Recovery Field Projects,* Taber et al (1997)

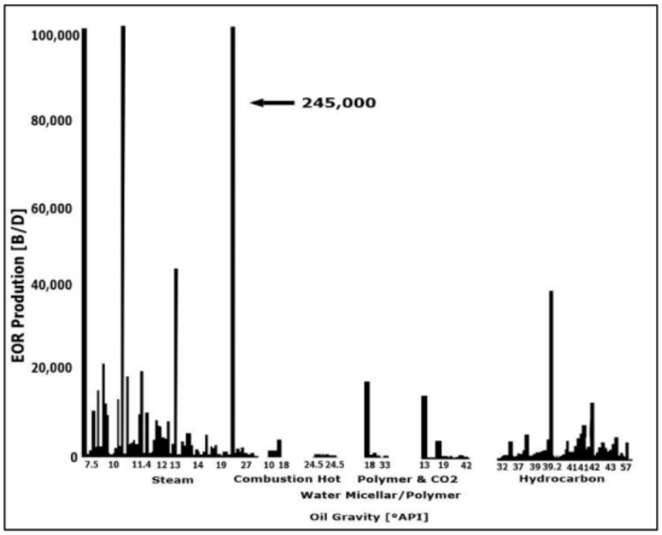

*Figure 3-4. EOR production vs. oil gravity outside the U.S.**

*Adopted from *EOR Screening Criteria Revisited-Part 1: Introduction to Screening Criteria and Enhanced Recovery Field Projects,* Taber et al (1997)

3.3 Suggested Criteria for EOR Methods

a. Taber (1997) – SPE 35385

Oil and reservoir characteristics for successful EOR methods are given in Table III-1. The table was compiled from field data for the projects shown in Figure III-2 through Figure III-3, and from the known oil-displacement mechanisms for each of the methods.

Table 3-1. Summary of Screening Criteria for EOR Methods

Properties	EOR Method								
	Nitrogen and flue gas	Hydrocarbon	Carbon Dioxide	Immiscible Gases	Miscellar/polymer, ASP, and alkaline flooding	Polymer flooding	Combustion	Steam	Surface Mining
Oil API Gravity	> 35 Average 48	> 23 Average 41	> 22 Average 36	> 12	> 20 Average 35	> 15	> 10 Average 16	> 8 to 13.5 Average 13.5	7 to 11
Oil Viscosity (cp)	< 0.4 Average 0.2	< 3 Average 0.5	< 10 Average 1.5	< 600	< 35 Average 13	> 10, < 150	< 5000 Average 1200	< 200000 Average 4700	zero cold flow
Composition	High % C1-C7	High % C2-C7	High % C5-C12	Not critical	Light, intermediate Some organic acids for alkaline floods	Not critical	Some asphaltic components	Not critical	Not critical
Oil Saturation (%PV)	> 40 Average 75	> 30 Average 80	> 20 Average 55	> 35 Average 70	> 35 Average 53	> 50 Average 80	> 50 Average 72	> 40 Average 66	>8% wt sand
Formation Type	Sandstone or Carbonate	Sandstone or Carbonate	Sandstone or Carbonate	Not critical	Sandstone Preferred	Sandstone Preferred	High porosity sandstone	High porosity sandstone	Mineable tar sand
Net Thickness (ft)	Thin unless dipping	Thin unless dipping	Wide range	Not critical if dipping and/or good vertical permeability	Not critical	Not critical	> 10 feet	> 20 feet	> 10 feet
Average Permeability (md)	Not critical	Not critical	Not critical	Not critical	> 10 md Average 450 md	> 10 md Average 800 md	> 50 md	> 200 md Average 2540 md	Not critical
Depth (ft)	> 6000	< 4000	> 2500	> 1800	< 9000 Average 3250	< 9000	< 11500 Average 3500	< 4500 Average 1500	< 3.1 overburden to sand ratio
Temperature (deg F)	Not critical	Not critical	Not critical	Not critical	< 200 Average 80	< 200 Average 140	< 100 Average 135	Not critical	Not critical

Screening criteria have been proposed for all enhanced oil recovery (EOR) methods. Data from EOR projects around the world have been examined and the optimum reservoir/oil characteristics for successful projects have been noted. The oil gravity ranges of oils of current EOR methods have been compiled and the results are presented in table above. The proposed screening criteria are based on both field results and oil recovery mechanisms. The current state of the art for all methods is presented briefly by that table, and relationships between them are described.

In general, the upper and lower values in Table III-1 (> or <) have come from process-mechanism understanding (laboratory experiments), and they also include parameters of successful field projects. For example, even though we are unaware of any miscible C02 projects in reservoirs with oils of less than 29°API, we list 22°API as the lower limit because extensive laboratory work shows that the required pressure [i.e., minimum miscibility pressure (MMP)] can be met in typical west Texas reservoirs with oils of that gravity. Also, we have lowered the oil gravity requirement to > 12° API for immiscible CO_2 floods to include a successful 13"API project in Turkey.

b. SPE 39234

Table 3-2. Screening Taber (revisited part 2) based on SPE 39234

Properties	EOR Method							
	Nitrogen and flue gas	Hydrocarbon	Carbon Dioxide	Immiscible Gasses	Miscellar/polymer, ASP, and alkaline flooding	Polymer flooding	Combustion	Steam
Oil API Gravity	>35 Average 48 CP: 38 to 54	> 23 Average 41 CP: 24 to 54	> 22 Average 36 CP: 27 to 44	> 12	>20 Average 35	> 15 CP: 14 to 43	> 10 Average 16 CP: 10 to 40	> 8 to 13.5 Average 13.5 CP: 8 to 27
Oil Viscosity (cp)	< 0.4 Average 0.2 CP: 0.07 to 0.3	< 3 Average 0.5 CP: 0.04 to 2.3	< 10 Average 1.5 CP: 0.3 to 6	<600	<35 Average 13	> 10, < 150 CP: 1 to 80	< 5000 Average 1200 CP: 6 to 5000	< 200000 Average 4700 CP: 10 to 137000
Composition	High % C1-C7	High % C2-C7	High % C5-C12	Not critical	Light, intermediate Some organic acids for alkaline floods	Not critical	Some asphaltic components	Not critical
Oil Saturation (%PV)	>40 Average 75 CP: 59 to 80	> 30 Average 80 CP: 30 to 98	> 20 Average 55 CP: 15 to 70	> 35 Average 70	>35 Average 53	> 50 Average 80 CP: 50 to 92	> 50 Average 72 CP: 62 to 94	> 40 Average 66 CP: 35 to 90
Formation Type	Sandstone or Carbonate	Sandstone or Carbonate	Sandstone or Carbonate	Not critical	Sandstone Preferred	Sandstone Preferred	High porosity sandstone	High porosity sandstone
Net Thickness (ft)	Thin unless dipping	Thin unless dipping	Wide range	Not critical if dipping	Not critical	Not critical	> 10 feet	>20 feet
Average Permeability (md)	Not critical	Not critical	Not critical	Not critical	> 10 md Average 450 md	> 10 md Average 800 md CP: 10 to 15000	>50 md CP: 85 to 4000	>200 md CP: 150 to 4500
Depth (ft)	>6000 CP: 10000 to 18500	<4000 CP: 4040 to 15900	Appropriate to allow injection pressure > MMP, which increase with temperature	> 1800	< 9000	< 9000 CP: 1300 to 9600	< 11500 Average 3500 CP: 400 to 11300	< 5000 150 to 4500
Temperature (deg F)	Not critical	Not critical	Not critical	Not critical	< 200	< 200 CP: 80 to 185	>100	Not critical CP: 60 to 280

Screening criteria are useful for cursory examination of many candidate reservoirs before expensive reservoir descriptions and economic evaluations are done. Screening criteria in this paper is based on a combination of the reservoir and oil characteristics of successful projects plus our understanding of the optimum conditions needed for good oil displacement by the different EOR fluids.

With the reservoir management practices of today, engineers consider the various IOR/EOR options much earlier in the productive life of a field. Obviously, economics always play the major role in "go/no-go" decisions for expensive injection projects, but a cursory examination with the technical criteria is helpful to rule out the less-likely candidates. The criteria are also useful for surveys of a large number of fields to determine whether specific gases or liquids could be used for oil recovery if an injectant was available at a low cost.

This paper provides screening criteria for the eight methods that are either the most important or still have some promise. These "current" EOR or IOR methods include the three gas (nitrogen, hydrocarbon, CO), three water [micellar/polymer plus alkaline/surfactant/polymer (ASP); polymer flooding; gel treatments] and the three thermal/mechanical (combustion, steam, surface mining) methods.

This paper is more familiar with the U.S. projects than those in other parts of the world. In addition to the very broad distribution of the EOR projects, the correlation between depth and oil gravity on various EOR method is based on the general trend, ranging from the many steam projects for the heavy oils at shallow depths in California to the very deep projects for the lightest oils that can be miscibly displaced by dry gas or nitrogen at high pressures.

c. SPE 100044

Table 3-3. Screening criteria for CO_2 huff and puff Injection based on SPE 10004

Parameters of Successful Reservoirs	Light Oils	Medium Oils	Heavy Oils
Oil Viscosity (cp)	0.4 to 8	32 to 46	415 to 3000
Oil Gravity (°API)	23 to 38	17 to 23	11 to 14
Porosity (%)	13 to 32	25 to 32	12 to 32
Depth (feet)	1200 to 12870	2600 to 4200	1150 to 4125
Thickness (feet)	6 to 60	36 to 220	200
Permeability (mD)	10 to 3000	150 to 388	250 to 350

As mentioned precedingly that the screening criteria designed by this paper is also based from the successful projects conducted from 30 oilfields located worldwide and came up with a conclusion of the parameters and category (for light oil, medium oil, and heavy oil that can be seen on above table).

In order to achieve the conclusion of the best parameters above, references from other successful projects were observed and it can be seen in Table III-4 below:

Table 3-4. Summary of Worldwide CO2 Huff and Puff Field Trials - Medium and Heavy Oils

SPE paper	15502	20883	15749	15749	24645	24645	This Work			
Field	Field G	Bati	Camarlu	Camarlu	Halfmoon	Halfmoon	Forest Reserve			
Basin		Raman	Camaru-11	Camaru-22						
Province	Texas				Wyoming	Wyoming				
Country	USA	Turkey	Turkey	Turkey	USA	USA	Trinidad			
Formation		limestone	limestone	limestone	Phosphoria	Tensleep	U forest	L forest	U cruse	LMLE
Depth (ft)	4200	4265	4125	4125	3400	3600	2600	3000	4200	1150
Thickness (ft)	36-68		200	200	40	98	55-220	73-213	210-309	200
Porosity (%)	25	18	12	12	14	15	30	32	31	32
Permeability (mD)	388	58	350	350	17	95	150	157	335	250
Sw Current (%)	25		23	25						
Pressure initial (psi)		1800	1736	1736			1300	1400	2200	
BHP (psi) current	660		1689	1637	450-900					
Temperature (°F)	135		116	116	135-141		120	120	130	95
Oil gravity (° API)	23.3	12	11-12	11-12	17	17	17	19	25	14
Oil viscosity (cp)	33.4	592	415	705	118	118	46	32	13	3000
Transmissibility(mDft/cp)	4507	6	295	174	2	76	489	770	8633	21
Produced WOR	23-106		small	small		40				
Pre-CO_2 oil rate (bbl/d)	5-39		15 -20	15 - 20		11	5	5	5	5
% Primary Recovery		1.5%	1%	1%						
So (start of cyclic CO2)	73									
Type of reservoir		primary	primary	primary	Weak WD	Strong WD	DD	DD	DD	DD
# of wells / # treatment		9					4	4	2	1
CO2 Util'n (Mcf/bbl)	4.9		5	1.3	15.5	11.6	22	12	139	5
Project Success		Success			Failure	Failure	Success	Success	Failure	Success
Incremental oil (STB)	1657		4704	6425	600	1150	9000	11100	1400	18000
No of cycles	2	Converted to Gas Drive	2	2	1	2	3	5	5	2
CO^2 injected (MMSCF)	8	30-50/well	21.01	12.43			56-558	72-170	12-379	141
Days of soak	31	21	10-13	12-13			3-5	3-5	3-5	3-5

Note: WF = water flood, DD= depletion drive, swd= strong water drive, wwd= weak water drive. LA & KY = Louisiana and Kentucky

Table 3-5. Summary of Worldwide CO2 Huff and Puff Field Trials – Light Oils

SPE paper	27677	15502	15502	15502	15502	15502	15502	15502	15502	15502	15502	15502
Field	Big Sink'g	Magnet	Picket Ridge	Field C	Field D	Withers N.	Field F	Thompson	Field I	Field J	Field K	W Col.
Basin	Appalachian	Withers									Manavel	
Province	Kentucky	Texas	Texas	Texas	Texas	Texas	Texas	Texas	Texas	Texas	Texas	Texas
Country	USA	USA	USA	USA	USA	USA	USA	USA	USA	USA	USA	USA
Formation		Magnet W	Picket Ridge					Frio			Olig	S Andres
Depth (ft)	1300	5500	4570	4900	4650	5250	5250	5200	7756	4100	5000	2600
Thickness (ft)	60	21	7	12	9	8	8	25	15	15	?	?
Porosity (%)	13	23	30	31.8	31	25	25	27	?	30	30	30
Permeability (mD)	19	1700	1200	534	350	450	400	500	15	500	1000	560
Sw Current (%)	50											
Pressure initial (psi)	400											
BHP (psi) current	150	1310	930	1430	1350	860	1030	1540	1200	750	900	500
Temperature (°F)	68	154	138	155	150	150	150	153	175	149	149	116
Oil gravity (° API)	38	26	25	24.4	23	25.7	25.7	25.2	37	25	26	30
Oil viscosity (cp)		2.3	2.5	4.6	3.2	2.5	2.9	2.7	1.6	4.4	4.2	8
Transmissibility(mDft/cp)		15522	3360	1393	984	1440	1103	4630	141	1705		
Produced WOR	90%	9-24	12-16	24-108	72	12-100	6.1	1.75	0.3	0	15-99	45536
Pre-CO_2 oil rate (bbl/d)		16-86	23-27	3-41	12	12-60	54	12	21	56	9-65	12-30
% Primary Recovery												
So (start of cyclic CO2)		73	80	68	69	80	75	73	?	85	?	?
Type of reservoir	WD											
# of wells / # treatment	240/290											
CO2 Util'n (Mcf/bbl)	1.1	1.1	8.2			2.8	10.2				2.4	10.2
Project Success	Success											
Incremental oil (STB)	180000	3697	122	0	0	1766	490	3	0	0	1656	391
CO^2 injected (MMSCF)	210	4	1	8	5	5	5	4	4	4	4	4
Days of soak	10	12	7	25	20	17	17	36	23	23	21	13

Note: WF = water flood, DD= depletion drive, swd= strong water drive, wwd= weak water drive: LA & KY = Louisiana and Kentucky

Table 3-6. Summary of World Wide CO2 Huff and Puff Field Trials – Light Oils

SPE paper	**18977**	**20208**	**20208**	**20208**	**20208**	**20208**	**20208**	**20208**	**20208**	**20208**	**20208**	**16720**
Field	Paradis	West Cote	b	c	d	e	f	g	h	I	k	Timbalier
Basin		Blanche Bay		Lake Barre					Bayou Sale	Lafitte		
Province	Louisiana	Louisiana	LA & Ky	Louisiana	LA & Ky	LA & Ky	LA & Ky	LA & Ky	Louisiana	Louisiana	LA & Ky	Louisiana
Country	USA	USA	USA	USA	USA	USA	USA	USA	USA	USA	USA	USA
Formation	Main py	Minnelusa	Sand	Up M	Sand	Sand	Sand	Sand	St. Marry	Sand	Sand	
Depth (ft)	10200	8140	10330	12870	4909	1200-3000	6248	1300	10060	8900	9837	4878
Thickness (ft)		21	46	20-50	12-17	6-24	7-35	34-58	30	na	15-34	
Porosity (%)	28	29	28	25	32	32	32	13-16	31	27	24	32
Permeability (mD)	1033	322	1033	139	2500	3000	300-500	10	500	250	252	500-2500
Sw Current (%)												25
Pressure initial (psi)												2390
BHP (psi) current		3847	2406	2500	2235	560-1400	2900	100	1795	3947	5100	2235
Temperature (°F)		185	212	240	138	80-100	166	68	206	185	192	138
Oil gravity (° API)	38	23-38	23-38	33	23-38	23-38	23-38	23-38	23-38	34	23-38	26
Oil viscosity (cp)	0.5	1.3		0.4						0.7		
Transmissibility(mDft/cp)		5202										
Produced WOR		9	15.6	1	71	8.3		5.5	0.37	0.43		99%
Pre-CO_2 oil rate (bbl/d)	23	19	25-31	47	13-18	9-53		1-70	54	72		15
% Primary Recovery												18
So (start of cyclic CO2)												34-60
Type of reservoir	tertiary	WF	WF	DD	SWD	SWD	SWD	DD	WWD	SWD	DD	b/water
# of wells / # treatment	11	1	2	3	4	9	2	66	1	1	3	2
CO2 Util'n (Mcf/bbl)	1.9	2.7	1.5-2.7	0.3	0.9-1.9	0.72-2.68		0.6-2.1	0.7	0.71		1.1-3.2
Project Success	Success											Success
Incremental oil (STB)	27000	3233	6148-11410	29830	5516-14863	2612-11051		321-6326	12115	9118		14000
CO^2 injected (MMSCF)	18											23
Days of soak	21	31	19-21	25-33	28-181	28-63	20-23	Jul-38	47	17	16-54	4-7 weeks

Note: WF = water flood, DD= depletion drive, swd= strong water drive, wwd= weak water drive: LA & KY = Louisiana and Kentucky

Most of those three tables show the previous successful projects that have effectuated CO_2 huff and puff injection in many fields. It shows the credibility of CO_2 injection to be applied and means that CO_2 has been an EOR method that applicable in the most field in the world with high increase of recovery after injection done.

This screening criteria reviews data 16 CO_2 huff and puff projects conducted in different wells in the Forest Reserve oilfield of Trinidad and Tobago for 20 years. It is concluded as one screening criteria and provides the facts about CO_2 huff and puff injection as shown three tables above. Specific interferences on conditions under which these projects succeeded in increasing oil production were generalized considering published results of similar projects elsewhere. By those tables, we can see the type of reservoir, which was successfully applied, and which one was not.

With variety of technical, operational and economic variable, a strong correlation or a definitive conclusion is difficult. However, by correlating various performance attributes with different parameters, certain inferences are drawn and tested which could be used to:

a. Determine if a candidate well could benefit from CO_2 huff and puff operations
b. Identify optimal design and operational configurations in specific situations, based on field experience and engineering considerations.

CO_2 huff and puff operations are essentially near wellbore stimulation techniques which can lead to increased oil recovery via removal of some productivity damage, reduced oil viscosity, increased dissolved gas content, oil swelling, and vaporization of lighter components of oil. In certain cases, they have also provided strategic information on injectivity and pressure communication with adjacent wells and helped attempts to demonstrate that by properly understanding relevant reservoir mechanisms, one can screen specific prospects.

3.4 Proposed Screening Process

- Proposed screening process based on SPE 100044, SPE 35385, and SPE 39234:

1. Define objectives – enhancing recovery from specific mechanism
2. Identify 'site-specific or time-specific' advantage (availability of CO_2 supplies at affordable costs, strong oil price) or disadvantages (high anticipated cost for the infrastructure).
3. Define method of CO_2 injection. Analyze it from fractured pressure reservoir. Pfrac>MMP can be either miscible or immiscible injection, Pfrac<MMP must be immiscible injection.

- In the above context, use screening criteria based on SPE 100044 with given reservoir properties.
- New ideas:
    1. Generate comparison between successful projects parameters and previous screening criteria to find possible new criteria (e.g. gravity<13 that is found successful) for CO_2 huff and puff injection.
    2. Define the correlation between *days of soak, number of cycle* and all parameters in the successful projects.

3.5 **Screening Result**

1. **Taber Meruap**

Table 3-7. Screening result for Langgak based on Taber Meruap

	Reservoir Characteristics					Score
	Oil Saturation	**Type of formation**	**Permeability (mD)**	**Depth (ft)**	**Temp (deg F)**	**Red =0 Yellow=1 Green =2**
Field Parameter Value	*30*	*High porosity (26%) high perm (500 mD)*	*500*	*1100-1300*	*136*	
Steam flooding	>40	High porosity and permeability sandstone	>200	<457.2	Not critical	6
In-situ combustion	>50	Sandstone with	>50	<1170	>140	5

		high porosity				
Gel treatment/polymer flooding	>50	Sandstone, carbonate	>10	<914.4	<194	6
Alkali surfactant polymer, alkali flooding, surfactant flooding	>35	Sandstone preferred	>10	<914.4	<194	6
CO2 flooding	>20	Sandstone, carbonate	Not critical if sufficient injection rate could be maintained	Appropriate to allow injection pressure > MMP, which increases with temperature	Appropriate to allow injection pressure > MMP, which increases with temperature	8

Hydrocarbon	>30	Sandstone, carbonate with few fractures	Not critical if uniform	>406.3	Temp can have significant effect on MMP	2
N2, flue gas	>40	Sandstone, carbonate with few fractures	Not critical	>610	Not critical	5

The table above shows comparison among all the EOR method based on Langgak field characteristics. The screening criteria above were obtained from the previous CO2 huff and puff injection before in Meruap which was successfully applied. The color shows its applicability in accordance with certain parameters. Green scores 2 and means that the Langgak field characteristic s aligned with the value attached in screening criteria. Yellow scores 1 and means that the parameter could be aligned but it depends on another parameter such as Minimum Miscibility Pressure (MMP) which highly depends on temperature. Red scores 0 because it is not included in the screening criteria established above and means utterly not recommended.

As shown above at the scoring table, CO2 flooding results the highest value with no reds on it compared to other EOR methods. Steam flooding, gel treatment, ASP, polymer flooding, surfactant flooding, alkali flooding, and also flue gas injection has two reds of depth and oil saturation. For in-situ combustion, it has two reds of oil saturation and temperature as well as yellow in depth. Lastly, hydrocarbon injection has two reds and two yellows which show that the EOR method is ill suited with Langgak field. Consequently, CO_2 flooding can be concluded as the best EOR method for Langgak Field as its score is the best without reds on it. Therefore, we can conclude that CO_2 flooding applicable for this field based on these screening criteria built in the previous CO_2 huff and puff injection.

2. SPE 35385

Table 3-8. Screening result for Langgak based on SPE 35385

Properties	EOR Method								
	Nitrogen and flue gas	Hydrocarbon	Carbon Dioxide	Immiscible Gases	Miscellar/polymer, ASP, and alkaline flooding	Polymer flooding	Combustion	Steam	Surface Mining
Oil API Gravity	> 35 Average 48	> 23 Average 41	> 22 Average 36	> 12	> 20 Average 35	> 15	> 10 Average 16	> 8 to 13.5 Average 13.5	7 to 11
Oil Viscosity (cp)	< 0.4 Average 0.2	< 3 Average 0.5	< 10 Average 1.5	< 600	< 35 Average 13	> 10, < 150	< 5000 Average 1200	< 200000 Average 4700	zero cold flow
Composition	High % C1-C7	High % C2-C7	High % C5-C12	Not critical	Light, intermediate Some organic acids for alkaline floods	Not critical	Some asphaltic components	Not critical	Not critical
Oil Saturation (%PV)	> 40 Average 75	D8:J17	> 20 Average 55	> 35 Average 70	> 35 Average 53	> 50 Average 80	> 50 Average 72	> 40 Average 66	>8% wt sand
Formation Type	Sandstone or Carbonate	Sandstone or Carbonate	Sandstone or Carbonate	Not critical	Sandstone Preferred	Sandstone Preferred	High porosity sandstone	High porosity sandstone	Mineable tar sand
Net Thickness (ft)	Thin unless dipping	Thin unless dipping	Wide range	Not critical if dipping and/or good vertical permeability	Not critical	Not critical	> 10 feet	> 20 feet	> 10 feet
Average Permeability (md)	Not critical	Not critical	Not critical	Not critical	> 10 md Average 450 md	> 10 md Average 800 md	> 50 md	> 200 md Average 2540 md	Not critical
Depth (ft)	> 6000	< 4000	> 2500	> 1800	< 9000 Average 3250	< 9000	< 11500 Average 3500	< 4500 Average 1500	< 3.1 overburden to sand ratio
Temperature (deg F)	Not critical	Not critical	Not critical	Not critical	< 200 Average 80	< 200 Average 140	> 100 Average 135	Not critical	Not critical
Score	11	14	16	16	18	17	15	16	-

A screening is conducted based on Langgak field's parameters that assigned to the screening criteria on the paper. Green, yellow, and red showing the compatibility from the most to the least, and the score for each color is 2,1,0 correspondingly. For further consideration, we will eliminate the EOR method that are less than 16, so that the EOR method that will be analyzed are CO_2 (16), Immiscible gases (16), micellar/polymer, ASP and alkaline flooding (18), polymer flooding (17), and steam (16).

ASP and alkaline flooding require many laboratory test and field experiments that will upheave the cost of the operation. That injection also needs a good mechanistic model which is very connected with the test and field experiments afterwards and mechanistic model depends on well spacing. ASP process is very sensitive to well spacing (Zhu et al., 2012) which in many cases causes failure such as slug breakdown or high chemical losses, occur beyond the distance reachable by tracers that costly as well. Accordingly, ASP flooding sometime cannot be strongly relied on.

Polymer flooding injection operation is very costly. For example, concentrated (~10%) broths of aqueous polymer (especially biopolymers), is more easily dissolved in the field, but is more costly per pound of polymer to transport to the field (Petrowiki). Polymer flooding will not pass the economic evaluation on Langgak field, so we will leave out the polymer flooding option.

Steam is one of the thermal EOR methods. Steam flooding is the most commonly used in heavy-oil reservoirs having high viscosity, so it is not compatible with Langgak Field. Moreover, in Indonesia average reservoir temperature is high even more than water boiling point which means steam flooding cannot be used efficiently in Indonesia.

That leaves us with CO_2 and immiscible gases. Indonesia having high temperature of reservoir as the volcanoes in Indonesia are among the most active of the Pacific Ring of Fire. For CO_2 miscible injection, it requires to meet a Minimum Miscibility Pressure (MMP). High temperature of reservoir in Indonesia cause the MMP of CO_2 injection is very high, even exceeding the fracture pressure of reservoir. Thus, the miscible injection of CO_2 is not feasible to conduct since it will break the formation. So, the most feasible EOR method to conduct in Langgak Field is CO_2 immiscible gases, with the injection pressure below MMP, as well as below its fracture pressure.

3. SPE 39234

Table 3-9. Screening result for Langgak Based on SPE 39234 (Taber Revisited Part 2)

Properties	EOR Method							
	Nitrogen and flue gas	Hydrocarbon	Carbon Dioxide	Immiscible Gasses	Miscellar/polymer, ASP, and alkaline flooding	Polymer flooding	Combustion	Steam
Oil API Gravity	> 35 Average 48 CP: 38 to 54	> 23 Average 41 CP: 24 to 54	> 22 Average 36 CP: 27 to 44	> 12	> 20 Average 35	> 15 CP: 14 to 43	> 10 Average 16 CP: 10 to 40	> 8 to 13.5 Average 13.5 CP: 8 to 27
Oil Viscosity (cp)	< 0.4 Average 0.2 CP: 0.07 to 0.3	< 3 Average 0.5 CP: 0.04 to 2.3	< 10 Average 1.5 CP: 0.3 to 6	< 600	< 35 Average 13	> 10, < 150 CP: 1 to 80	< 5000 Average 1200 CP: 6 to 5000	< 200000 Average 4700 CP: 10 to 137000
Composition	High % C1-C7	High % C2-C7	High % C5-C12	Not critical	Light, intermediate Some organic acids for alkaline floods	Not critical	Some asphaltic components	Not critical
Oil Saturation (%PV)	> 40 Average 75 CP: 59 to 80	> 30 Average 80 CP: 30 to 98	> 20 Average 55 CP: 15 to 70	> 35 Average 70	> 35 Average 53	> 50 Average 80 CP: 50 to 92	> 50 Average 72 CP: 62 to 94	> 40 Average 66 CP: 35 to 90
Formation Type	Sandstone or Carbonate	Sandstone or Carbonate	Sandstone or Carbonate	Not critical	Sandstone Preferred	Sandstone Preferred	High porosity sandstone	High porosity sandstone
Net Thickness (ft)	Thin unless dipping	Thin unless dipping	Wide range	Not critical if dipping	Not critical	Not critical	> 10 feet	> 20 feet
Average Permeability (md)	Not critical	Not critical	Not critical	Not critical	> 10 md Average 450 md	> 10 md Average 800 md CP: 10 to 15000	> 50 md CP: 85 to 4000	> 200 md CP: 150 to 4500
Depth (ft)	> 6000 CP: 10000 to 18500	< 4000 CP: 4040 to 15900	Appropriate to allow injection pressure > MMP, which increase with temperature	> 1800	< 9000	< 9000 CP: 1300 to 9600	< 11500 Average 3500 CP: 400 to 11300	< 5000 150 to 4500
Temperature (deg F)	Not critical	Not critical	Not critical	Not critical	< 200	< 200 CP: 80 to 185	> 100	Not critical CP: 60 to 280
Score	11	12	16	16	18	17	15	16

In this study, in order to select the most appropriate EOR method for applying in our case study, table scoring was used. Therefore, the values of most critical parameters such as API degree, depth, oil viscosity and saturation, formation type, reservoir thickness, composition, reservoir temperature and rock permeability have been matched to the table. The results show that the most appropriate method for implementation in the reservoir is micellar/polymer, alkaline/surfactant/polymer (ASP), alkaline flooding; because this reservoir has high API degree, light oil, low depth and, etc.

Table III-9 summarized the results of the quick screening. This Table shows that the polymer methods are placed on the second rank in terms of accuracy with 17 points. The accuracy of CO2 flooding, immiscible, and steam flooding method are 16 points, and this method can be used in the reservoir after micellar/polymer, ASP, and alkaline flooding; and polymer flooding methods according to its screening criteria. Moreover, the accuracy of in-situ combustion is reported 15 points, respectively. Also, the quick screening indicated that the gas injection methods including nitrogen and hydrocarbon flooding are not strongly recommended for applying in the reservoir due to being contradictory of their criteria with the reservoir condition.

ASP flooding and alkaline flooding emerge as the highest score for this screening. However, the screening criteria for the ASP and alkaline flooding process have noticeably changed over the last decade due to improvements in application and chemical technology. At the beginning in late 1990, several ASP field projects were also conducted in the United States in smaller fields in the Minnelusa formation. It is conducted as secondary recovery process in the early stages of waterflood so that the amount of true incremental recovery by ASP over that of waterflood remains questionable. Finally, ambiguity of whether the incremental oil recovered was due to sweep improvement by the use ASP or other process. This application lacks analysis and the significance and true contribution of the additional surfactants in this test is not clear.

Also, even if polymer flooding has the best score, we have to consider a lot of things that related to this screening. As an example, there was a polymer injection in Tambaredjo field in Suriname. The pilot had three injectors and nine offset producers. The produced oil viscosity ranged from 1260 to 3057 mPa-s with an average of 1728 mPa-s with high permeability. The nine production wells produced 10-60% of the injected polymer concentration. Oil rates in producer were increased while the water cuts were decreased. However, the responses from polymer injection were modest because perhaps there was a near wellbore fracture formed. Moreover, the dissolved oxygen was ambient (3-8ppm).

Also, there must have been issues that polymer injection forms such as:

1. A small range of injection pressure may occur, along with less liquid production at the initial stage of polymer injection (when water cut is still increasing).
2. Poor connectivity between oil strata, poor injectivity, large decreases in liquid production, and large pressure differences may occur in production wells when water cut decreases or is stable. High flow pressures may occur within production wells, as well as unresponsive wells at the corners or edges of patterns.
3. Differences exist between producers or the polymer volume injected and the change in water cut. This leads to asymmetry responses in oil production well, and to rapid water cut increases for some oil wells.
4. Differences in polymer volume injected may occur if injection is switched back to water at different times.

Three aspects may be responsible for the above issues, besides the heterogeneity and well pattern. First, oil saturation before polymer injection may be low in the low permeability layer due to serious interference between layers. Second, water intake profile reversal may occur during polymer injection. Sweep may be poor within thick high permeability. Third, large well-to-well variations in water cut may occur at the late stage of polymer flooding. Refer to Langgak field, it may occur since the permeability is high and thickness is wide enough.

Other than that, we have to see the facilities and economic evaluation itself. CO_2 has been a type of gas that easily to find and cheap to buy instead of polymer and another chemical compound to be injected in certain reservoir. Therefore, it is not always going to be as smooth as the screening result.

Based on the James J. Sheng's book (EOR Field Cases), the EOR is highly depending on oil prices. In the low oil prices, polymer flooding and other chemical injection hardly achieve economic condition with bigger benefit. Accordingly, CO_2 flooding can be an efficient way to conquer that problem as well as results high recovery since it has already been proved by the successful projects that have been mentioned before in the previous sections.

4. SPE 100044

Table 3-10. Langgak Oil Properties

API Gravity	30.8
Oil Viscosity (cp)	14
Porosity (%)	26
Thickness(ft)	200
Depth (ft)	1100-1300
Temperature (deg F)	136
Permeability (mD)	500

Based on the value of Langgak's oil properties above, screening based on the criteria from SPE 10044 is conducted to ensure as if SPE 10044 is considered to be a valid screening standard so that CO_2 huff and puff injection could be done in Langgak Field. The screening criteria from SPE 10044 are as follow:

Table 3-11. SPE 100044 CO2 huff and puff injection screening criteria

Parameters of Successful Reservoirs	Light Oils	Medium Oils	Heavy Oils
Oil Viscosity (cp)	0.4 to 8	32 to 46	415 to 3000
Oil Gravity (°API)	23 to 38	17 to 23	11 to 14
Porosity (%)	13 to 32	25 to 32	12 to 32
Depth (feet)	1200 to 12870	2600 to 4200	1150 to 4125
Thickness (feet)	6 to 60	36 to 220	200
Permeability (mD)	10 to 3000	150 to 388	250 to 350

Previously it is stated that Langgak Oil is categorized as light oil through various From the incision above, the screening criteria from SPE 10044 is proving that Langgak oil has the criteria for CO_2 huff and puff injection and is categorized to light oil based on most of the value of its parameters such as oil gravity, porosity, depth, and permeability which belongs to light oil criteria based on SPE 10044. There are 2 parameters which is slightly deviated, the thickness which is 200 feet belongs to the heavy oil criteria, while the viscosity which is 14 cp doesn't belong to any type neither light, medium, or heavy oil itself, but overall screening using SPE 10044 criteria is proving that CO_2 huff and puff injection is very potential to be conducted in Langgak field.

CHAPTER IV
LABORATORY WORK: OIL SWELLING

4.1 Introduction

Swelling is one of the main mechanism that is expected on the CO_2 immiscible flooding process. After we inject CO_2 into the reservoir, we could get more volume of oil and its density is become less (more mobile) and its volume also increased. Swelling factor measures the ratio between volume of oil after CO_2 was injected at certain mole percent and volume of oil before the injection happened.

Swelling ratio is a good means to know how effective CO2 flooding is in improving the recovery. Swelling ratio is the ratio between volumes of crude oil at given pressure to its initial volume at atmospheric condition. Tsau et al. (2010) mentioned the ability of CO_2 to extract hydrocarbon from crude oil depends on its density. The swelling ratio indicate how well CO_2 can increase the volume of crude oil and help mobilize it to the surface. The amount of swelling is dependent on the pressure, temperature, composition, and physical properties of the solvent and the reservoir fluid.

Swelling ratio is one of the parameters that is important in CO2 flooding preparation. It is the ratio of the oil at a given pressure to its initial volume at atmospheric condition. Swelling ratio will increase with increasing pressure at constant temperature and decrease with increasing temperature under constant pressure. It is related to the solubility of CO_2 into the crude oil. If temperature is increased, the solubility of CO_2 will decrease, hence it affects the swelling factor. Swelling ratio can be measured by using Swelling Experiment with a PVT Cell or using a simulation model to generate the PVT of crude oil after being injected with CO_2 at various pressure, temperature, and CO_2 concentration.

Simon and Graue (1964) made a correlation of swelling factor based on mole fraction of CO_2 injected and molecular weight of crude oil as shown in Figure IV-1 below.

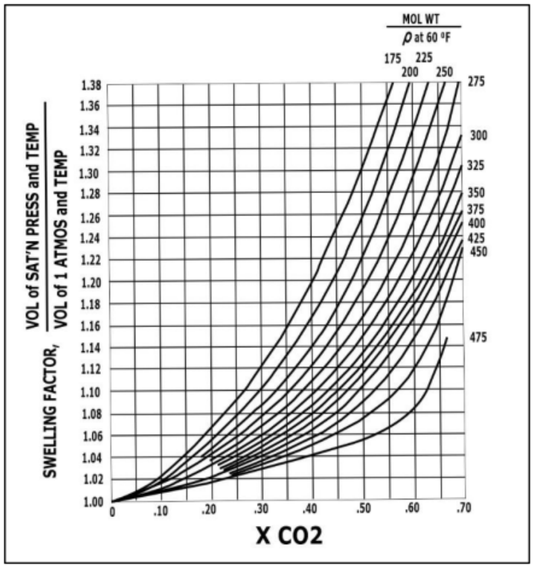

Figure 4-1. Swelling Factor vs Mol Fraction of CO_2

4.2 CO_2 Solubility

The solubility of a substance is the amount of that substance that will dissolve in a given amount of solvent. In this CO_2 Flooding case, CO_2 will be dissolve into water and oil phase. CO_2 solubility in oil can be determined by several ways. One of them is by using the nomograph as shown in Figure IV-2 below. From the Figure IV-2, it can be known that CO_2 solubility is depend on the saturation pressure, temperature, and oil gravity.

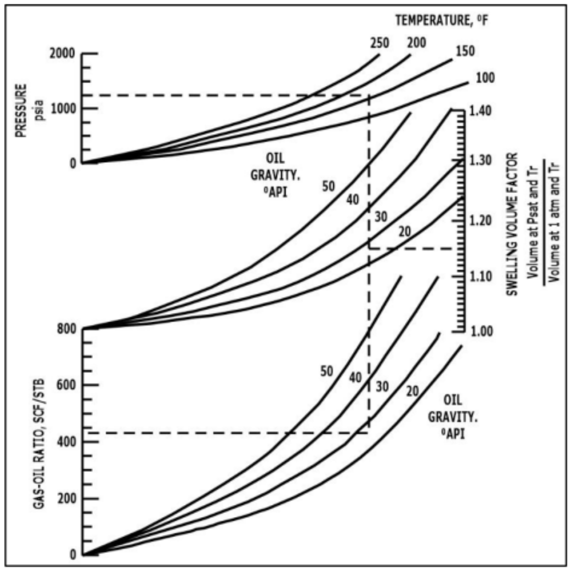

Figure 4-2. CO_2 solubility and swelling on dead oil

Simon and Graue (1964) mentioned that CO_2 solubility is also depend on the oil characterization factor or UOP K factor. They produced an equation to predict the CO_2 solubility based on different temperature, pressure (also CO_2 fugacity) and also oil characterization factor. Characterization factor is used for characterizing crude oils and components. And also it is useful because they remain constant for chemically similar hydrocarbons. K factor of 12.5 or greater indicates a hydrocarbon compound predominantly paraffinic in nature. Lower values of this factor indicate hydrocarbons with more naphthenic or aromatic components. Characterization factor can be calculated using the following equation:

$K_w = \frac{T_b^{1/3}}{\gamma_o}$, with Kw is Watson characterization factor, $^oR^{1/3}$; γ_o is oil specific gravity; and Tb is mean average boiling point temperature, ^oR.

Table 4-1. Watson Characterization Factors for Selected Compounds

Series	Compound	Formula	Boiling Point Temperature (°R)	Molecular Weight	Specific Gravity	Watson Characterization Factor
Paraffins	n-Hexane	C_6H_{14}	615.4	86.178	0.6640	12.8
	2-Methylpentane	C_6H_{14}	600.1	86.178	0.6579	12.8
	n-Heptane	C_7H_{16}	668.8	100.205	0.6882	12.7
Naphthenes	Cyclohexane	C_6H_{12}	637.0	84.162	0.7834	11.0
	Methylcyclohexane	C_7H_{14}	673.4	98.189	0.7740	11.3
Aromatics	Benzene	C_6H_6	635.8	78.114	0.8844	9.7
	Toluene	C_7H_8	690.8	92.141	0.8718	10.1

The results of the solubility study conducted by Simon and Graue are shown in Figure IV-3, IV-4, and IV-5 below.

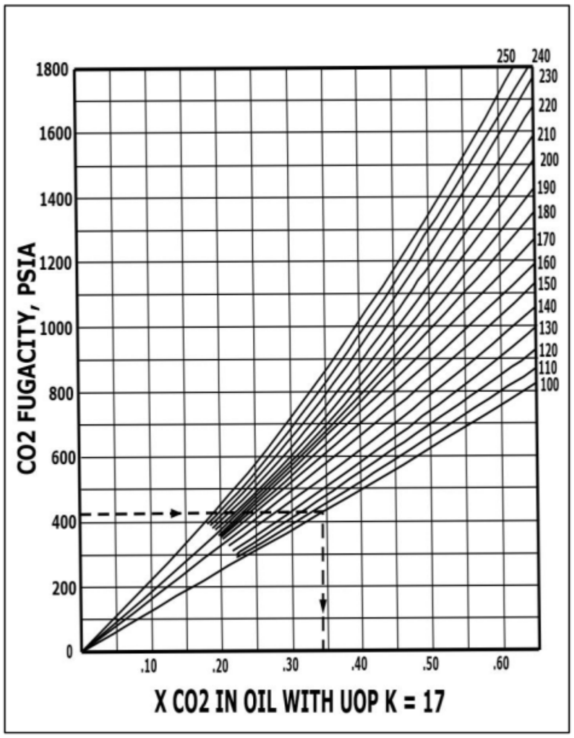

Figure 4-3. CO_2 solubility vs T and CO_2 Fugacity

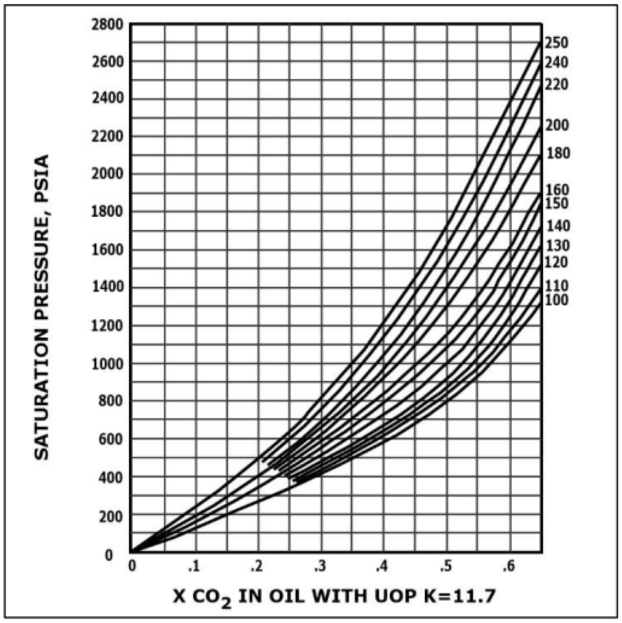

Figure 4-4. CO_2 Solubility vs T and Pressure

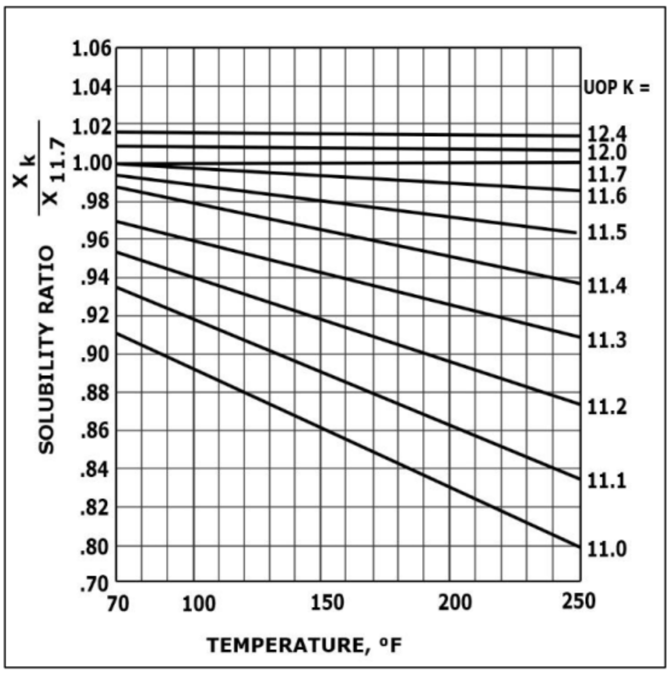

Figure 4-5 . CO2 Solubility vs T and Pressure

4.3 Swelling Experiment

4.3.1 Previous Experiment

Because swelling effect is important to be known before doing CO_2 project, there were a lot of researchers which already studied the effect of swelling of crude oil during CO2 injection. Ali Abedini (2014) provide the swelling experiment schematic diagram which can be seen at Figure IV-6.

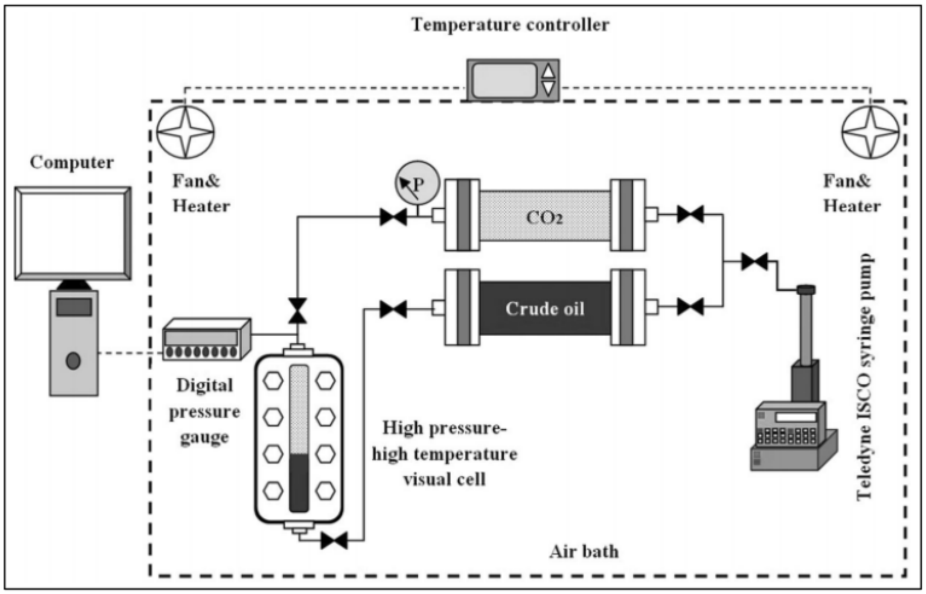

Figure 4-6. Swelling Experiment Schematic Diagram (Ali Abedini, 2014)

In the experiment, he used crude oil from Bakken oil field in South Saskatchewan, Canada, with density and viscosity of the oil are 802 kg/m^3 and 2.92 mPa s, respectively. The apparatus mainly consisted of a see through windowed high pressure cell, a magnetic stirrer, and a high-pressure CO_2 cylinder. To control the experimental temperature and maintain the temperature at a constant value, a temperature controller as also used. The function of magnetic stirrer was to create a consistent turbulence inside the cell. It will significantly accelerated the CO_2 dissolution into the oil by creating convective mass transfer. During the process, the pressure inside the windowed cell was measured and recorded using digital pressure gauge. Once the visual cell was pressurized with CO_2 to a pre-specified pressure (Pi), the pressure of the cell was allowed to stabilize while CO_2 was dissolving into the crude oil. The test was terminated when the final CO_2 pressure (Pf) inside the cell reached a stable value and no further pressure decay was observed. It was considered as an equilibrium pressure (Peq) of the system. Lastly, initial and final CO_2 volume in visual cell were determined by taking photos and utilizing image analysis technique.

Throughout this study, the solubility of CO_2 in the oil (xCO_2) was defined as the ratio of the total mass of dissolved CO_2 in 100 gr of the original crude oil sample and was calculated using the mass balance equations as given by the following relationships:

$$m_{CO_2,dissolved} = m_{CO_2,i} - m_{CO_2,f}$$

$$= \left(\frac{P_i V_{CO_2,i} MW_{CO_2}}{Z_i RT}\right) - \left(\frac{P_f V_{CO_2,f} MW_{CO_2}}{Z_f RT}\right)$$

$$= \frac{MW_{CO_2}}{RT}\left[\left(\frac{P_i V_{CO_2,i}}{Z_i}\right) - \left(\frac{P_f V_{CO_2,f}}{Z_f}\right)\right] \quad (1)$$

$$m_{oil} = (\rho_{oil} V_{oil}) \quad (2)$$

$$\chi_{CO_2} = \frac{m_{CO_2,dissolved}}{m_{oil}} \times 100$$

$$= \frac{MW_{CO_2}}{\rho_{oil} V_{oil} RT}\left[\left(\frac{P_i V_{CO_2,i}}{Z_i}\right) - \left(\frac{P_f V_{CO_2,f}}{Z_f}\right)\right] \quad (3)$$

4.3.2 Swelling Experiment Equipment

a. *Pressure Cell*

The pressure cell used in swelling test is composed of cylindrical metal with the cylindrical sapphire inside. The cylindrical sapphire used to make the observation easier and also it can hold the pressure until 5,000 psi. The pressure cell can be seen at Figure IV-7.

Figure 4-7. Pressure cell for swelling experiment

b. Magnetic Stirrer

To agitate the crude oil during the experiment, magnetic stirrer was needed. The magnetic stirrer can be seen at Figure IV-8.

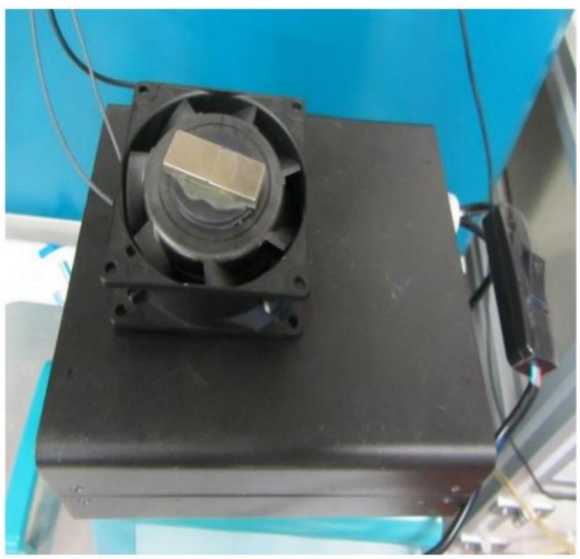

Figure 4-8. Magnetic Stirrer

c. Temperature Controller

The temperature controller was used to control the temperature of the experiment set up. The temperature that was controlled by using this device is 58°C. The temperature controller can be seen at Figure IV-9.

Figure 4-9. Temperature Controller

d. CO_2 Pressure Bomb

The CO_2 that was used is 99.99% pure CO_2 that was contained in pressure bomb which has initial pressure around 900 psi. The CO_2 pressure bomb then was connected with the ISCO pump 260D model. The pressure bomb can be seen at Figure IV-10.

Figure 4-10. CO_2 pressure bomb

e. ISCO Pump 260D

ISCO pump is a piston-driven model pump that can give displacement to the fluid using constant flow or constant pressure mode. For CO2 injection, specialized ISCO pump (260D Syringe pump) was used because it was specifically for refilling under high pressure to handle supercritical fluids. The ISCO pump can be seen at Figure 11.

Figure 4-11. ISCO pump 260D

f. Pump Controller

The pump controller was used for controlling the 260D ISCO pump. We can set the rate for constant pressure mode, or the pressure for the constant rate mode of the ISCO pump. Pump controller can be seen at Figure 12.

Figure 4-12. Pump controller

g. Cooling Water Bath

Cooling water bath from Lab. Compression was used to easily compress CO_2 gas in ISCO pump to reach high pressure. The temperature of the water bath was set up at 4°C. The cooling water bath can be seen at Figure IV-13.

Figure 4-13. Cooling water bath

4.3.3 Swelling Experiment Procedure

Procedure of swelling experiment is:

- Do pressure leak test on the swelling cell before doing the experiment.
- Set the swelling apparatus in the box / oven with pressure and temperature controllable environment (for safety cause).
- Pasang dan atur peralatan eksperimen swelling ke dalam oven.
- Put the crude oil into the pressure cell, with minimum crude oil volume injected was 3 ml.
- After that, tighten all the connection and fittings that connecting the pressure cell and also the ISCO pump (CO_2 inlet).
- Control the sample temperature reach reservoir temperature (58^{o}C).
- Inject CO_2 by considering the density of CO_2 that were injected at certain pressure and temperature using constant pressure mode in the ISCO pump.
- To control volume of CO2 injected, control the valve in ISCO pump.

- Set pressure starts with low pressure and step by step increases the pressure until it reaches desired pressure.
- Measure the difference of the height of the oil column for each set pressure and the height of the initial oil column before it was injected by CO2 (atmospheric condition).
- Calculate the Swelling Factor when the equilibrium time was reached.

4.3.4 Swelling Calculation/Determination Method

The swelling factor can be determined by measuring the initial volume of oil injected and the volume of oil after injected by CO_2. The swelling ratio (swelling factor) is defined as the volume of oil after it was injected by CO_2 divided by initial oil volume in the pressure cell before injection of CO_2.

4.3.5 Swelling Experiment Result

Swelling experiments have been conducted at reservoir temperature 58°C where swelling is measured under various CO_2 injection pressure conditions. Swelling experiments have been performed with CO_2 injection pressures up to 3300 psi. Oil volume change is observed every 1 hour. The observation data of Langgak oil swelling experiment is shown below:

Table 4-2. Observation data of swelling experiment at 300 psi

Date	Pressure, psi	Observation Time, hrs	Initial Height, cm	Final Height, cm	Isco Pump Vol. Initial, cc	Isco Pump Vol. Final, cc	S. F.	Percentage
16-Apr-18	300	1	2.20	2.13	222.55	198.56	0.97	-3.18%
		2	2.20	2.14	198.56	195.65	0.97	-2.73%
		3	2.20	2.15	195.65	193.16	0.98	-2.27%
		4	2.20	2.16	193.16	190.65	0.98	-1.82%
		5	2.20	2.16	190.65	187.70	0.98	-1.82%
		6	2.20	2.16	187.70	185.33	0.98	-1.82%
		7	2.20	2.16	185.33		0.98	-1.82%
		8	2.20	2.17		179.31	0.99	-1.36%
		9	2.20	2.17	179.31	176.27	0.99	-1.36%
		10	2.20	2.17	176.27		0.99	-1.36%
		11	2.20	2.18			0.99	-0.91%
		12	2.20	2.18			0.99	-0.91%
		13	2.20	2.19			1.00	-0.45%
		14	2.20	2.19			1.00	-0.45%
		15	2.20	2.20			1.00	0.00%
		16	2.20	2.20			1.00	0.00%
		17	2.20	2.20			1.00	0.00%
		18	2.20	2.20			1.00	0.00%
		19	2.20	2.20			1.00	0.00%
		20	2.20	2.20			1.00	0.00%
		21	2.20	2.20		142.44	1.00	0.00%
		22	2.20	2.21	142.44	140.70	1.00	0.45%
		23	2.20	2.21	140.70	138.23	1.00	0.45%
		24	2.20	2.21	138.23	136.02	1.00	0.45%

tidak teramati

Table 4-3. Observation data of swelling experiment at 400 psi

Date	Pressure, psi	Observation Time, hrs	Initial Height, cm	Final Height, cm	Isco Pump Vol. Initial, cc	Isco Pump Vol. Final, cc	S. F.	Percentage
13-Apr-18	400	1	2.14	2.08	198.75	175.17	0.97	-2.80%
		2	2.14	2.09	175.17	171.61	0.98	-2.34%
		3	2.14	2.10	171.61		0.98	-1.87%
		4	2.14	2.11		164.50	0.99	-1.40%
		5	2.14	2.11	164.50	161.40	0.99	-1.40%
		6	2.14	2.12	161.40	158.01	0.99	-0.93%
		7	2.14	2.13	158.01	154.80	1.00	-0.47%
		8	2.14	2.14	154.80	151.79	1.00	0.00%
		9	2.14	2.14	151.79		1.00	0.00%
		10	2.14	2.14			1.00	0.00%
		11	2.14	2.15			1.00	0.47%
		12	2.14	2.15			1.00	0.47%
		13	2.14	2.15			1.00	0.47%
		14	2.14	2.15			1.00	0.47%
		15	2.14	2.15			1.00	0.47%
		16	2.14	2.16			1.01	0.93%
		17	2.14	2.16			1.01	0.93%
		18	2.14	2.17		117.54	1.01	1.40%
		19	2.14	2.17	117.54	114.01	1.01	1.40%
		20	2.14	2.17	114.01	110.87	1.01	1.40%
		21	2.14	2.18	110.87		1.02	1.87%
		22	2.14	2.18		104.14	1.02	1.87%
		23	2.14	2.18	104.14	100.87	1.02	1.87%
		24	2.14	2.18	100.87	97.63	1.02	1.87%

tidak teramati

Table 4-4. Observation data of swelling experiment at 500 psi

Date	Pressure, psi	Observation Time, hrs	Initial Height, cm	Final Height, cm	Isco Pump Vol. Initial, cc	Isco Pump Vol. Final, cc	S. F.	Percentage
12-Apr-18	500	1	2.22	2.18	113.30	89.03	0.98	-1.80%
		2	2.22	2.20	89.03	85.34	0.99	-0.90%
		3	2.22	2.20	85.34	82.42	0.99	-0.90%
		4	2.22	2.21	82.42	79.06	1.00	-0.45%
		5	2.22	2.23	79.06	75.85	1.00	0.45%
		6	2.22	2.24	75.85	72.24	1.01	0.90%
		7	2.22	2.24	72.24	68.64	1.01	0.90%
		8	2.22	2.25	68.64		1.01	1.35%
		9	2.22	2.25		61.66	1.01	1.35%
		10	2.22	2.25	61.66	57.99	1.01	1.35%
		11	2.22	2.26	57.99		1.02	1.80%
		12	2.22	2.26			1.02	1.80%
		13	2.22	2.27			1.02	2.25%
		14	2.22	2.27			1.02	2.25%
		15	2.22	2.28			1.03	2.70%
		16	2.22	2.28			1.03	2.70%
		17	2.22	2.28			1.03	2.70%
		18	2.22	2.29			1.03	3.15%
		19	2.22	2.29			1.03	3.15%
		20	2.22	2.29			1.03	3.15%
		21	2.22	2.29			1.03	3.15%
		22	2.22	2.29		13.88	1.03	3.15%
		23	2.22	2.30	13.88	10.24	1.04	3.60%
		24	2.22	2.30	10.24	6.64	1.04	3.60%

tidak teramati

Table 4-5. Observation data of swelling experiment at 600 psi

Date	Pressure, psi	Observation Time, hrs	Initial Height, cm	Final Height, cm	Isco Pump Vol. Initial, cc	Isco Pump Vol. Final, cc	S. F.	Percentage
10-Apr-18	600	1	2.20	2.16	178.11	173.85	0.98	-1.82%
		2	2.20	2.19	173.85	173.93	1.00	-0.45%
		3	2.20	2.20	173.93	173.31	1.00	0.00%
		4	2.20	2.22	173.31		1.01	0.91%
		5	2.20	2.23		171.74	1.01	1.36%
		6	2.20	2.24	171.74	170.46	1.02	1.82%
		7	2.20	2.25	170.46	169.33	1.02	2.27%
		8	2.20	2.25	169.33		1.02	2.27%
		9	2.20	2.26			1.03	2.73%
		10	2.20	2.26			1.03	2.73%
		11	2.20	2.26			1.03	2.73%
		12	2.20	2.26			1.03	2.73%
		13	2.20	2.26			1.03	2.73%
		14	2.20	2.27			1.03	3.18%
		15	2.20	2.27			1.03	3.18%
		16	2.20	2.27			1.03	3.18%
		17	2.20	2.27		162.99	1.03	3.18%
		18	2.20	2.28	162.99	162.78	1.04	3.64%
		19	2.20	2.28	162.78	161.89	1.04	3.64%
		20	2.20	2.28	161.89	161.45	1.04	3.64%
		21	2.20	2.29	161.45	160.92	1.04	4.09%
		22	2.20	2.29	160.92	160.34	1.04	4.09%
		23	2.20	2.29	160.34	159.73	1.04	4.09%
		24	2.20	2.29	159.73	158.81	1.04	4.09%

tidak teramati

Table 4-6. Observation data of swelling experiment at 700 psi

Date	Pressure, psi	Observation Time, hrs	Initial Height, cm	Final Height, cm	Isco Pump Vol. Initial, cc	Isco Pump Vol. Final, cc	S. F.	Percentage
9-Apr-18	700	1	2.10	2.07	184.35	180.11	0.99	-1.43%
		2	2.10	2.09	180.11	179.57	1.00	-0.48%
		3	2.10	2.12	179.57	179.12	1.01	0.95%
		4	2.10	2.14	179.12	178.60	1.02	1.90%
		5	2.10	2.15	178.60	178.19	1.02	2.38%
		6	2.10	2.17	178.19	177.89	1.03	3.33%
		7	2.10	2.17	177.89	177.19	1.03	3.33%
		8	2.10	2.18	177.19	176.49	1.04	3.81%
		9	2.10	2.19	176.49		1.04	4.29%
		10	2.10	2.19		174.92	1.04	4.29%
		11	2.10	2.19	174.92	174.26	1.04	4.29%
		12	2.10	2.19	174.26		1.04	4.29%
		13	2.10	2.20			1.05	4.76%
		14	2.10	2.20			1.05	4.76%
		15	2.10	2.20			1.05	4.76%
		16	2.10	2.20			1.05	4.76%
		17	2.10	2.20			1.05	4.76%
		18	2.10	2.20			1.05	4.76%
		19	2.10	2.20			1.05	4.76%
		20	2.10	2.21			1.05	5.24%
		21	2.10	2.21			1.05	5.24%
		22	2.10	2.21		165.28	1.05	5.24%
		23	2.10	2.21	165.28	164.49	1.05	5.24%
		24	2.10	2.21	164.49	164.34	1.05	5.24%

tidak teramati

Table 4-7. Observation data of swelling experiment at 800 psi

Date	Pressure, psi	Observation Time, hrs	Initial Height, cm	Final Height, cm	Isco Pump Vol. Initial, cc	Isco Pump Vol. Final, cc	S. F.	Percentage
24-Apr-18	800	1	2.21	2.15	195.88	189.85	0.97	-2.71%
		2	2.21	2.19	189.85	189.98	0.99	-0.90%
		3	2.21	2.21	189.98	189.90	1.00	0.00%
		4	2.21	2.23	189.90	189.55	1.01	0.90%
		5	2.21	2.24	189.55	188.98	1.01	1.36%
		6	2.21	2.25	188.98		1.02	1.81%
		7	2.21	2.27			1.03	2.71%
		8	2.21	2.28			1.03	3.17%
		9	2.21	2.29			1.04	3.62%
		10	2.21	2.29			1.04	3.62%
		11	2.21	2.30			1.04	4.07%
		12	2.21	2.30			1.04	4.07%
		13	2.21	2.30			1.04	4.07%
		14	2.21	2.30			1.04	4.07%
		15	2.21	2.30		182.24	1.04	4.07%
		16	2.21	2.30	182.24	181.73	1.04	4.07%
		17	2.21	2.31	181.73	181.22	1.05	4.52%
		18	2.21	2.31	181.22	180.77	1.05	4.52%
		19	2.21	2.31	180.77		1.05	4.52%
		20	2.21	2.32		179.69	1.05	4.98%
		21	2.21	2.32	179.69	179.18	1.05	4.98%
		22	2.21	2.33	179.18	178.54	1.05	5.43%
		23	2.21	2.33	178.54	177.93	1.05	5.43%
		24	2.21	2.33	177.93		1.05	5.43%

tidak teramati

Table 4-8. Observation data of swelling experiment at 900 psi

Date	Pressure, psi	Observation Time, hrs	Initial Height, cm	Final Height, cm	Isco Pump Vol. Initial, cc	Isco Pump Vol. Final, cc	S. F.	Percentage
17-Apr-18	900	1	2.19	2.14	209.45	201.92	0.98	-2.28%
		2	2.19	2.17	201.92	200.64	0.99	-0.91%
		3	2.19	2.20	200.64	199.58	1.00	0.46%
		4	2.19	2.21	199.58	198.65	1.01	0.91%
		5	2.19	2.23	198.65	197.78	1.02	1.83%
		6	2.19	2.25	197.78	196.91	1.03	2.74%
		7	2.19	2.25	196.91	195.97	1.03	2.74%
		8	2.19	2.27	195.97		1.04	3.65%
		9	2.19	2.28			1.04	4.11%
		10	2.19	2.28			1.04	4.11%
		11	2.19	2.29			1.05	4.57%
		12	2.19	2.29			1.05	4.57%
		13	2.19	2.30			1.05	5.02%
		14	2.19	2.30			1.05	5.02%
		15	2.19	2.30			1.05	5.02%
		16	2.19	2.30			1.05	5.02%
		17	2.19	2.30		186.94	1.05	5.02%
		18	2.19	2.31	186.94	185.79	1.05	5.48%
		19	2.19	2.31	185.79	186.27	1.05	5.48%
		20	2.19	2.31	186.27	185.72	1.05	5.48%
		21	2.19	2.32	185.72	184.78	1.06	5.94%
		22	2.19	2.32	184.78	183.55	1.06	5.94%
		23	2.19	2.32	183.55	182.38	1.06	5.94%
		24	2.19	2.32	182.38	181.20	1.06	5.94%

tidak teramati

Table 4-9. Observation data of swelling experiment at 1000 psi

Date	Pressure, psi	Observation Time, hrs	Initial Height, cm	Final Height, cm	Isco Pump Vol. Initial, cc	Isco Pump Vol. Final, cc	S. F.	Percentage
27-Apr-18	1000	1	2.30	2.23	172.66	162.85	0.97	-3.04%
		2	2.30	2.29	162.85		1.00	-0.43%
		3	2.30	2.31			1.00	0.43%
		4	2.30	2.33		159.25	1.01	1.30%
		5	2.30	2.36	159.25	158.27	1.03	2.61%
		6	2.30	2.38	158.27		1.03	3.48%
		7	2.30	2.39			1.04	3.91%
		8	2.30	2.39			1.04	3.91%
		9	2.30	2.40			1.04	4.35%
		10	2.30	2.40			1.04	4.35%
		11	2.30	2.41			1.05	4.78%
		12	2.30	2.42			1.05	5.22%
		13	2.30	2.43			1.06	5.65%
		14	2.30	2.43			1.06	5.65%
		15	2.30	2.43			1.06	5.65%
		16	2.30	2.43		149.77	1.06	5.65%
		17	2.30	2.44	149.77	148.63	1.06	6.09%
		18	2.30	2.44	148.63	144.88	1.06	6.09%
		19	2.30	2.45	144.88		1.07	6.52%
		20	2.30	2.45			1.07	6.52%
		21	2.30	2.45			1.07	6.52%
		22	2.30	2.45		141.89	1.07	6.52%
		23	2.30	2.45	141.89	141.73	1.07	6.52%
		24	2.30	2.45	141.73	143.56	1.07	6.52%

tidak teramati

Table 4-10. Observation data of swelling experiment at 1100 psi

Date	Pressure, psi	Observation Time, hrs	Initial Height, cm	Final Height, cm	Isco Pump Vol. Initial, cc	Isco Pump Vol. Final, cc	S. F.	Percentage
26-Apr-18	1100	1	2.00	1.94	218.22	201.83	0.97	-3.00%
		2	2.00	2.01	201.83	200.65	1.01	0.50%
		3	2.00	2.03	200.65		1.02	1.50%
		4	2.00	2.05		199.00	1.03	2.50%
		5	2.00	2.07	199.00	197.25	1.04	3.50%
		6	2.00	2.09	197.25	195.91	1.05	4.50%
		7	2.00	2.10	195.91	195.39	1.05	5.00%
		8	2.00	2.11	195.39	194.61	1.06	5.50%
		9	2.00	2.11	194.61		1.06	5.50%
		10	2.00	2.12		192.11	1.06	6.00%
		11	2.00	2.12	192.11	191.17	1.06	6.00%
		12	2.00	2.12	191.17	190.17	1.06	6.00%
		13	2.00	2.13	190.17		1.07	6.50%
		14	2.00	2.14			1.07	7.00%
		15	2.00	2.14			1.07	7.00%
		16	2.00	2.14			1.07	7.00%
		17	2.00	2.15			1.08	7.50%
		18	2.00	2.15			1.08	7.50%
		19	2.00	2.15			1.08	7.50%
		20	2.00	2.16			1.08	8.00%
		21	2.00	2.16			1.08	8.00%
		22	2.00	2.16			1.08	8.00%
		23	2.00	2.16			1.08	8.00%
		24	2.00	2.16		178.91	1.08	8.00%

tidak teramati

Table 4-11. Observation data of swelling experiment at 1300 psi

Date	Pressure, psi	Observation Time, hrs	Initial Height, cm	Final Height, cm	Isco Pump Vol. Initial, cc	Isco Pump Vol. Final, cc	S. F.	Percentage
2-May-18	1300	1	2.24	2.21	243.36	226.29	0.99	-1.34%
		2	2.24	2.26	226.29	224.33	1.01	0.89%
		3	2.24	2.31	224.33		1.03	3.12%
		4	2.24	2.33		222.84	1.04	4.02%
		5	2.24	2.34	222.84	221.50	1.04	4.46%
		6	2.24	2.37	221.50	218.89	1.06	5.80%
		7	2.24	2.39	218.89		1.07	6.70%
		8	2.24	2.40			1.07	7.14%
		9	2.24	2.41			1.08	7.59%
		10	2.24	2.41			1.08	7.59%
		11	2.24	2.41			1.08	7.59%
		12	2.24	2.42			1.08	8.04%
		13	2.24	2.44			1.09	8.93%
		14	2.24	2.44			1.09	8.93%
		15	2.24	2.45			1.09	9.38%
		16	2.24	2.45			1.09	9.38%
		17	2.24	2.46			1.10	9.82%
		18	2.24	2.46			1.10	9.82%
		19	2.24	2.46			1.10	9.82%
		20	2.24	2.46		203.73	1.10	9.82%
		21	2.24	2.47	203.73	202.58	1.10	10.27%
		22	2.24	2.47	202.58	302.38	1.10	10.27%
		23	2.24	2.47	302.38	200.05	1.10	10.27%
		24	2.24	2.47	200.05	199.51	1.10	10.27%

tidak teramati

Table 4-12. Observation data of swelling experiment at 1600 psi

Date	Pressure, psi	Observation Time, hrs	Initial Height, cm	Final Height, cm	Isco Pump Vol. Initial, cc	Isco Pump Vol. Final, cc	S. F.	Percentage
3-May-18	1600	1	2.31	2.27	182.70	161.44	0.98	-1.73%
		2	2.31	2.36	161.44	159.48	1.02	2.16%
		3	2.31	2.41	159.48	157.54	1.04	4.33%
		4	2.31	2.44	157.54		1.06	5.63%
		5	2.31	2.46			1.06	6.49%
		6	2.31	2.49		152.07	1.08	7.79%
		7	2.31	2.50	152.07	150.16	1.08	8.23%
		8	2.31	2.52	150.16	147.99	1.09	9.09%
		9	2.31	2.52	147.99	145.79	1.09	9.09%
		10	2.31	2.53	145.79	144.13	1.10	9.52%
		11	2.31	2.54	144.13	142.24	1.10	9.96%
		12	2.31	2.55	142.24	140.30	1.10	10.39%
		13	2.31	2.56	140.30	138.51	1.11	10.82%
		14	2.31	2.56	138.51		1.11	10.82%
		15	2.31	2.57			1.11	11.26%
		16	2.31	2.57			1.11	11.26%
		17	2.31	2.58			1.12	11.69%
		18	2.31	2.58			1.12	11.69%
		19	2.31	2.59			1.12	12.12%
		20	2.31	2.60			1.13	12.55%
		21	2.31	2.60			1.13	12.55%
		22	2.31	2.60			1.13	12.55%
		23	2.31	2.60			1.13	12.55%
		24	2.31	2.60		117.60	1.13	12.55%

tidak teramati

Table 4-13. Observation data of swelling experiment at 1900 psi

Date	Pressure, psi	Observation Time, hrs	Initial Height, cm	Final Height, cm	Isco Pump Vol. Initial, cc	Isco Pump Vol. Final, cc	S. F.	Percentage
4-May-18	1900	1	1.90	1.85	214.80	190.76	0.97	-2.63%
		2	1.90	1.92	190.76	187.41	1.01	1.05%
		3	1.90	2.01	187.41	184.72	1.06	5.79%
		4	1.90	2.02	184.72	181.58	1.06	6.32%
		5	1.90	2.05	181.58	178.62	1.08	7.89%
		6	1.90	2.07	178.62	175.16	1.09	8.95%
		7	1.90	2.09	175.16	171.94	1.10	10.00%
		8	1.90	2.11	171.94		1.11	11.05%
		9	1.90	2.12			1.12	11.58%
		10	1.90	2.12			1.12	11.58%
		11	1.90	2.12			1.12	11.58%
		12	1.90	2.13			1.12	12.11%
		13	1.90	2.14			1.13	12.63%
		14	1.90	2.15			1.13	13.16%
		15	1.90	2.15			1.13	13.16%
		16	1.90	2.15			1.13	13.16%
		17	1.90	2.15			1.13	13.16%
		18	1.90	2.17			1.14	14.21%
		19	1.90	2.17			1.14	14.21%
		20	1.90	2.17			1.14	14.21%
		21	1.90	2.18			1.15	14.74%
		22	1.90	2.18			1.15	14.74%
		23	1.90	2.18			1.15	14.74%
		24	1.90	2.18			1.15	14.74%

tidak teramati

Table 4-14. Observation data of swelling experiment at 2000 psi

Date	Pressure, psi	Observation Time, hrs	Initial Height, cm	Final Height, cm	Isco Pump Vol. Initial, cc	Isco Pump Vol. Final, cc	S. F.	Percentage
2-Jun-18	2000	1	2.07		135.03			
		2	2.07					
		3	2.07	2.39		82.39	1.15	15.46%
		4	2.07	2.44	82.39		1.18	17.87%
		5	2.07	2.46			1.19	18.84%
		6	2.07	2.47			1.19	19.32%
		7	2.07	2.47			1.19	19.32%
		8	2.07	2.48			1.20	19.81%
		9	2.07	2.48			1.20	19.81%
		10	2.07	2.50			1.21	20.77%
		11	2.07	2.52			1.22	21.74%
		12	2.07	2.52			1.22	21.74%
		13	2.07	2.52			1.22	21.74%
		14	2.07	2.52			1.22	21.74%
		15	2.07	2.53			1.22	22.22%
		16	2.07	2.53			1.22	22.22%
		17	2.07	2.55			1.23	23.19%
		18	2.07	2.55			1.23	23.19%
		19	2.07	2.56			1.24	23.67%
		20	2.07	2.56			1.24	23.67%
		21	2.07	2.56			1.24	23.67%
		22	2.07	2.56			1.24	23.67%
		23	2.07	2.56		46.05	1.24	23.67%
		24	2.07	2.56	46.05	44.12	1.24	23.67%

tidak teramati

Table 4-15. Observation data of swelling experiment at 2200 psi

Date	Pressure, psi	Observation Time, hrs	Initial Height, cm	Final Height, cm	Isco Pump Vol. Initial, cc	Isco Pump Vol. Final, cc	S. F.	Percentage
23-May-18	2200	1	1.99	2.34	202.35	177.31	1.18	17.59%
		2	1.99	2.34	177.31	173.49	1.18	17.59%
		3	1.99	2.36	173.49		1.19	18.59%
		4	1.99	2.40			1.21	20.60%
		5	1.99	2.41			1.21	21.11%
		6	1.99	2.44			1.23	22.61%
		7	1.99	2.44			1.23	22.61%
		8	1.99	2.45			1.23	23.12%
		9	1.99	2.45			1.23	23.12%
		10	1.99	2.45			1.23	23.12%
		11	1.99	2.45			1.23	23.12%
		12	1.99	2.45			1.23	23.12%
		13	1.99	2.45			1.23	23.12%
		14	1.99	2.45			1.23	23.12%
		15	1.99	2.45			1.23	23.12%
		16	1.99	2.45			1.23	23.12%
		17	1.99	2.45			1.23	23.12%
		18	1.99	2.46			1.24	23.62%
		19	1.99	2.46		110.81	1.24	23.62%
		20	1.99	2.46	110.81	107.01	1.24	23.62%
		21	1.99	2.46	107.01	103.76	1.24	23.62%
		22	1.99	2.46	103.76	100.16	1.24	23.62%
		23	1.99	2.46	100.16	96.17	1.24	23.62%
		24	1.99	2.46	96.17	92.42	1.24	23.62%

tidak teramati

Table 4-16. Observation data of swelling experiment at 2400 psi

Date	Pressure, psi	Observation Time, hrs	Initial Height, cm	Final Height, cm	Isco Pump Vol. Initial, cc	Isco Pump Vol. Final, cc	S. F.	Percentage
4-Jun-18	2400	1	1.83	2.06	233.71	209.46	1.13	12.57%
		2	1.83	2.18	209.46	207.17	1.19	19.13%
		3	1.83	2.20	207.17	204.86	1.20	20.22%
		4	1.83	2.22	204.86		1.21	21.31%
		5	1.83	2.24			1.22	22.40%
		6	1.83	2.24			1.22	22.40%
		7	1.83	2.24			1.22	22.40%
		8	1.83	2.24			1.22	22.40%
		9	1.83	2.24			1.22	22.40%
		10	1.83	2.24			1.22	22.40%
		11	1.83	2.25			1.23	22.95%
		12	1.83	2.25			1.23	22.95%
		13	1.83	2.25			1.23	22.95%
		14	1.83	2.25			1.23	22.95%
		15	1.83	2.25			1.23	22.95%
		16	1.83	2.25			1.23	22.95%
		17	1.83	2.25			1.23	22.95%
		18	1.83	2.25			1.23	22.95%
		19	1.83	2.25			1.23	22.95%
		20	1.83	2.25		167.24	1.23	22.95%
		21	1.83	2.25	167.24	164.77	1.23	22.95%
		22	1.83	2.25	164.77	162.34	1.23	22.95%
		23	1.83	2.25	162.34	160.05	1.23	22.95%
		24	1.83	2.25	160.05	157.98	1.23	22.95%

tidak teramati

Table 4-17. Observation data of swelling experiment at 2600 psi

Date	Pressure, psi	Observation Time, hrs	Initial Height, cm	Final Height, cm	Isco Pump Vol. Initial, cc	Isco Pump Vol. Final, cc	S. F.	Percentage
9-May-18	2600	1	1.80	2.00	240.13		1.11	11.11%
		2	1.80	2.10			1.17	16.67%
		3	1.80	2.14			1.19	18.89%
		4	1.80	2.18		200.53	1.21	21.11%
		5	1.80	2.19	200.53	196.64	1.22	21.67%
		6	1.80	2.19	196.64	192.09	1.22	21.67%
		7	1.80	2.19	192.09		1.22	21.67%
		8	1.80	2.19			1.22	21.67%
		9	1.80	2.19			1.22	21.67%
		10	1.80	2.19			1.22	21.67%
		11	1.80	2.19			1.22	21.67%
		12	1.80	2.19			1.22	21.67%
		13	1.80	2.19			1.22	21.67%
		14	1.80	2.19			1.22	21.67%
		15	1.80	2.19			1.22	21.67%
		16	1.80	2.19		151.42	1.22	21.67%
		17	1.80	2.19	151.42	146.85	1.22	21.67%
		18	1.80	2.19	146.85	142.71	1.22	21.67%
		19	1.80	2.19	142.71	139.03	1.22	21.67%
		20	1.80	2.19	139.03	135.04	1.22	21.67%
		21	1.80	2.19	135.04	130.77	1.22	21.67%
		22	1.80	2.19	130.77		1.22	21.67%
		23	1.80	2.19		122.47	1.22	21.67%
		24	1.80	2.19	122.47	118.31	1.22	21.67%

tidak teramati

Table 4-18. Observation data of swelling experiment at 3000 psi

Date	Pressure, psi	Observation Time, hrs	Initial Height, cm	Final Height, cm	Isco Pump Vol. Initial, cc	Isco Pump Vol. Final, cc	S. F.	Percentage
11-May-18	3000	1	2.23	2.50	229.73	201.06	1.12	12.11%
		2	2.23		201.06	196.51		
		3	2.23		196.51			
		4	2.23					
		5	2.23					
		6	2.23			176.46		
		7	2.23		176.46	171.53		
		8	2.23		171.53	166.64		
		9	2.23		166.64			
		10	2.23					
		11	2.23					
		12	2.23					
		13	2.23					
		14	2.23					
		15	2.23					
		16	2.23					
		17	2.23					
		18	2.23					
		19	2.23					
		20	2.23	2.72		107.92	1.22	21.97%
		21	2.23	2.72	107.92	103.38	1.22	21.97%
		22	2.23	2.72	103.38	98.65	1.22	21.97%
		23	2.23	2.72	98.65	93.97	1.22	21.97%
		24	2.23	2.72	93.97	89.28	1.22	21.97%

tidak teramati

Table 4-19. Observation data of swelling experiment at 3300 psi

Date	Pressure, psi	Observation Time, hrs	Initial Height, cm	Final Height, cm	Isco Pump Vol. Initial, cc	Isco Pump Vol. Final, cc	S. F.	Percentage
25-May-18	3300	1	2.28	2.55	218.05		1.12	11.84%
		2	2.28	2.72		176.62	1.19	19.30%
		3	2.28	2.75	176.62	169.72	1.21	20.61%
		4	2.28	2.79	169.72		1.22	22.37%
		5	2.28	2.83			1.24	24.12%
		6	2.28	2.83			1.24	24.12%
		7	2.28	2.83			1.24	24.12%
		8	2.28	2.83			1.24	24.12%
		9	2.28	2.83			1.24	24.12%
		10	2.28	2.84			1.25	24.56%
		11	2.28	2.84			1.25	24.56%
		12	2.28	2.84			1.25	24.56%
		13	2.28	2.84			1.25	24.56%
		14	2.28	2.84			1.25	24.56%
		15	2.28	2.82			1.24	23.68%
		16	2.28	2.79			1.22	22.37%
		17	2.28	2.76			1.21	21.05%
		18	2.28	2.76			1.21	21.05%
		19	2.28	2.74			1.20	20.18%
		20	2.28	2.74		67.25	1.20	20.18%
		21	2.28	2.73	67.25	60.97	1.20	19.74%
		22	2.28	2.69	60.97	54.76	1.18	17.98%
		23	2.28	2.67	54.76	48.42	1.17	17.11%
		24	2.28	2.65	48.42	41.93	1.16	16.23%

tidak teramati

Then calculate the swelling factor and the percentage based on the observation data. Percentage is percentage of changing oil volume. Percentage can be determined with equation below:

$$Percentage = \frac{finale\ volume - initial\ volume}{initial\ volume} \times 100\%$$

After that, plot the swelling factor and percentage with observation time for each CO_2 injection pressure.

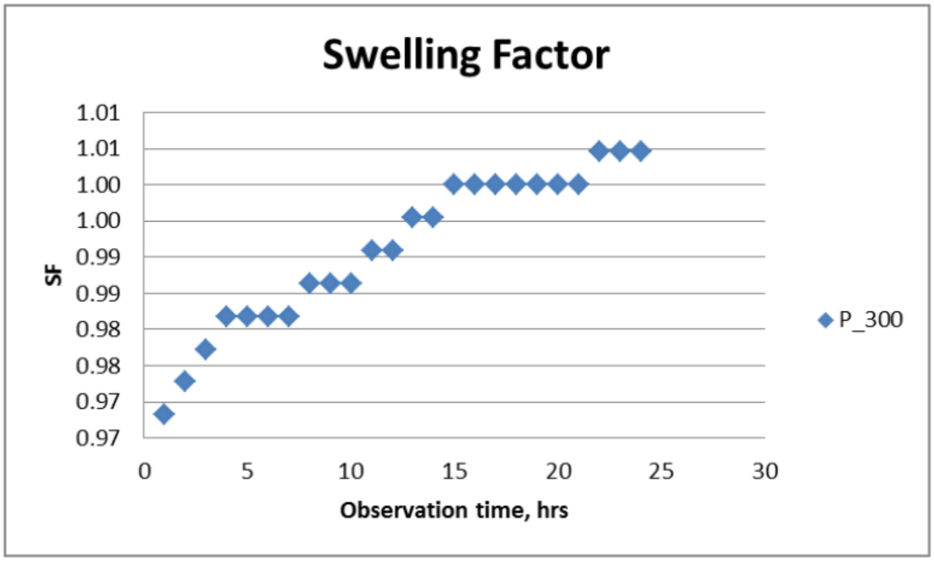

Figure 4-14. Swelling factor vs. observation time at 300 psi

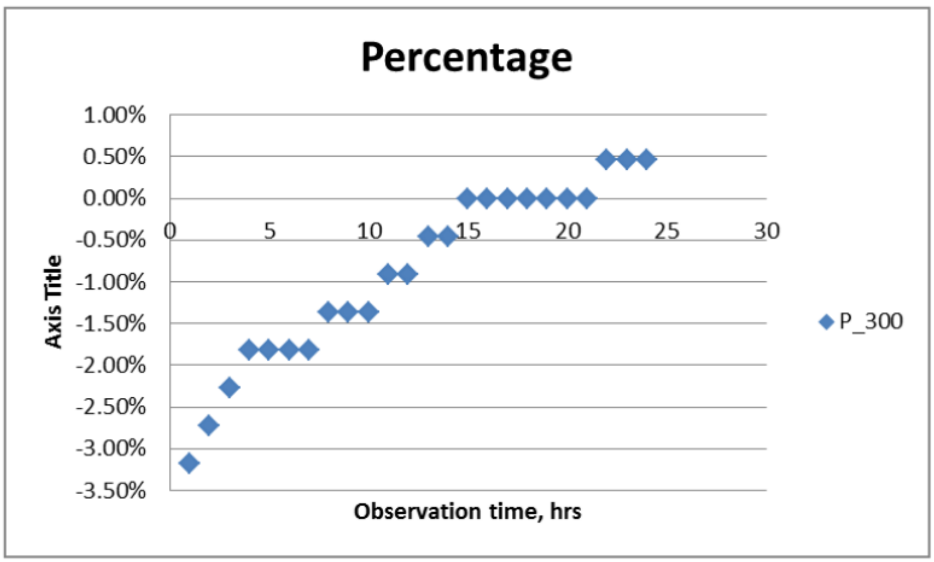

Figure 4-15. Percentage vs. observation time at 300 psi

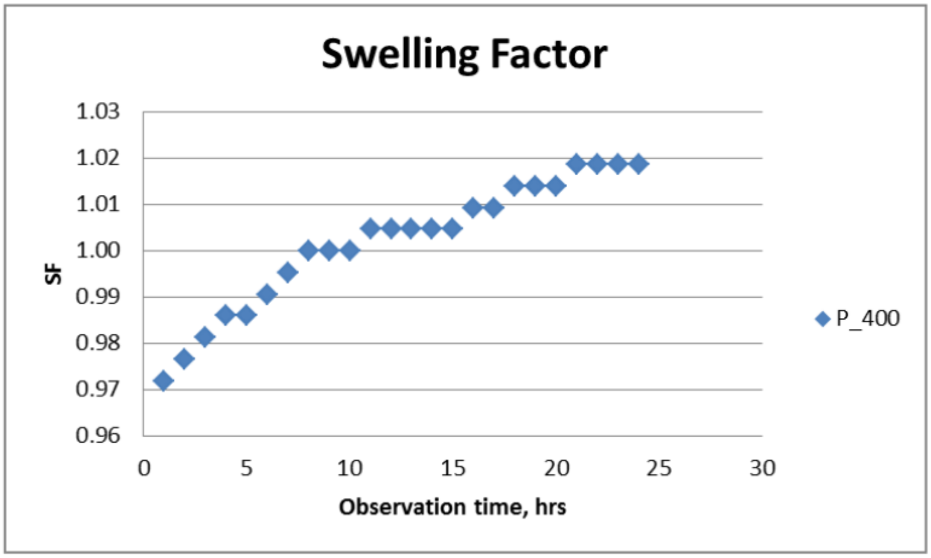

Figure 4-16. Swelling factor vs. observation time at 400 psi

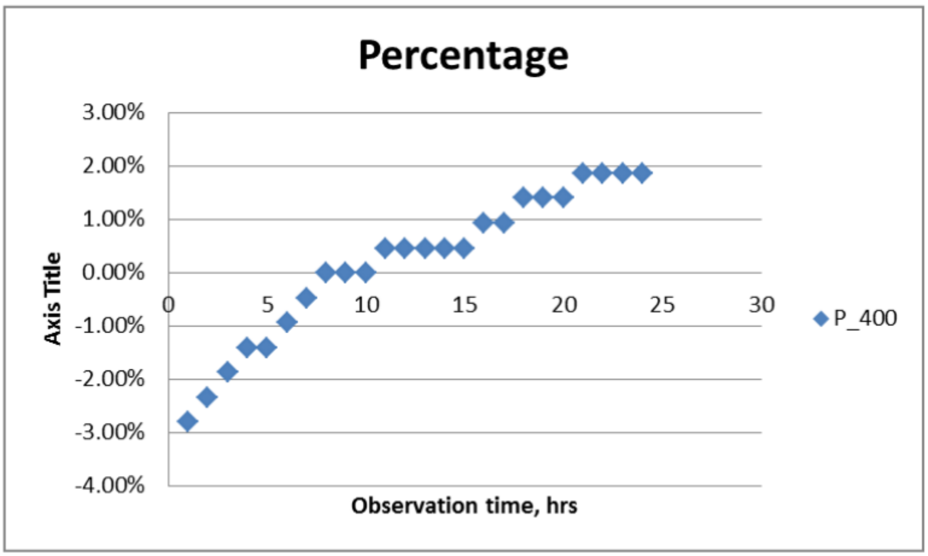

Figure 4-17. Percentage vs. observation time at 400 psi

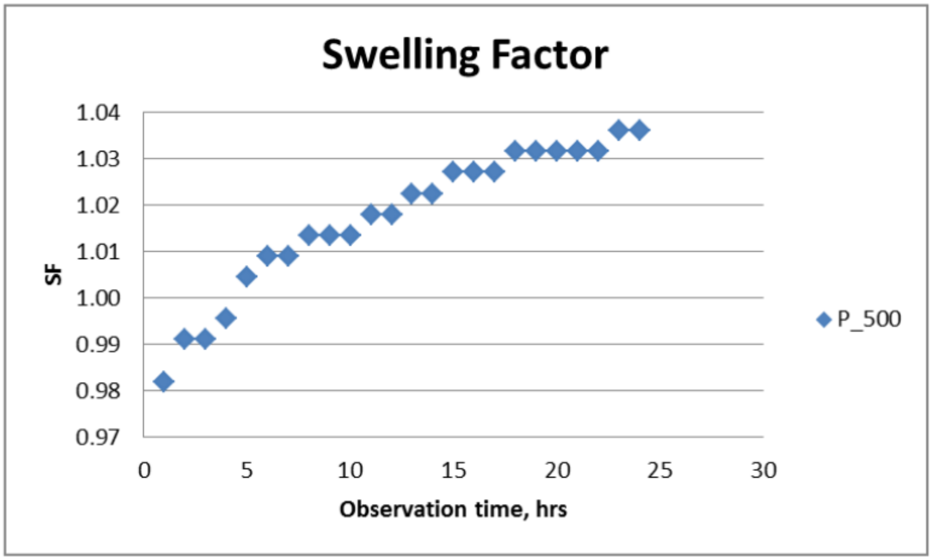

Figure 4-18. Swelling factor vs. observation time at 500 psi

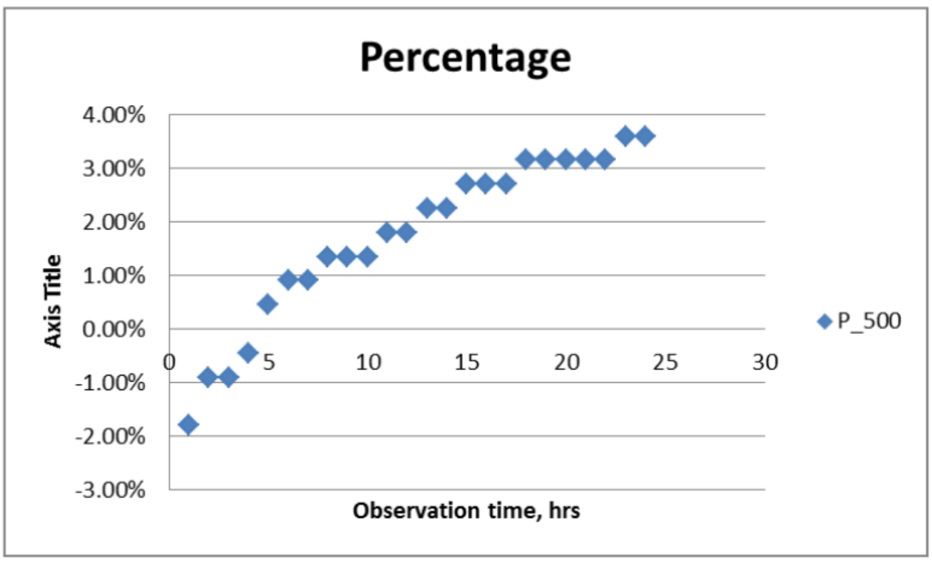

Figure 4-19. Percentage vs. observation time at 500 psi

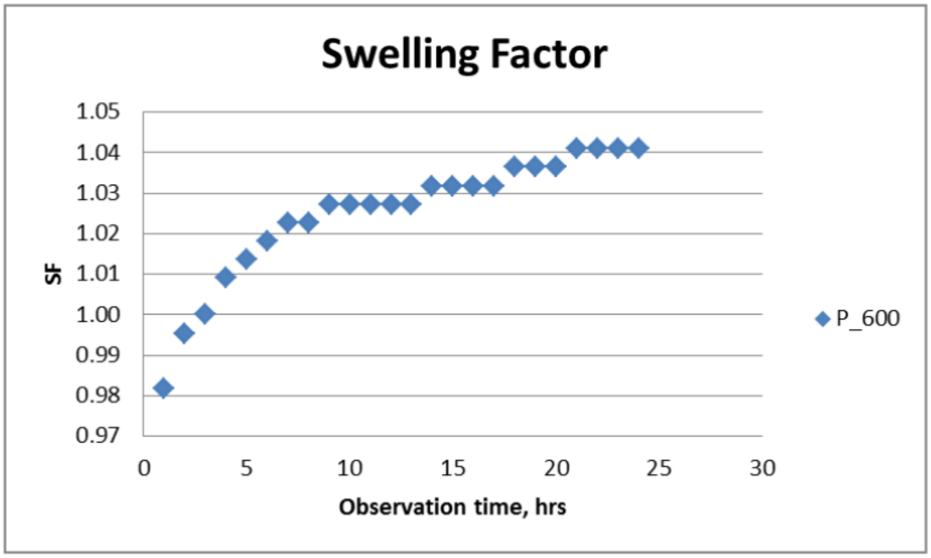

Figure 4-20. Swelling factor vs. observation time at 600 psi

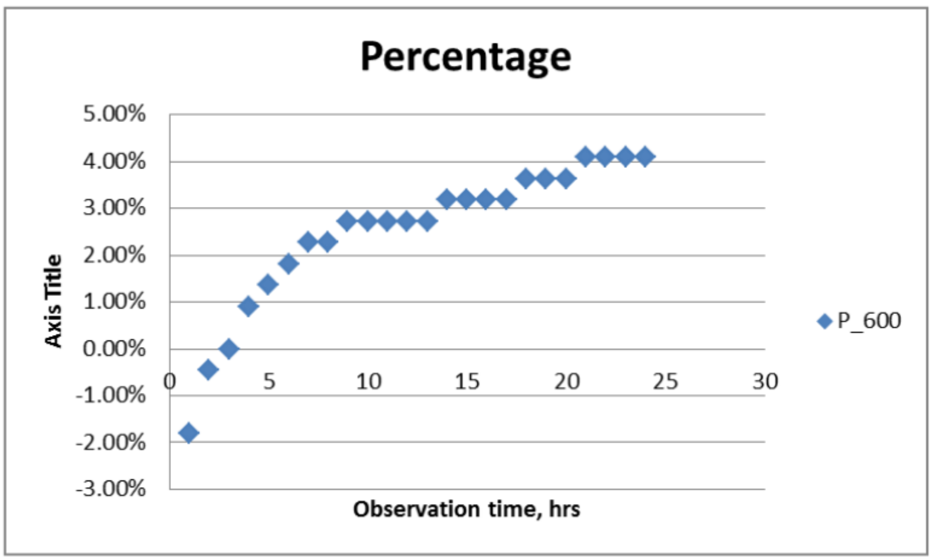

Figure 4-21. Percentage vs. observation time at 600 psi

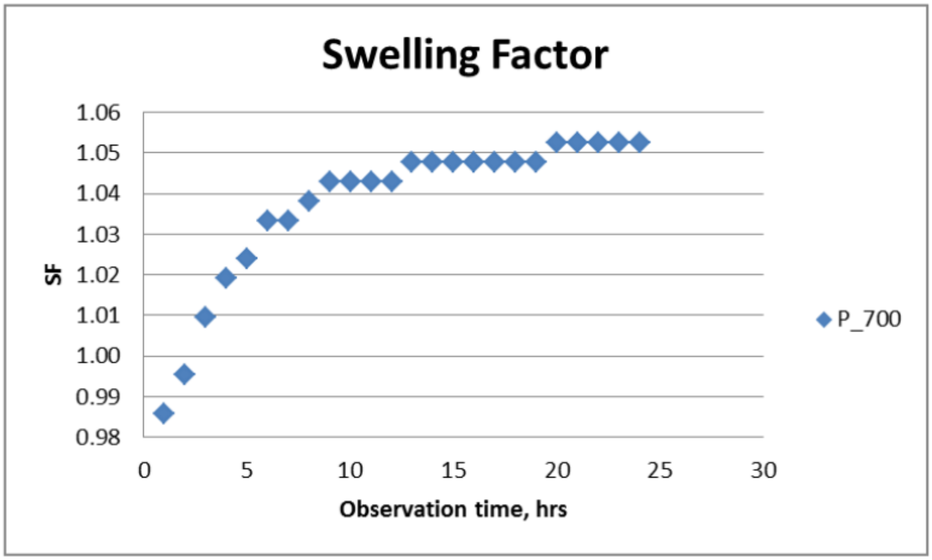

Figure 4-22. Swelling factor vs. observation time at 700 psi

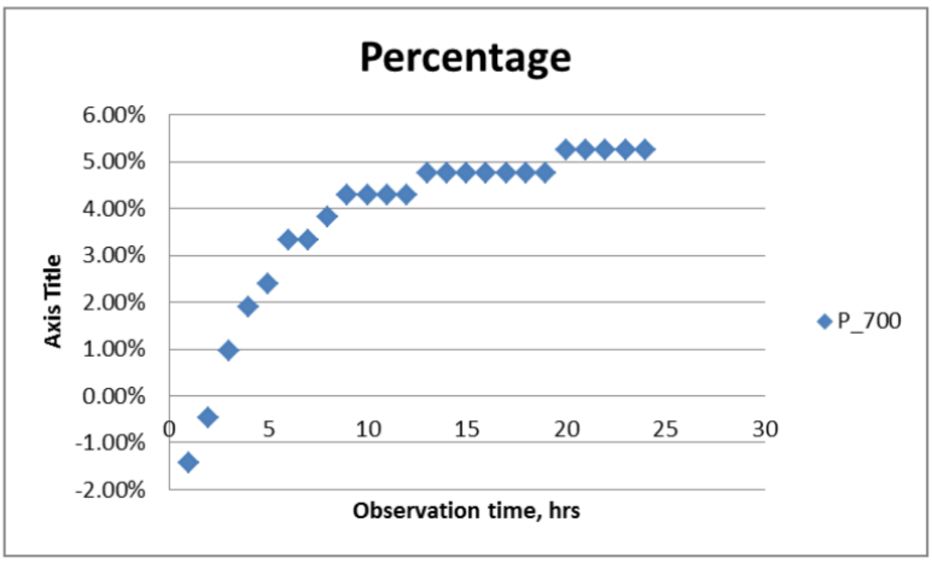

Figure 4-23. Percentage vs. observation time at 700 psi

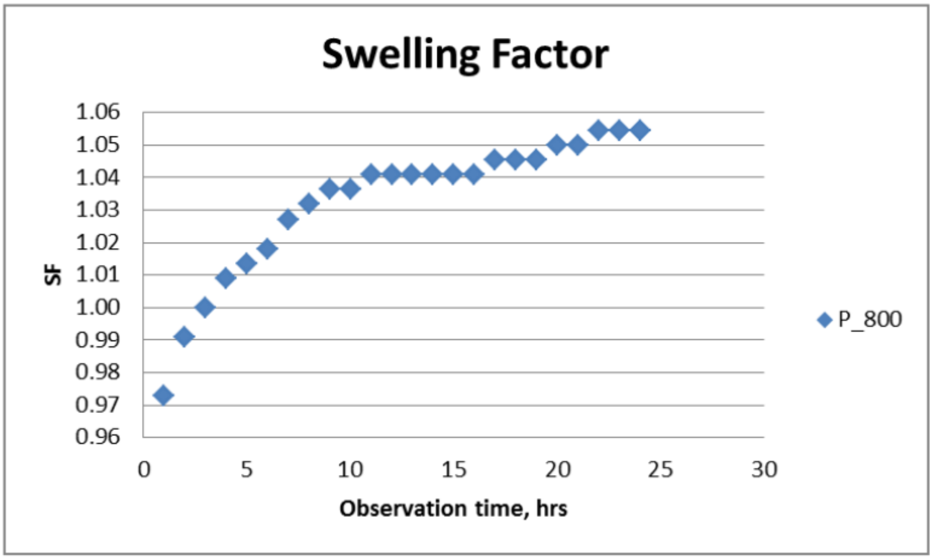

Figure 4-24. Swelling factor vs. observation time at 800 psi

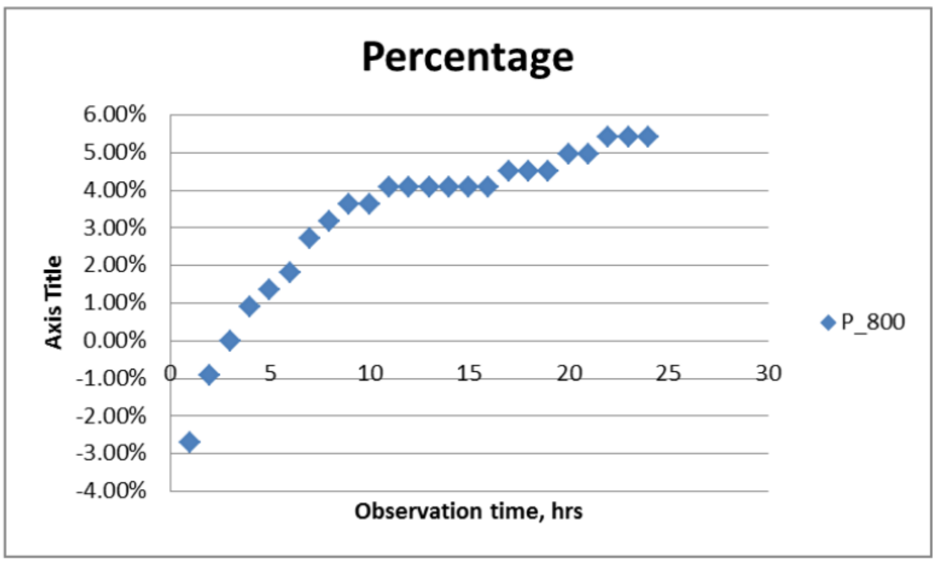

Figure 4-25. Percentage vs. observation time at 800 psi

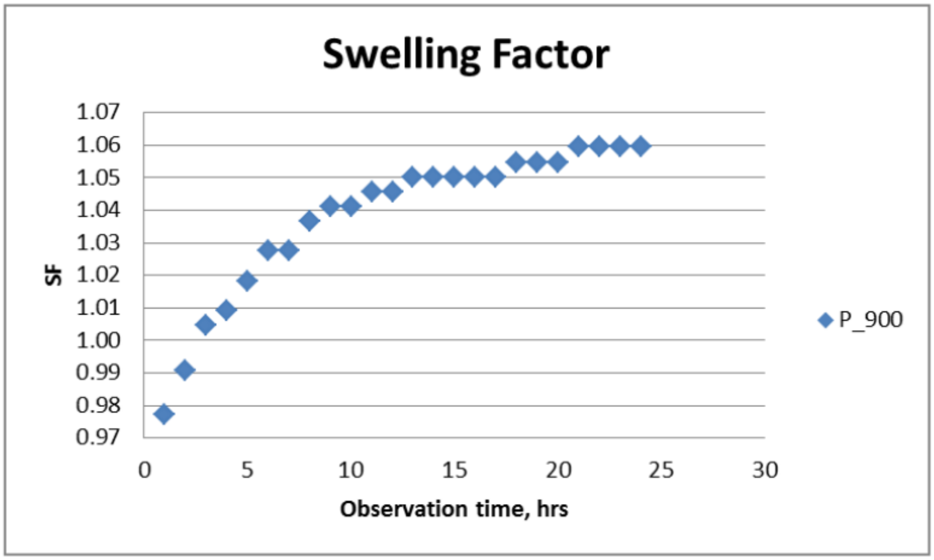

Figure 4-26. Swelling factor vs. observation time at 900 psi

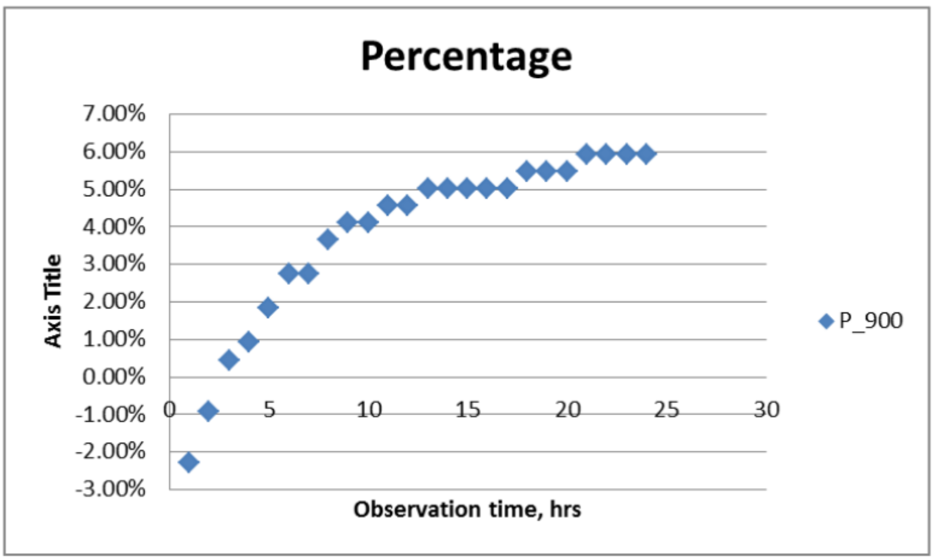

Figure 4-27. Percentage vs. observation time at 900 psi

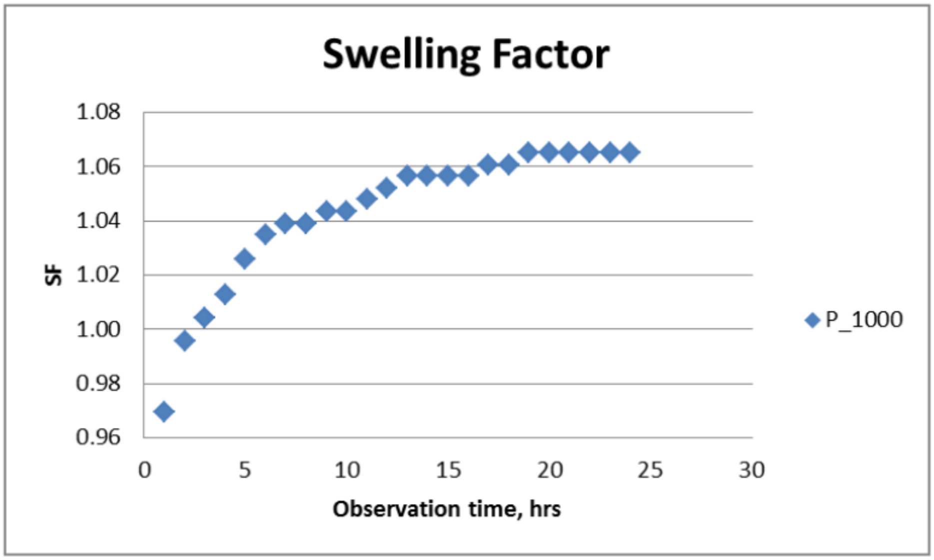

Figure 4-28. Swelling factor vs. observation time at 1000 psi

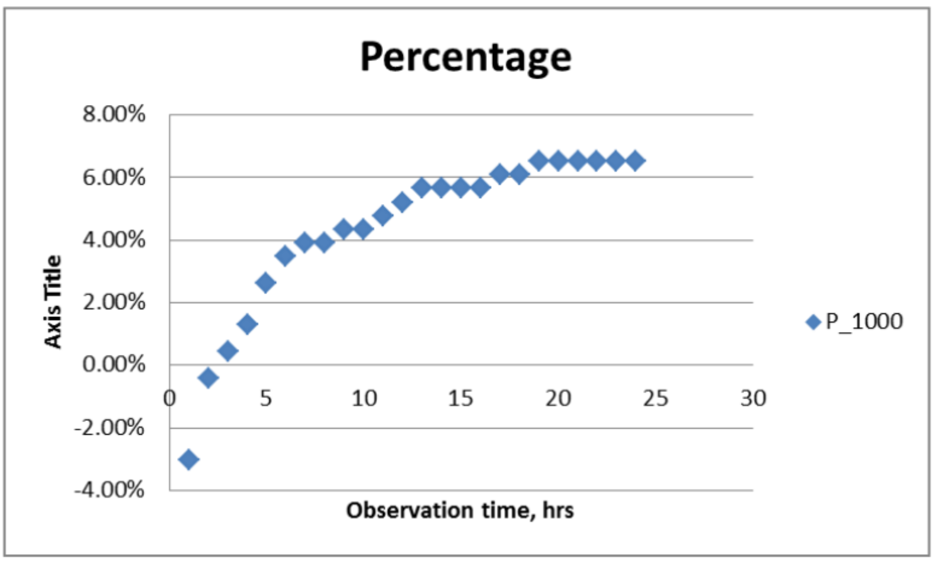

Figure 4-29. Percentage vs. observation time at 1000 psi

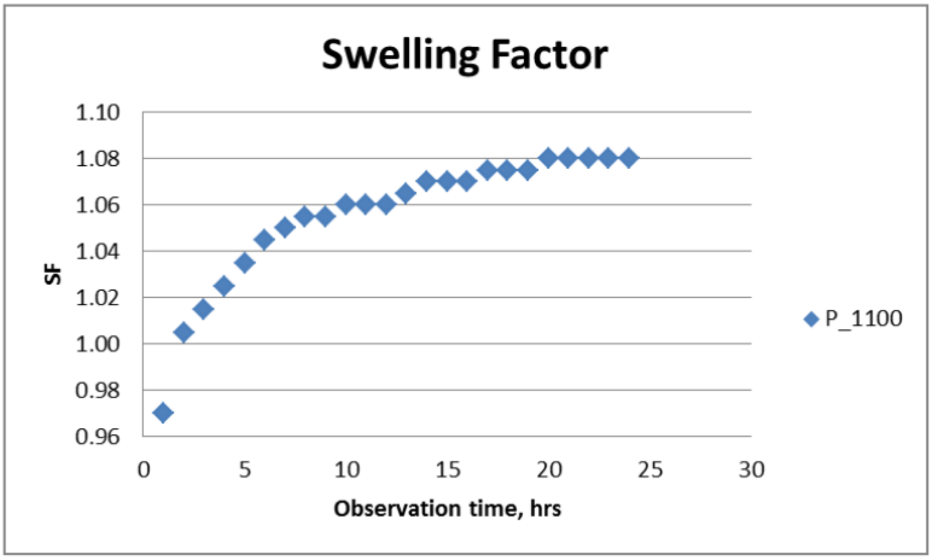

Figure 4-30. Swelling factor vs. observation time at 1100 psi

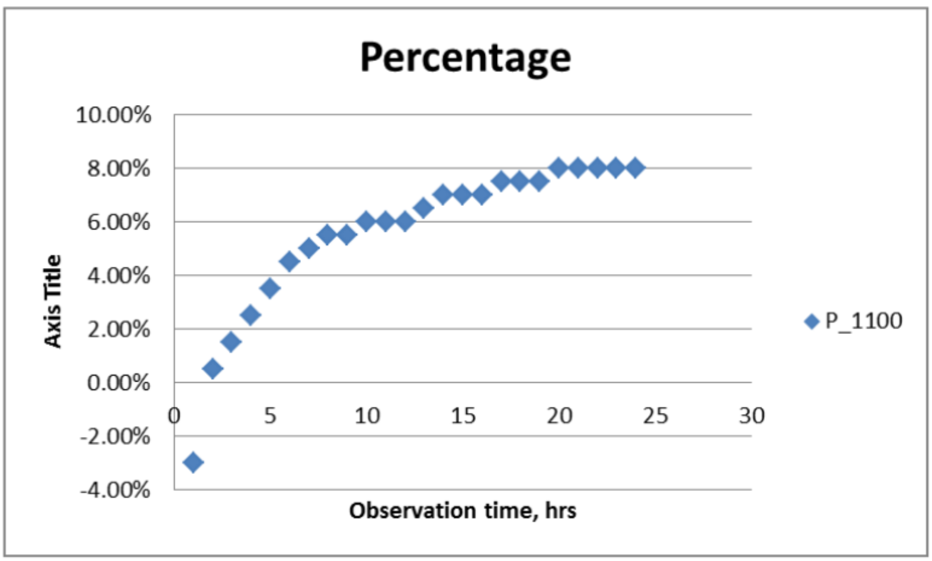

Figure 4-31. Percentage vs. observation time at 1100 psi

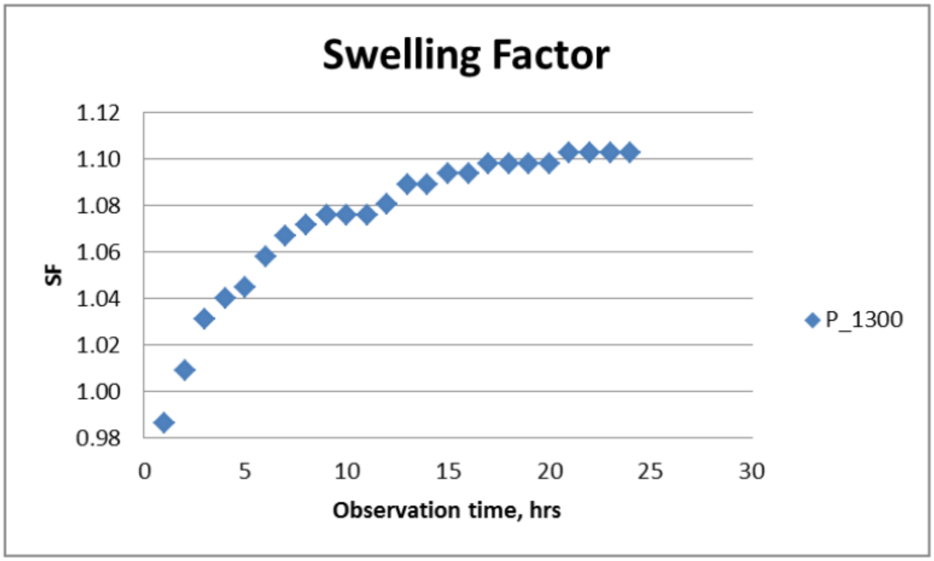

Figure 4-32. Swelling factor vs. observation time at 1300 psi

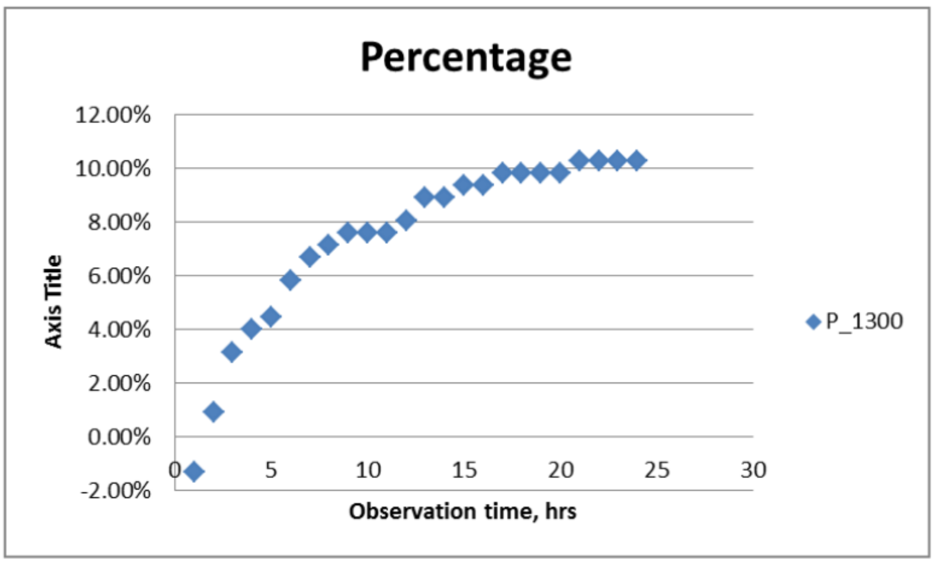

Figure 4-33. Percentage vs. observation time at 1300 psi

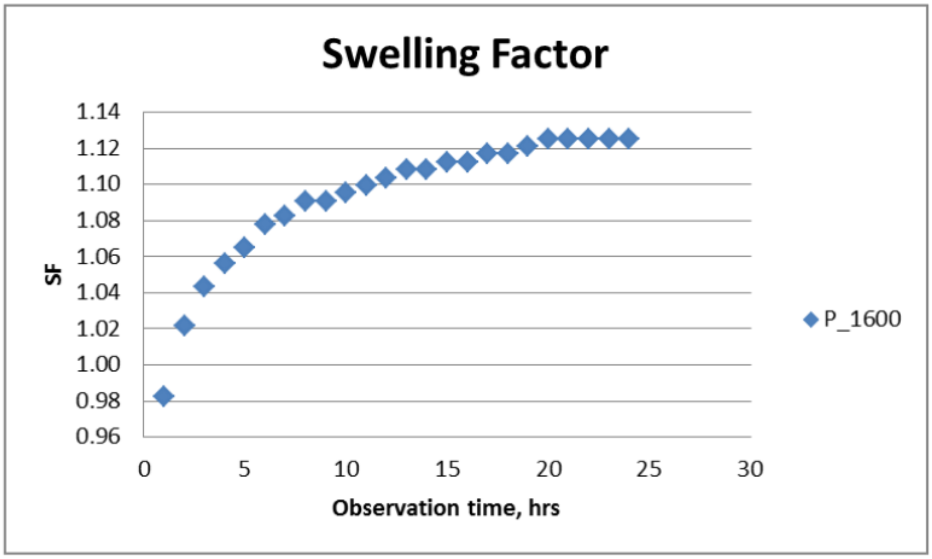

Figure 4-34. Swelling factor vs. observation time at 1600 psi

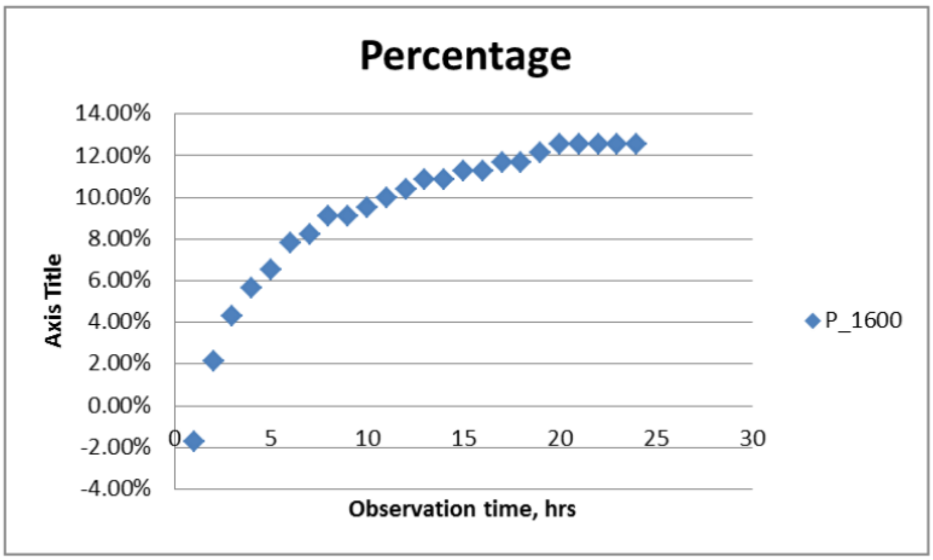

Figure 4-35. Percentage vs. observation time at 1600 psi

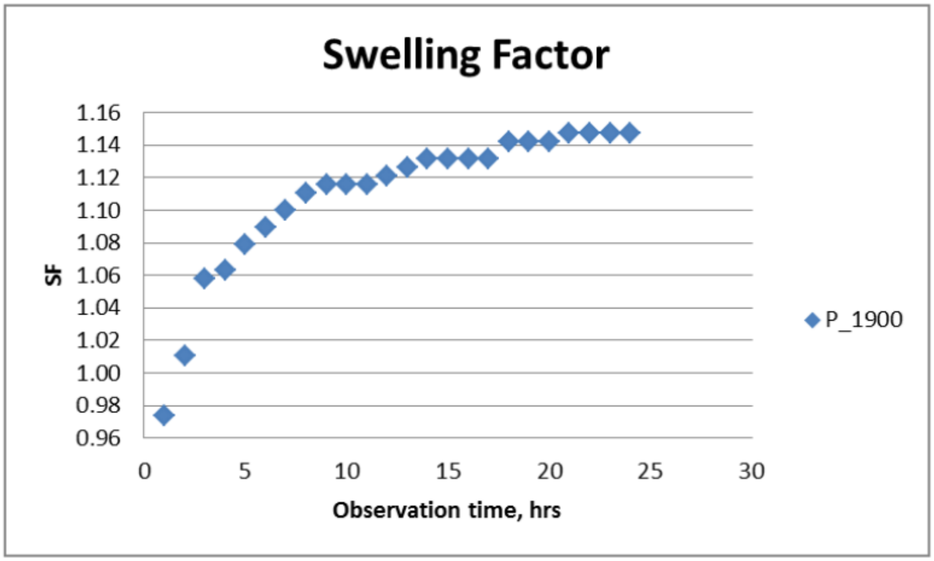

Figure 4-36. Swelling factor vs. observation time at 1900 psi

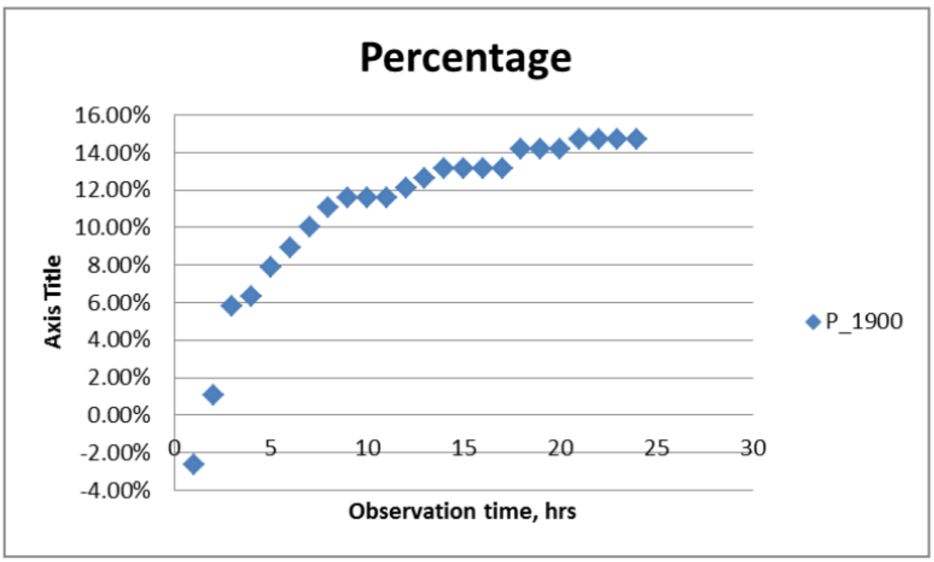

Figure 4-37. Percentage vs. observation time at 1900 psi

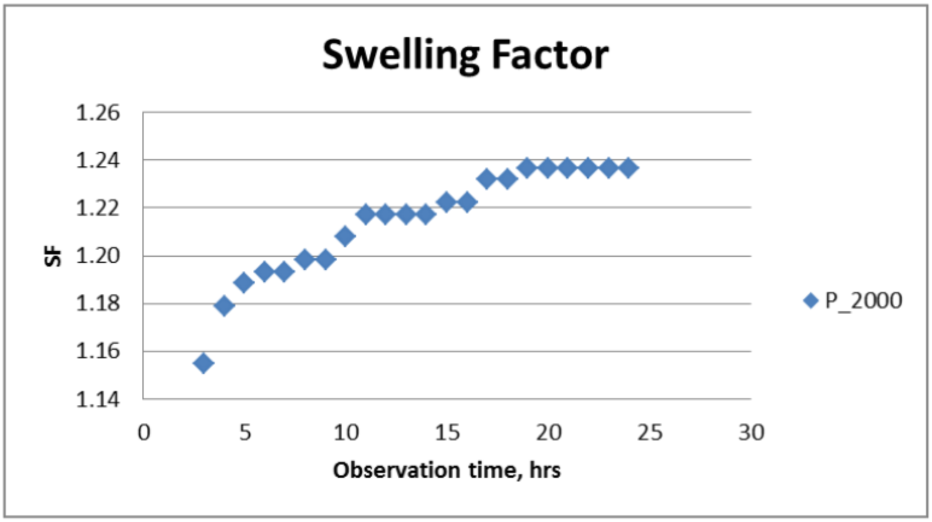

Figure 4-38. Swelling factor vs. observation time at 2000 psi

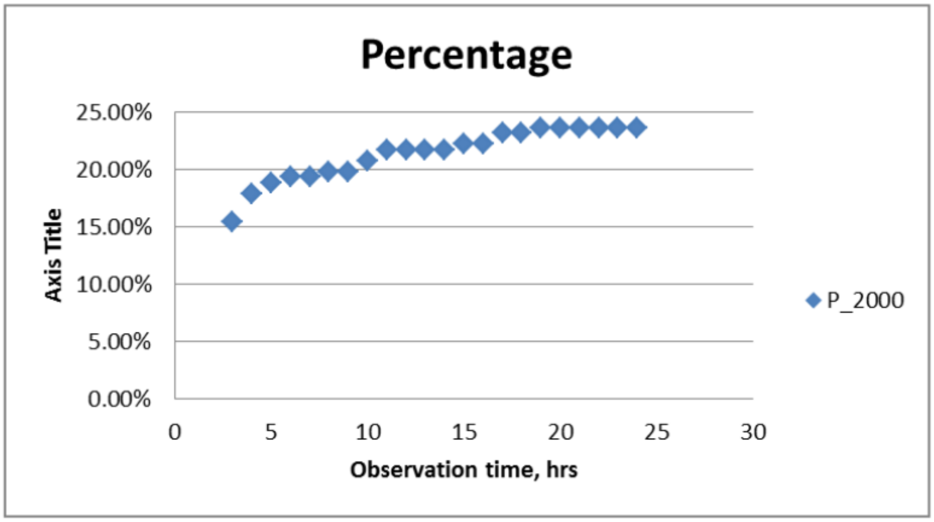

Figure 4-39. Percentage vs. observation time at 2000 psi

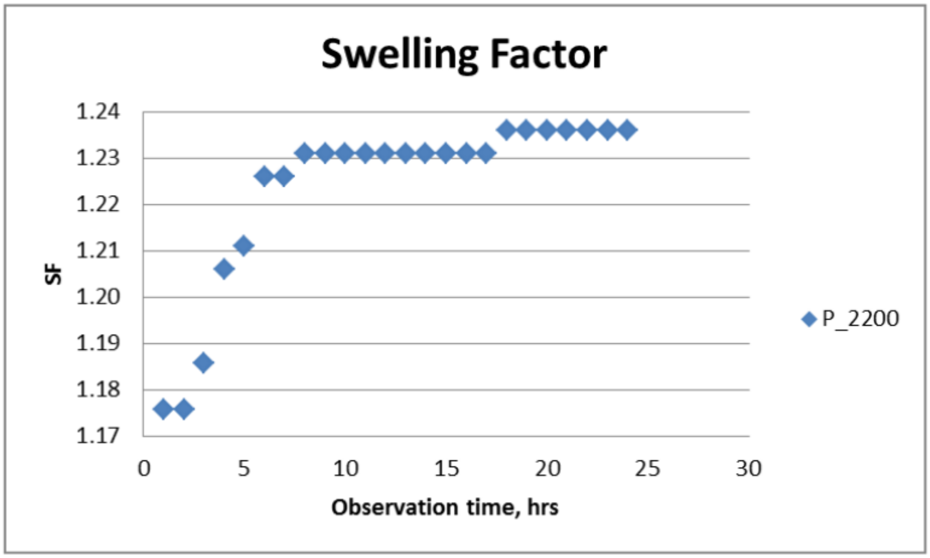

Figure 4-40. Swelling factor vs. observation time at 2200 psi

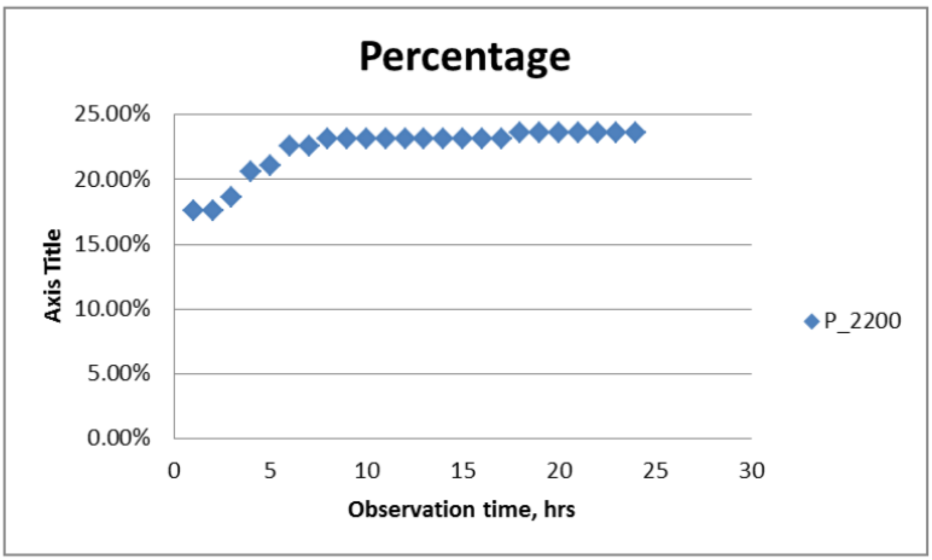

Figure 4-41. Percentage vs. observation time at 2200 psi

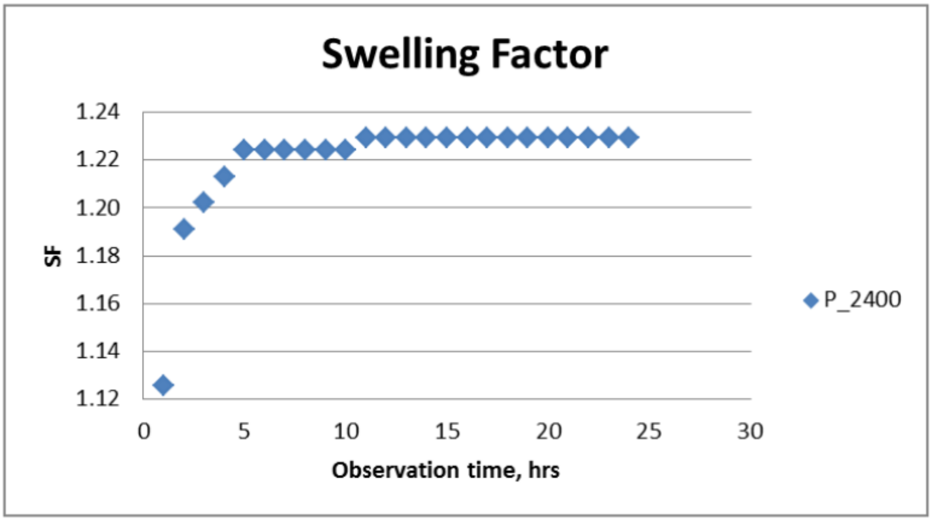

Figure 4-42. Swelling factor vs. observation time at 2400 psi

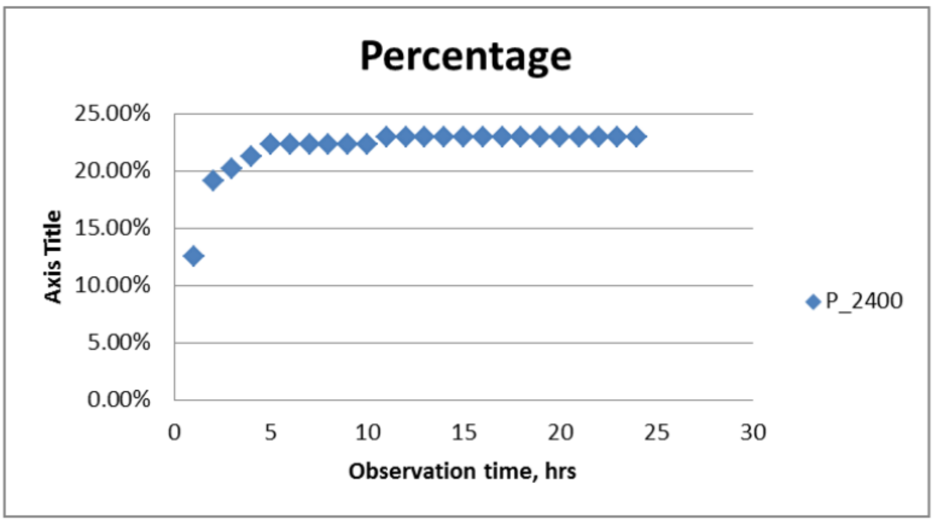

Figure 4-43. Percentage vs. observation time at 2400 psi

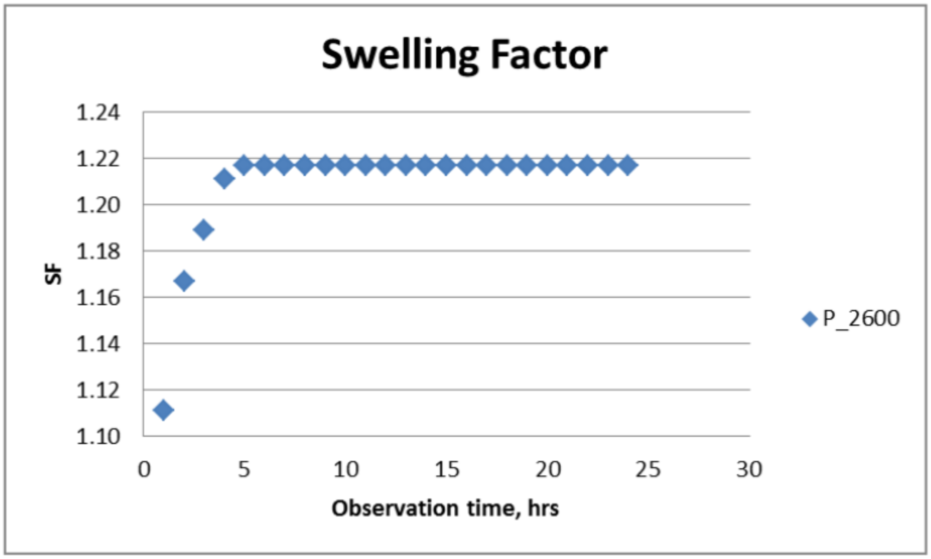

Figure 4-44. Swelling factor vs. observation time at 2600 psi

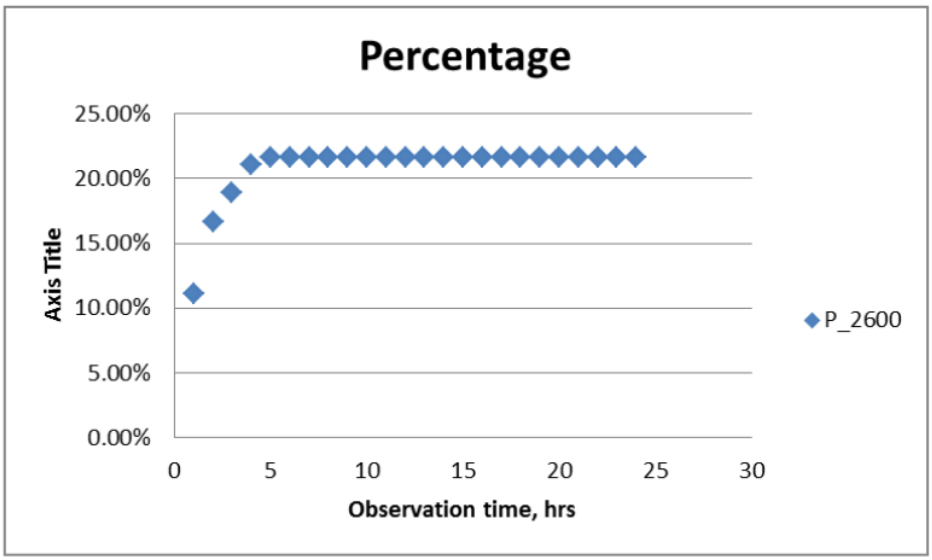

Figure 4-45. Percentage vs. observation time at 2600 psi

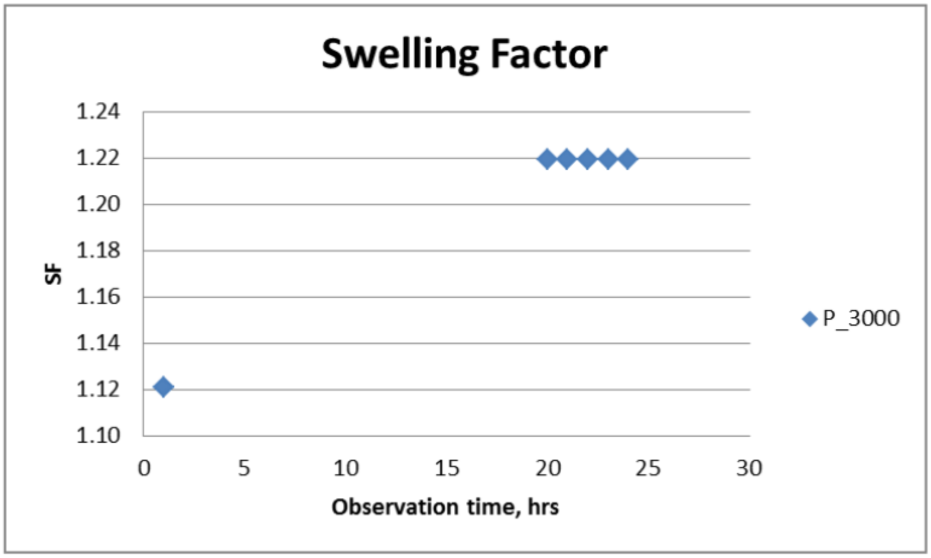

Figure 4-46. Swelling factor vs. observation time at 3000 psi

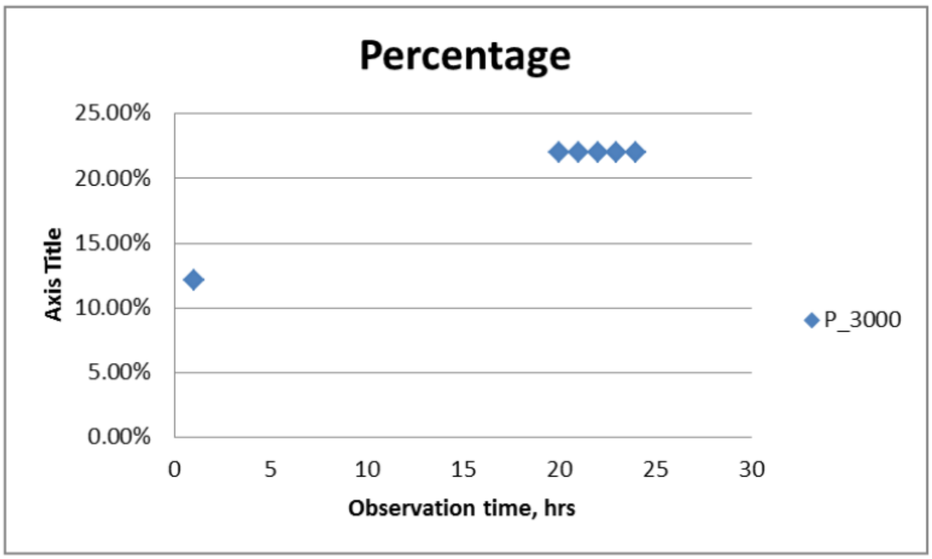

Figure 4-47. Percentage vs. observation time at 3000 psi

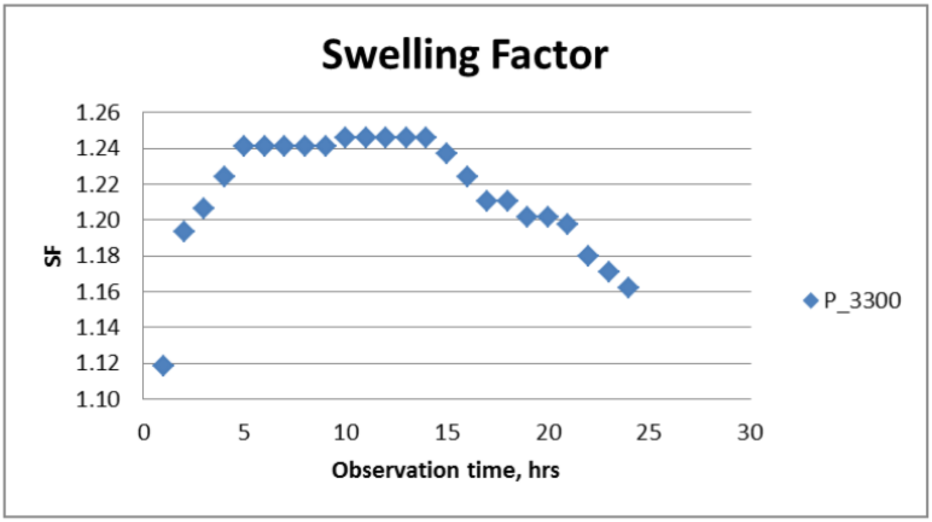

Figure 4-48. Swelling factor vs. observation time at 3300 psi

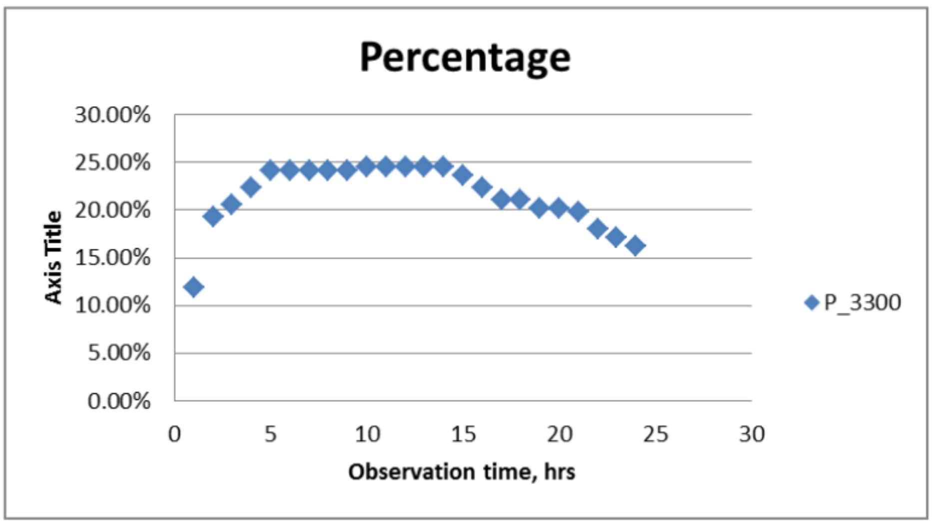

Figure 4-49. Percentage vs. observation time at 3300 psi

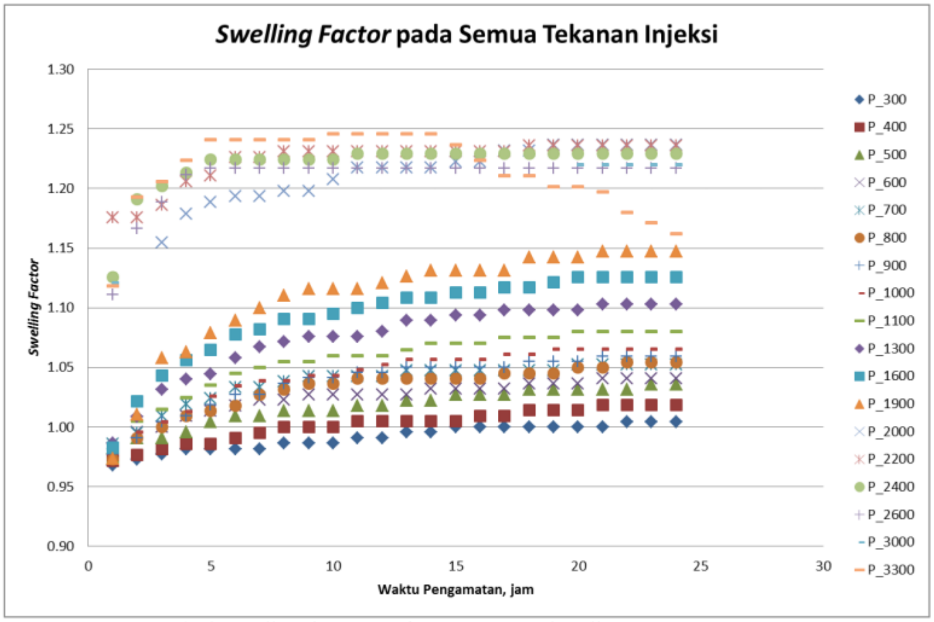

Figure 4-50. Swelling factor vs. observation time for all injection pressure

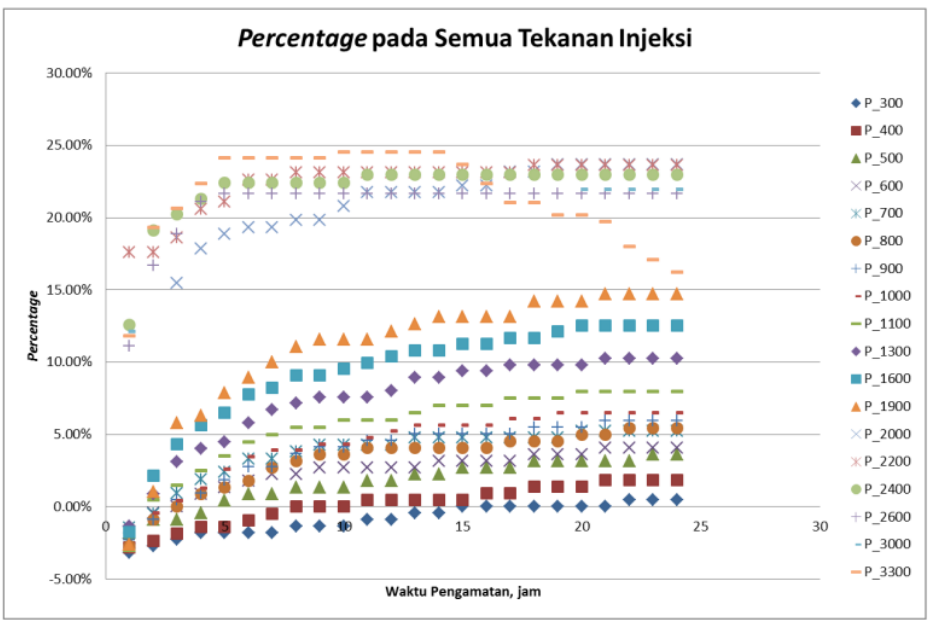

Figure 4-51. Percentage vs. observation time for all injection pressure

From Figure 4-50, it can be seen that after 20 hours CO_2 injection, the oil swelling factor is not significantly increase. And for injection pressure 3.300 psi, the swelling factor is decrease after 15 hours.

After that, the swelling at 24 hours observation time can be plotted for each injection pressure.

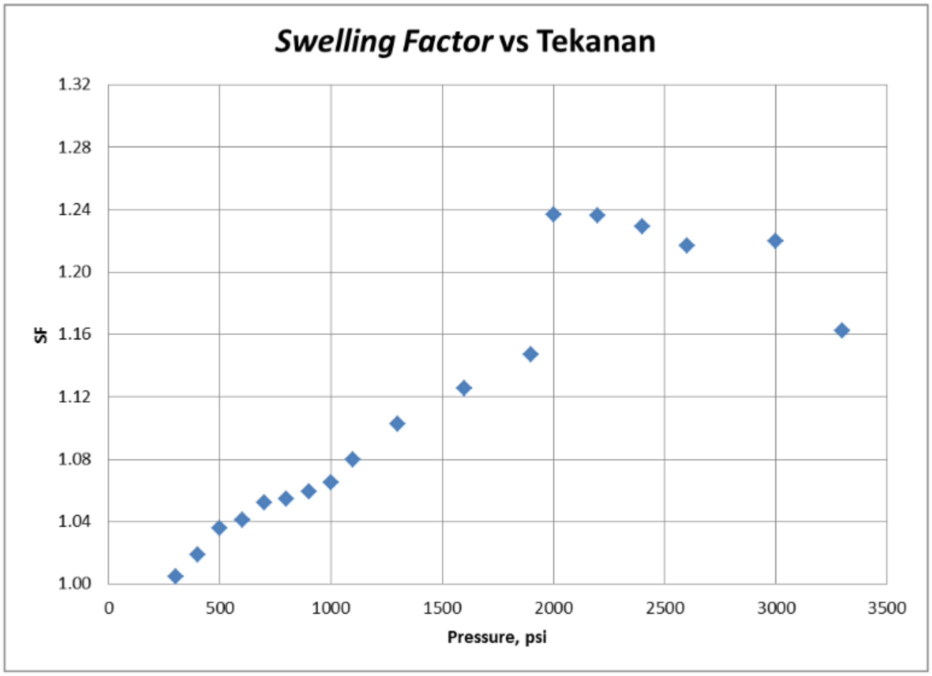

Figure 4-52. Swelling factor vs. pressure

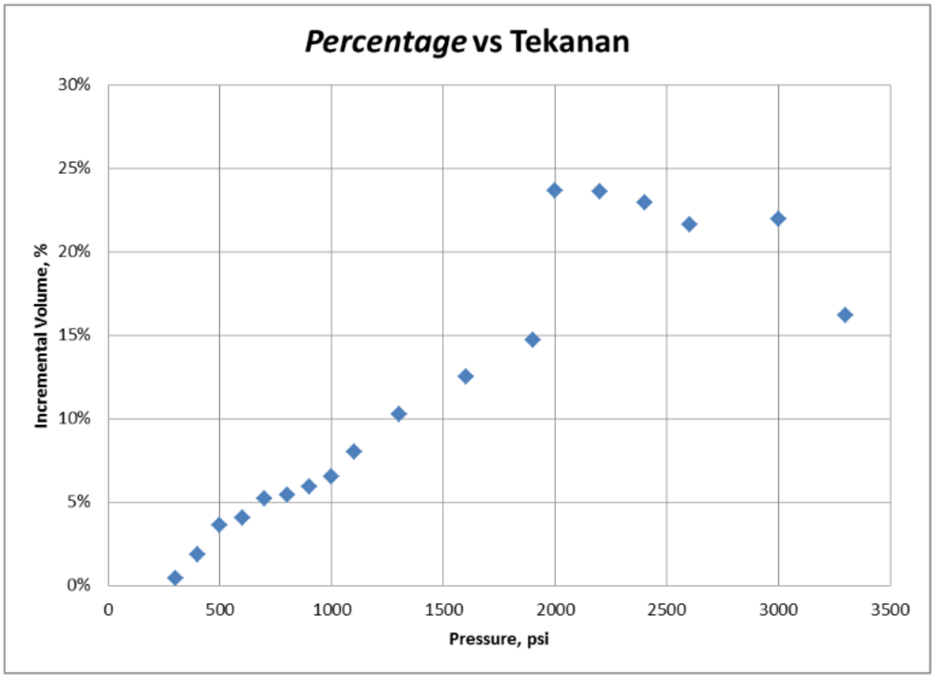

Figure 4-53. Percentage vs. pressure

From Figure 52, it can be seen that the swelling factor increases with increasing pressure up to 2000 psi injection pressure. This occurs because at constant temperature, the solubility of CO2 increases with increasing pressure. Then, at an injection pressure greater than 2000 psi, the trend of the swelling factor value decreases with increasing pressure. This happens because there is evaporation and condensation process before miscibility occurs. And the condensation process will be dominant due to Langgak oil has much heavy component. The condensation mechanism occurs when the gas is injected into an oil having a small intermediate carbon fraction component and has a heavy fractional component. The oil will take the intermediate fraction component of the gas (gas condensed into the oil) until the oil component becomes more like a gas component.

CHAPTER V

LABORATORY WORK: VISCOSITY REDUCTION

5.1 Introduction

Viscosity is a measure of fluid resistance to flow. The process of CO_2 injection in oil will affect the viscosity of the oil itself. This is closely related to CO_2 solubility and swelling factor. In the CO_2 injection process and there is CO_2 dissolved in oil then the oil will expand or increase the volume (swelling). When oil is swelling then the oil will flow easier (viscosity down). Therefore it is very important to know the change of oil viscosity in CO_2 injection process

5.2 Viscosity Reduction Experiment

5.2.1 Experiment Equipment

a. PVS Rheometer

PVS Rheometer is a tool designed to measure fluid viscosity. PVS Rheometer measures with coaxial cylinder and can measure accurately. PVS rheometer also have thermobatch that allowing to measure fluid viscosity at certain temperatures. PVS rheometer shown in Figure V-1.

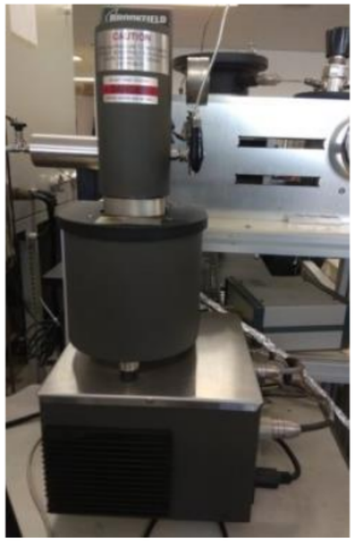

Figure 5-1. PVS Rheometer

b. PVS Rheometer Software

PVS Rheometer software is used to set parameters in fluid viscosity measurements, perform tool calibration, and ensure parameters in the measurement. There are some parameters that can be adjusted in the PVS rheometer software, for example temperature and RPM. The maximum pressure of PVS rheometer tool in measuring the viscosity of fludia is 1000 psi. PVS Rheometer software is shown in Figure V-2.

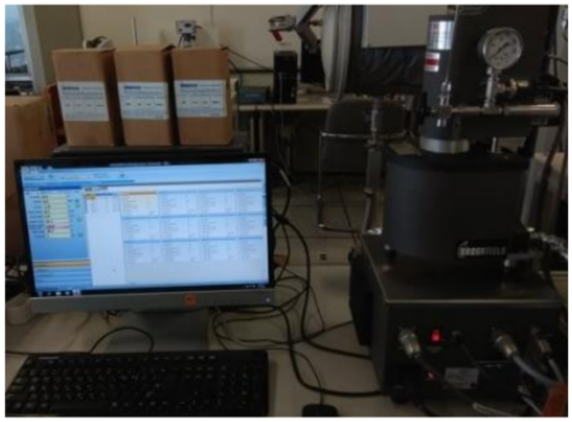

Figure 5-2. Rheometer Software

c. CO_2 Pressure Bomb

The CO_2 that was used is 99.99% pure CO_2 that was contained in pressure bomb which has initial pressure around 900 psi. The CO_2 pressure bomb then was connected with the ISCO pump 260D model. The pressure bomb can be seen at Figure V-36.

Figure 5-3. CO_2 pressure bomb

d. ISCO Pump 260D

ISCO pump is a piston-driven model pump that can give displacement to the fluid using constant flow or constant pressure mode. For CO_2 injection, specialized ISCO pump (260D Syringe pump) was used because it was specifically for refilling under high pressure to handle supercritical fluids. The ISCO pump can be seen at Figure V-4.

Figure 5-4. ISCO pump 260D

e. Pump Controller

The pump controller was used for controlling the 260D ISCO pump. We can set the rate for constant pressure mode, or the pressure for the constant rate mode of the ISCO pump. Pump controller can be seen at Figure V-5.

Figure 5-5. Pump controller

f. Cooling Water Bath

Cooling water bath from Lab. Compression was used to easily compress CO_2 gas in ISCO pump to reach high pressure. The temperature of the water bath was set up at 4°C. The cooling water bath can be seen at Figure V-6.

Figure 5-6. Cooling water bath

5.2.2 Viscosity Reduction Experiment Procedure

Procedure of viscosity reduction experiment is:

- Lift and turn the PVS rheometer head and remove it from the thermobath.
- Remove the sample cup by holding the sample cup and rotating the locking ring.
- Put the oil into 12 ml sample cup.
- Lubricate the surface of the upper cup sample.
- Attach a sample cup to the PVS Rheometer by holding the sample cup and rotating the locking ring.
- Rotate the sample cup and observe it visually to check whether there is a tool problem or not.
- Rotate and lower the PVS rheometer head into the thermobath.
- Adjust the fluid temperature and inject CO_2 gas at a desired pressure.
- Perform viscosity measurements after 24 hours of CO_2 injection.

5.2.3 Calculation Method

a. Torque Multiplier

The torque multiplier is a calibration tool. Range of torque multiplier value are 450 to 550. Torque multipliers are strongly related to the torque cylinder torque sensor.

b. Viscosity Calculation

The viscosity of various rheometer models and geometries is calculated by the following equation:

$$Viscosity\ [cp] = \frac{TM \times \%torsi \times 10.000}{RPM \times SCM \times SRC}$$

Where:

TM = torque multiplier,

SMC = torque geometry constant,

SRC = shear rate constant.

c. Shear Stress Calculation

Shear stress for various rheometer models and geometry can be calculated by the following equation:

$$Shear\ stress\ \left[\frac{dyne}{cm^2}\right] = \frac{TM \times \%torsi \times 100}{SMC}$$

Where:

TM = torque multiplier,

SMC = torque geometry constant.

d. Shear Rate Calculation

The shear rate for various geometries can be calculated by the following equation:

$$Shear\ rate\ \left[\frac{1}{sec^1}\right] = RPM \times SRC$$

Where:

SRC = shear rate constant.

5.2.4 Eksperiment Result

Viscosity reduction test has been carried out at reservoir temperature with some different pressure. The result of viscosity reduction test can be seen in Table V-1 and Figure V-7.

Table 5-1. Result of viscosity reduction test

Tekanan (psi)	Viskostitas (cp)
0	16.8
400	14.0
600	11.1
900	10.2

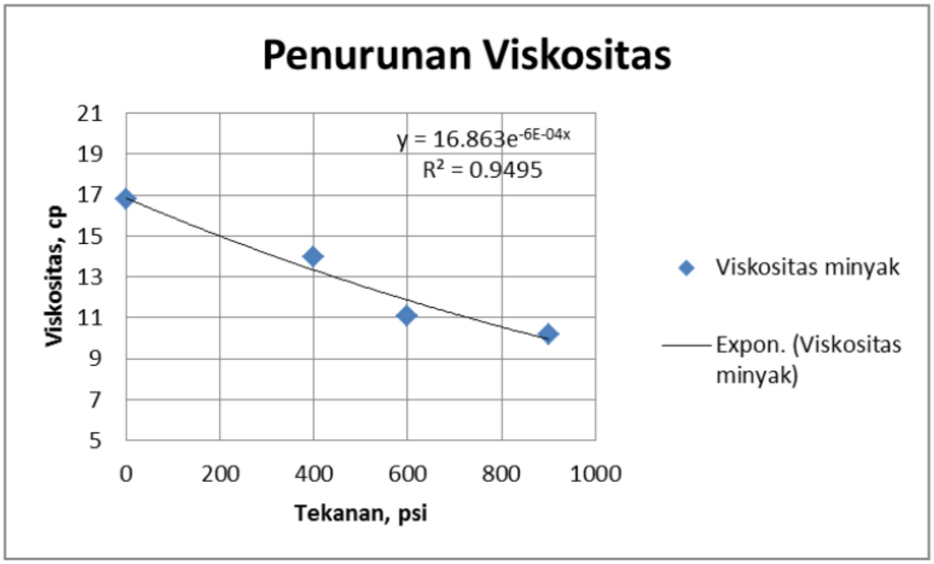

Figure 5-7. Viscosity reduction profile

Based on the result of viscosity reduction test and viscosity reduction profile (Figure V-7), it can be seen that the oil viscosity decrease up to 40% with increasing CO_2 injection pressure up to 900 psi. The relationship between oil viscosity with CO_2 injection pressure is as follow:

$$viskosity = 16{,}863 \times e^{-6\times10^{-4}\times tekanan}$$

CHAPTER VI
MINIMUM MISCIBLE PRESSURE (MMP) DETERMINATION

6.1 Introduction

Minimum miscible pressure is the lowest pressure needed to achieve miscible state of the system. There are two kinds of MMP that could happen base on the how many contact it needed to achieve the MMP. There are first contact miscibility (FCM) and multiple contact miscibility (MCM). We can differentiate the process that will happen by looking at ternary diagram of the crude oil system. The example of first contact miscibility is a reaction between ethanol and water. (Jarrell et al. 2002) They will form one phase of fluid without observable interface (no interface, IFT = 0). Butane and crude oil also can form one phase of fluid (first contact miscibility), but the cost of butane is high, so we must consider the economics if we want to apply the butane (LPG) flooding into the reservoir.

MMP can be defined as:

- Maximum oil recovery at 1.2 PV of CO_2 injected, can be seen at Figure 1.1 (Yellig and Metcalfe, 1980).
- The pressure that causes 80% oil recovery at CO_2 breakthrough and 94% of oil in place ultimately recovered (Holm and Josendal, 1974).
- The pressure that causes 90 % oil recovery at 1.2 PV of CO_2 injected (William, 1980).

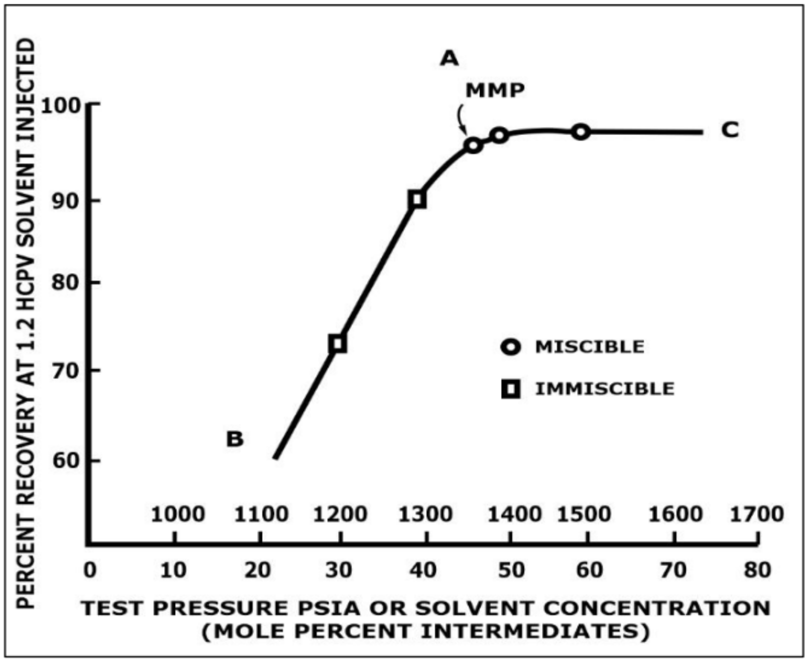

Figure 6-1 . MMP menurut Metcalfe (1980)

There are three main parameters that affecting MMP such as gas injection composition, intermediate, component (C_{5+}) of crude oil, and reservoir temperature. Also there are two different mechanisms that could happen on miscibility process, which are vaporizing and condensing mechanism. (Holm, 1986).

a. Vaporizing Mechanism

The light component from crude oil is vaporized by CO_2 and it will continue until CO_2 become more like the oil and thus become easier to soluble in the oil. Upon contact with the oil, light and intermediate molecular-weight hydrocarbons transfer from the oil into the gas phase,thus vaporizing into the gas. Formation of miscibility may require several contacts between gas containing vaporized components and fresh reservoir oil.

b. Condensing Mechanism

The rich gas is injected into the oil with less intermediate carbon fraction, but have heavier fraction in the component. The crude oil will take the intermediate fraction from the gas (the gas is condensed into the oil) until the crude oil will be similar in component with the rich gas. That is when the miscibility will happen.

The process of vaporizing and condensing mechanism are explained at Figure VI-2.

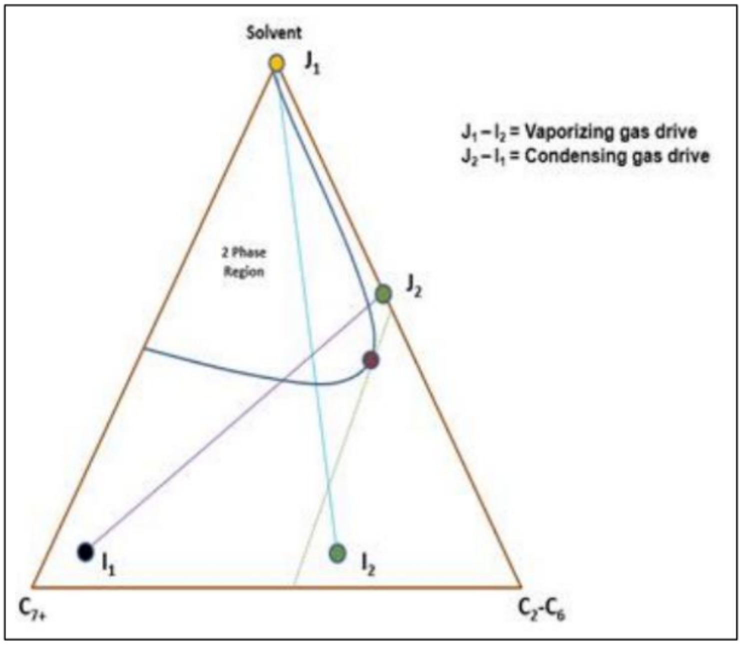

Figure 6-2. Vaporizing and condensing mechanisms

6.2 **MMP Determination Using Correlations**

6.2.1 National Petroleum Council (1976)

National Petroleum Council (NPC) proposed the MMP correlation based on the API gravity and temperature only. Table VI-1 below shows the MMP correlation from NPC.

Table 6-1. MMP Correlation from NPC

Gravity (^{o}API)	MMP (psi)

< 27	4.000
27 - 30	3.000
> 30	1.200

Table 6-2. Reservoir temperature correction from NPC

T (^{o}F)	Tambahan Tekanan (psi)
< 120	0
120 - 150	+ 200
150 - 200	+ 350
200 - 250	+ 500

6.2.2 Cronquist (1978)

In 1978, Cronquist proposed the following CO_2 MMP correlation:

$$MMP = 15.988 \times T_{res}^{(0.7442+0.0011MW_{C5}+0.0015M_{C1})}$$

Where:

MMP = minimum miscibility pressure, psi

T_{res} = temperatur reservoir, ^{o}F

MWC_{5+} = molecular weight of the pentanes plus fraction of the reservoir fluid

M_{ci} = mole fraction of methane and nitrogen in the reservoir fluid

The reservoir fluid was characterized using the molecular weight of the C5+ fraction and the mole fraction of nitrogen and methane in the reservoir fluid. The correlation was based on 58 experimental MMP measurement from a number of sources using oil ranging from 23.7 to 44 ^{0}API and reservoir temperatures from 77 to 248^{0}F. The MMP values ranged from 1076 to 5000 psia..

6.2.3 Yellig dan Metcalfe (1980)

Yellig and Metcalfe in 1980 proposed a pure CO_2 MMP correlation based on the reservoir temperature. They also stated that if the calculated MMP is less than the bubble point pressure of the reservoir fluid that the bubble point pressure should be taken as the MMP. The correlation can be expressed as:

$$MMP = 1833.7217 + 2.2518T_{res} + 0.018T_{res}^2 - \frac{103949.93}{T_{res}}$$

Or can also be seen in the following Figure VI-3.

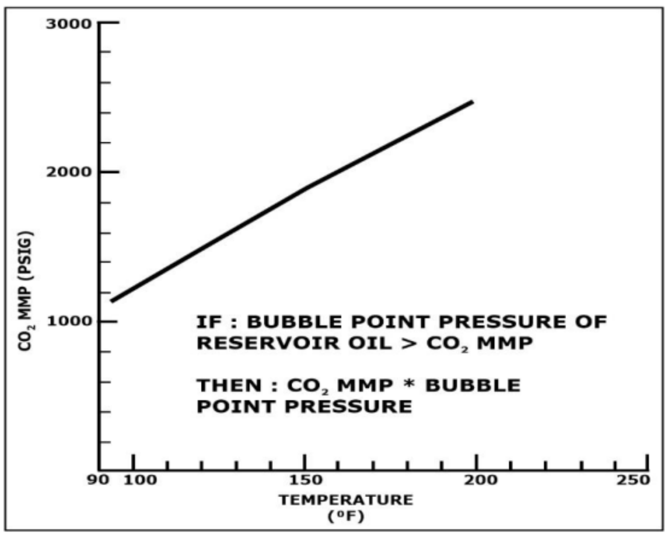

Figure 6-3. Yellig-Metcalfe MMP correlation diagram

6.2.4 Johnson dan Pollin (1981)

In 1981, Johnson and Pollin developed a CO2 MMP correlation for the temperature range of 300 K to 410 K, which tolerated up to 20 mole % methane and nitrogen impurities.

$$MMP - Pc_{,inj} = \alpha_{inj}\left(T_{Res} - T_{c,inj}\right) + I(0{,}285MW - MW_{inj})^2$$

Where:

$P_{c,inj}$ = Critical pressure of injection gas (psia)

T_{res} = Reservoir temperature (K)

$T_{c,inj}$ = Critical temperature of injected gas(K)

MW = Molecular weight of reservoir fluid

MW_{inj} = Molecular weight of injected gas

I = oil characterization index

α = 18.9 psia/K for pure CO_2

The oil characterization index is a function of a molecular weight and API gravity and is expressed by the following equation:

$$I = C_{11} + C_{21}MW + C_{31}MW^2 + C_{41}MW^3 + (C_{12} + C_{22}MW)\rho + C_{13}\rho^2$$

Where:

C_{11} = -11,73

C_{12} = 0.1362

C_{13} = -7,222 x 10^{-5}

C_{21} = 6,313 x 10^{-2}

C_{22} = 1,138 x 10^{-5}

C_{31} = -1,954 x 10^{-4}

C_{41} = 2,502 x 10^{-7}

For gas mixtures of CO2 with N2, the injection as constant (α_{inj}) becomes:

$$\alpha_{inj} = 10{,}5 \times \left(1{,}8 + \frac{10^3 y_2}{T_{res} - T_{c,inj}}\right)$$

If CO2 mix with CH4, the injection as constant (α_{inj}) becomes:

$$\alpha_{inj} = 10{,}5 \times \left(1{,}8 + \frac{10^2 y_2}{T_{res} - T_{c,inj}}\right)$$

WHere: y_2 = mole fraction of non-CO_2 component in injected gas.

6.2.5 VI.2.5. Glaso (1985)

Glaso in 1985 modelled CO_2 MMP by the following equation:

$$MMP = 810 - 3{,}404MW_{C7+} + \left(1{,}7 \times 10^{-9} MW_{C7}^{3,73} \times e^{786,8MW_{C7+}^{-1,058}}\right) T_{res}$$

Where, MW_{C7+} = molecular weight of C_{7+} component in stock tank oil..

When the mole fraction of intermediates (Fr) < 18%, the correlation is:

$$MMP = 2947{,}9 - 3{,}404MW_{C7+} + \left(1{,}7 \times 10^{-9} MW_{C7}^{3,73} \times e^{786,8MW_{C7+}^{-1,058}}\right) T_{res} - (121{,}2F_r)$$

Where, F_R = % mole fraction of ethane to butane in reservoir fluid.

6.2.6 VI.2.6. Yuan, Johns, dan Egwuenu (2005)

Yuan et al. (2005) developed pure and impure CO2 MMP correlations. The input data for temperature is in the range of 120ºF to 300ºF. The correlation used three input parameters which are the reservoir temperature, the C2-C6 mole fraction in the oil and the molecular weight of the C_{7+} fraction. The correlation gave an absolute average error of 6.6% and is expressed as follows::

$$MMP_{pure} = a_1 + a_2 M_{C7+} + a_3 P_{C2-6} + \left(a_4 + a_5 M_{C7+} + a_6 \frac{P_{C2-6}}{M_{C7+}^2}\right) T + (a_7 + a_8 M_{C7+} + a_9 M_{C7+}^2 + a_{10} P_{C2-6}) T^2$$

Where:

a_1 = $-1{,}4634 \times 10^3$

a_2 = 6,612

a_3 = -44,979

a_4 = 2,139

a_5 = 0,11667

a_6 = 8,1661 x 10^3

a_7 = -0,12258

a_8 = 1,2883 x 10^{-3}

a_9 = -4,0152 x 10^{-6}

a_{10} = -9,2577 x 10^{-4}

For impure CO_2 stream, the correlation is shown below:

$$\frac{MMP_{impure}}{MMP_{pure}} = 1 + m(P_{CO2} - 100)$$

with m:

$$m = a_1 + a_2 M_{C7+} + a_3 P_{C2-6} + \left(a_4 + a_5 M_{C7+} + a_6 \frac{P_{C2-6}}{M_{C7+}^2}\right) T + (a_7 + a_8 M_{C7+} + a_9 M_{C7+}^2 + a_{10} P_{C2-6}) T^2$$

Where:

a_1 = -6,599 x 10^{-2}

a_2 = -1,5246 x 10^{-4}

a_3 = 1,3807 x 10-^{3}

a_4 = 6,2384 x 10^{-4}

a_5 = -6,7725 x 10^{-7}

a_6 = -2,7344 x 10^{-2}

a_7 = -2,6953 x 10^{-6}

a_8 = 1,7279 x 10^{-8}

a_9 = -3,1436 x 10^{-11}

a_{10} = -1,9566 x 10^{-8}

6.2.7 VI.2.7. Petroleum Recovery Institute

Petroleum Recovery Institute, Canada, made a MMP correlation which only consider the temperature of the system.

$$MMP = 1071{,}82893 \times 10^{b}, \text{ dengan } b = \left[2{,}772 - \left(\frac{1519}{T}\right)\right]$$

with:

T = temperature, ^{o}R

MMP = minimum miscible pressure, psia.

6.3 MMP Determination Using Swelling Experiment

Hand and Pinczweski (1990) point out that swelling/extraction tests are simple single contact phase behavior experiments that offer a measurement of the amount of hydrocarbon that CO_2 can extract or vaporize from crude oil. However, Tsau et al. (2010) proposed for predicting the MMP through swelling test. This its method has been proved by Abdurrahman et al. (2015). In their experiments, the MMP through swelling test is close to the slim tube measurement. The discrepancies between both of method are in the range of 0.6% – 0.7% of Tsau et al. (2010) and 1.2% - 3.9% of Abdurrahman et al., 2015). Figure VI-4 shows plots swelling test vs pressure to predict the MMP.

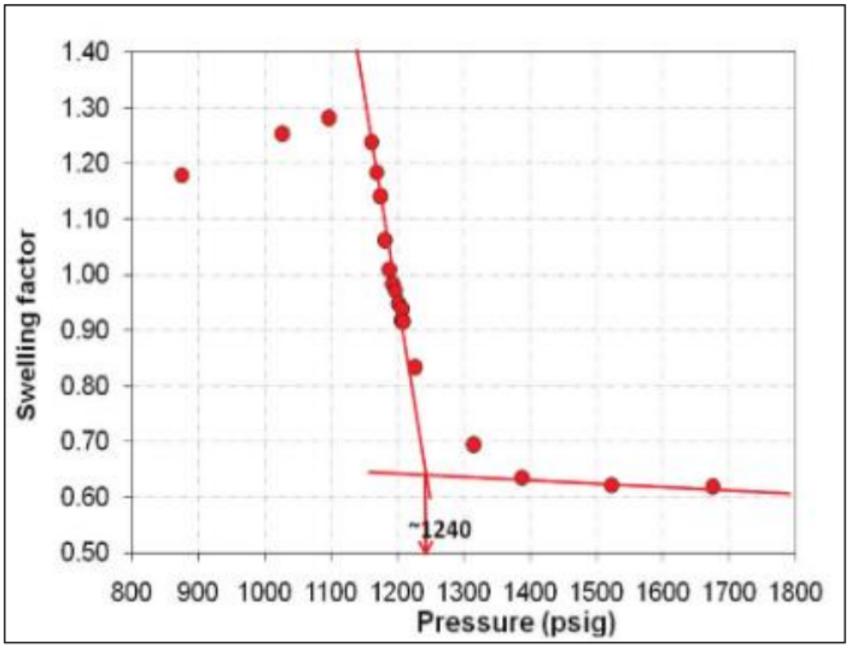

Figure 6-4. Estimation of MMP from swelling test (Tsau dkk, 2010)

Tsau et al. (2010) proposed the MMP to be determined through swelling tests when the straight-line curve of the extraction-condensation stage and the extraction stage intersects each other. However, the MMP cannot be determined graphically from the plot when it lacks of the extraction stage (Figure VI-5).

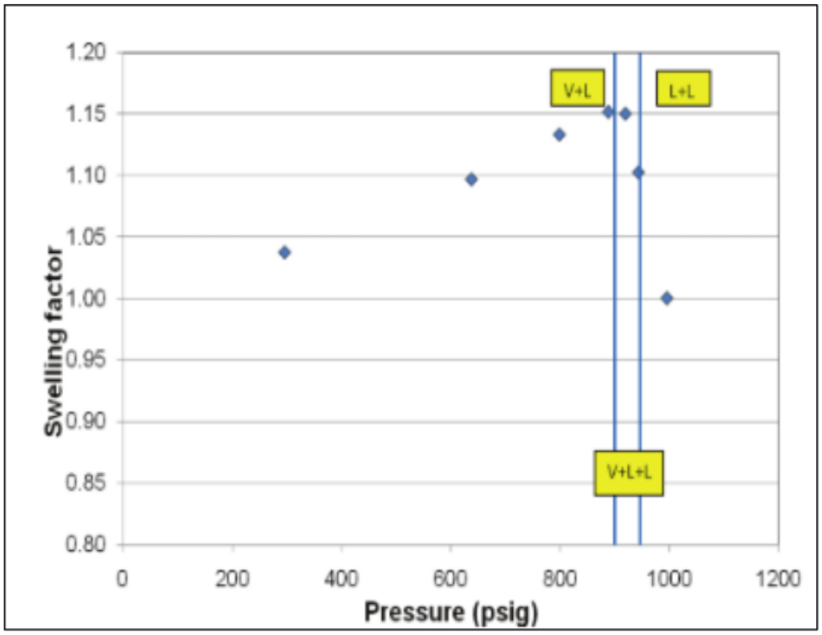

Figure 6-5. The MMP cannot be determined due to lack of extraction stage (Tsau dkk, 2010)

6.4 MMP Determination for Langgak Oil

6.4.1 Based on Correlation

Based on Yellig correlation is:

$$MMP = 1833.7217 + 2.2518T_{res} + 0.018T_{res}^2 - \frac{103949.93}{T_{res}}$$

Where: Tres = 136°F.

So, the MMP result based on Yellig correlation is:

$$MMP_{Yellig} = 1708{,}56\ psi$$

Based on Petroleum Recovery Institute (PRI) correlation is:

$$MMP = 1071{,}82893 \times 10^b, \text{dengan } b = \left[2{,}772 - \left(\frac{1519}{T}\right)\right]$$

Where, T = 595.67°R

So, the MMP result based on Petroleum Recovery Institute (PRI) correlation is:

$$MMP_{PRI} = 1786{,}72\ psi$$

Based on Glaso correlation model is:

$$MMP = 810 - 3{,}404 MW_{C7+} + \left(1{,}7 \times 10^{-9} MW_{C7}^{3{,}73} \times e^{786{,}8 MW_{C7+}^{-1{,}058}}\right) T_{res}$$

Where, $MW_{C7+} = 323$ and $T_{res} = 136^{o}F$.

And then, the MMP result based on Glaso correlation is:

$$MMP_{Glaso} = 810 - (3{,}404 \times 323) + \left(1{,}7 \times 10^{-9} \times 323^{3{,}73} \times e^{786{,}8 \times 323^{-1{,}058}}\right) 136$$

$$MMP_{Glaso} = 2730{,}41\ psi$$

Based on Yuan dkk (2005) correlation model:

$$MMP_{pure} = a_1 + a_2 M_{C7+} + a_3 P_{C2-6} + \left(a_4 + a_5 M_{C7+} + a_6 \frac{P_{C2-6}}{M_{C7+}^2}\right) T + (a_7 + a_8 M_{C7+} + a_9 M_{C7+}^2 + a_{10} P_{C2-6}) T^2$$

Where:

a_1 = -1,4634 x 10^3

a_2 = 6,612

a_3 = -44,979

a_4 = 2,139

a_5 = 0,11667

a_6 = 8,1661 x 10^3

a_7 = -0,12258

a_8 = 1,2883 x 10^{-3}

a_9 = -4,0152 x 10^{-6}

a_{10} = -9,2577 x 10^{-4}

P_{C2-6} = 0.0806

M_{C7+} = 323

T = 136°F

So, the MMP result based on Yuan correlation is:

$$MMP_{Yuan} = 3765{,}44\,psi$$

6.4.2 Based on Swelling Experiment

The MMP can be determined through swelling tests when the straight-line curve of the extraction-condensation stage and the extraction stage intersects each other.

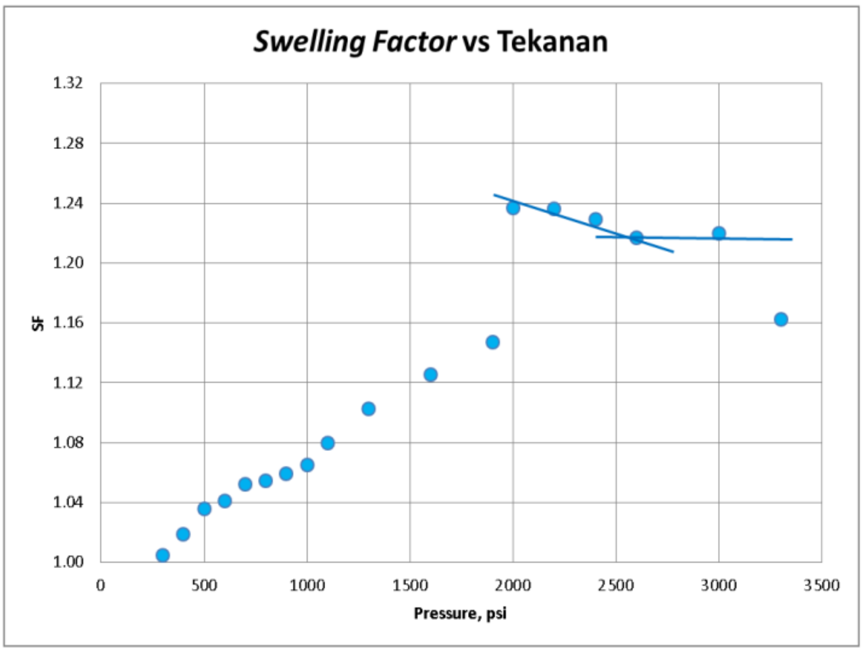

Figure 6-6. MMP determination based oil swelling test

Tsau et al. (2010) proposed the MMP to be determined through swelling tests when the straight-line curve of the extraction-condensation stage and the extraction stage intersects each other. Based on the result of swelling experiment using Langgak oil sample, it can be seen in Figure 6-6. However, it is hard to determine the MMP graphically from the plot when it lacks of the extraction stage.From Figure 6-6, it can be seen that the extraction-condensation stage from 2.000 psi until 2.600 psi, and the extraction stage from 2600 until 3000 psi. From the intersection between the line of extraction-condensation stage and line of extraction stage, it can be estimated the MMP of Langgak oil is in the range of 2.400 to 2.600 psi.

CHAPTER VII
MMP DETERMINATION:
EOS & 1-D SLIMTUBE SIMULATION

7.1 Introduction

The number of producing fields in Indonesia has reached peak production so that the current production has decreased. Nowadays, majority of the oil production still in the primary and secondary recovery stage. Traditional primary recovery methods as well as secondary recovery techniques can only recover around one third of the Original Oil in Place (OOIP) (Lake et al. 1992). This condition indicates that there is still a consequential amount of the remaining oil in place that could potentially be produced through tertiary recovery or Enhanced Oil Recovery. EOR processes are designed to do one of two things—improve sweep efficiency or improve displacement efficiency (Hite, 2005). It is needed to increase reserves and the production. One favorable method to improve oil recovery is gas injection.

Among of the existed gases, use of the carbon dioxide (CO_2) is one of the proposed methods with relatively low cost and high efficiency to improve oil recovery (Ali and Thomas 1996; Alvarado and Manrique 2010; Moritis 2004). The study of CO2 injection originally appeared in 1930's and had a great development in the 1970's since many CO_2 EOR screening criteria have been published by Brashear, et al. (1978), Goodlett, et al. (1986), Taber, et al. (1987), and Klins (1984). In 1964, a first field test was conducted at Mead Strawn Field, which involved the injection of a large slug of CO_2 followed by carbonated water at reservoir condition. Results indicated that 53 to 82 percent more oil was produced by CO_2 flood than was produced by water in the best areas of the waterflood (Holm, et.al. 1971). Following this success, laboratory and pilot test continued including in Indonesia.

A key design parameter in miscible CO_2 Injection is the minimum miscibility pressure (MMP). Miscible injection occurs when the injection pressure is set above MMP. MMP is a function of reservoir temperature, oil composition and injected gas composition. Most of Indonesian reservoirs have high temperature and as MMP is a direct function of temperature and it increases linearly corresponding to the temperature (Bashir, et al., 2012), most of reservoir oil in Indonesia have relatively high value of MMP. High MMP which also sometimes exceeds fracture pressure makes miscible injection is impossible.

7.1.1 CO_2 Flooding

Carbon dioxide is a molecule that consists of two oxygen atoms covalently bonded to a single carbon atom. Its molecular weight is about 44 g/mol. Depending on temperature and pressure, CO_2 can exist as a solid, liquid, or gas. As a supercritical fluid, CO_2 develops miscibility with crude oil to improves oil recovery (Ansarizadeh et al. 2015). The phase diagram of CO_2 can be seen in Figure 1. CO_2 can make-up multi-contact and first contact miscibility with oil at reasonable reservoir pressures while other miscible gases may not reach this point for up to a couple of thousand psi more (Behzadi and Towler, 2009).

Generally, the effect of CO2 compound in increasing the recovery factor are related strongly to three main mechanism which are oil swelling, viscosity reduction, and IFT reduction (Li, et.al. 2012). In oil swelling mechanism, carbon dioxide is highly soluble in hydrocarbons oils which yields a 10 to 40 percent increase in volume (Interstate Oil Compact Commission, 1974). This effect of this mechanism depends on saturation pressure, reservoir temperature and composition of crude oil. In viscosity reduction mechanism, as carbon dioxide gas saturates oil, large reduction in oil viscosity occurs. In IFT reduction mechanism, miscibility can be reached when there is no interfacial tension between oil and carbon dioxide. Mixture of carbon dioxide and oil leads to lower interfacial tension. These three mechanisms are best when the oil and CO_2 are acting as one phase or miscible condition.

Condition of miscibility for reservoir gas flooding depends on the composition of the flooded gas, composition of oil, and temperature (Green and Willhite 1998; Gu et al. 2013). The latest study (Chen. 2013; Ju.2012) summarize the detail effect of the three factors as follows:

- On the constant condition of the components in the injected gas and the components and properties of oil, the MMP increases with increasing the reservoir temperature.
- On the constant condition of the components in the injected gas and the reservoir temperature, the higher the content of C2~C6 and the lower the molecular weight in the crude oil, the smaller MMP. On the contrary, the more the heavy components in the crude oil are, the less favorable it will be for miscibility
- On the constant condition of the reservoir temperature and the components and properties of oil, the MMP decreases with increasing the content of intermediate components (CO_2, H_2S, and C2~C6) and increases with increasing the content of volatile components (CH_4 and N_2) in the injected gas.

Miscible CO_2 Injection may give a better recovery than hydrocarbon flood even though both of mechanisms appear to be the same. CO_2 has a much higher solubility in water than hydrocarbons and has been observed in laboratory experiments to diffuse through the water phase to swell bypassed oil until the oil is mobile. Thus, not only are screening criteria for depth and oil viscosity easier to meet in CO_2 flooding, but the ultimate recovery may be better than with hydrocarbons.

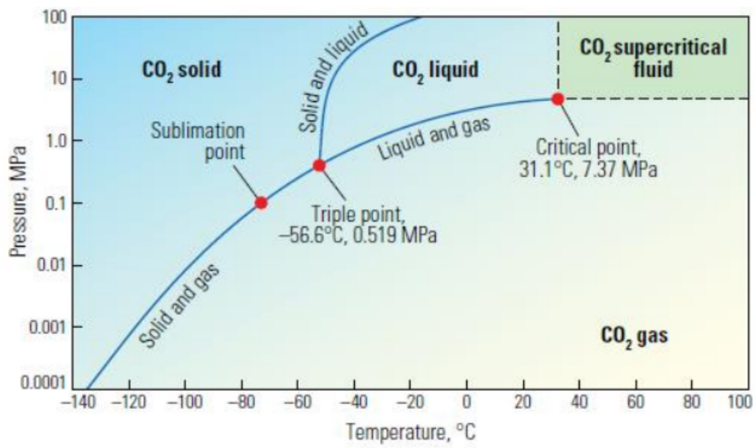

Figure 7-1. Carbon dioxide phases (M. Ansarizadeh, 2015)

7.1.2 Minimum Miscibility Pressure (MMP)

Miscibility in CO_2 flooding is defined as the physical condition between crude oil and CO_2 that will permit them to form a single homogeneous phase and mix in all proportions without the existence of an interface (Holm, 1986). Minimum Miscibility pressure (MMP) is defined as the lowest pressure at which a crude oil and solvent develop miscibility dynamically. Composition of the fluids (oil, gas, or solvent), pressure, and temperature of reservoir affect the miscibility.

7.1.3 Miscibility Behavior

Miscibility is defined as the physical condition between two or more fluids that permits them to mix in all proportions without the existence of an interface (IFT = 0). Miscibility conditions mainly depends on pressure, temperature and the fluids compositions. It is a condition at which two fluids can be mixed together so that no separation can be identified.

The miscibility behavior can be visualized using ternary diagram. Miscibility can be divided into first contact miscibility (FCM) and multiple contact miscibility (MCM). When crude oil and the injection fluids are directly miscible at the first contact, it is called FCM. However, first contact miscibility in field application of CO_2 injection is hard to achieve. For most reservoir temperature, high reservoir pressures are required to reduce the two phases region so that both the reservoir oil and injected fluid are in the single phase region. Multiple contact miscibility happens commonly at relatively lower pressure and after several contacts. So, the separation process occurs. Each separation process creates a new equilibrium and repeat again until miscibility is achieved.

Multi-contact miscibility can happen in three types which are vaporizing gas drive, condensing gas drive and condensing/vaporizing (CV) drive. In a vaporizing gas drive, when gas contact with oil, some oil intermediate components are vaporized to gas and enriched the gas. The enriched gas moves along and contacts fresh oil at the front, and the new contacts further enriches the gas. Within a finite number of contacts, the gas may be sufficiently enriched to develop miscibility with fresh oil. In a condensing gas drive (or enriched-gas drive), the gas is relatively enriched with intermediate components while the oil is relatively heavy. When gas first contacts the oil, some intermediate components condense from the gas to the oil, resulting in lighter oil. This lighter and enriched oil does not move as fast therefore is left behind and contacted by fresh gas. As a result, the enriched oil becomes further enriched, and after repeated contacts, the oil is sufficiently enriched to be miscible with fresh gas. The condensing/vaporizing gas drive, first described by Zick (1986) and Stalkup (1987), has features of both a vaporizing and a condensing gas drive. The transfer of intermediate components from gas to oil (condensation) and from oil to gas (vaporization) creates a condition whereby both oil and gas become miscible.

Pseudo-ternary phase diagram is used to illustrate the miscible displacement process. Schematic view of the phase triangles of CO_2 flooding processes at constant pressure and temperature. The miscibility behavior mainly includes these following behavior [9]:

1. Miscibility achieved by first-contact miscible

FCM procedure visualized by Figure 2a. When the oil composition lays closer to the side of the lighter components (C_{1-6}), the path of CO_2 injection is straight ahead from 100% CO_2 side to where the oil lays. Miscibility will be directly achieved by the first contact because CO_2 injection bypasses the two-phases area.

2. Miscibility achieved by multiple-contact miscible

When the oil composition lays on the right-hand side of the phase triangle but not close enough to the side of the lighter components, C_{1-6} and closer to critical tie-line, the injection pathway of CO_2 injection will cross the two-phases area (miscibility gap) and originate a transition zone as presented in Figure 2b. New equilibrated CO_2-rich injection gas and new extraction phase converge. This process continues until miscibility is achieved by multiple-contact miscible.

3. Miscibility cannot be achieved

When the oil composition has a high ratio of heavier components (C_{7+}), it lays on the left-hand side of critical tie-line. For each new injection, the pathway of CO_2 will always cross the two-phase area. There is no way to achieve miscibility because the heavier parts of the crude are not extracted by the CO_2 remain in the formation. This kind of immiscible behavior is given in Figure 2c.

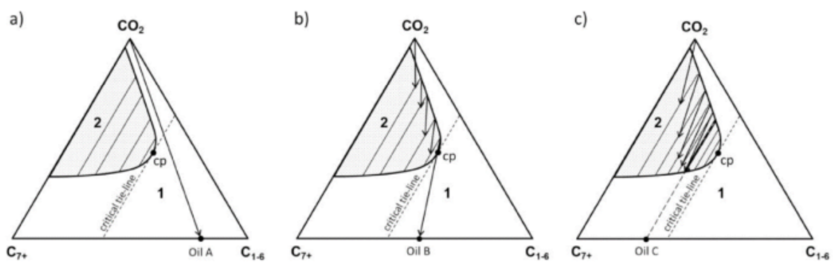

Figure 7-2. Miscibility behavior (Rommerkirchen et al. 2016)

7.1.4 MMP Determination Method

MMP can be estimated either experimentally, empirically or using computational method. In laboratory, it can be measured using slim-tube test (Yelling and Metcalfe, 1980), rising-bubble experiments (Christianson and Haines, 1987) and vanishing-interfacial-tension tests (Rao, 1997). Slim-tube results are reliable as real fluids are used. However, it is time consuming and expensive to conduct. The rising bubble and vanishing interfacial test can not completely capture the multiple contacts mechanism. Many empirical correlations have been developed to estimate MMP by fitting experimental data based on range of reservoir condition, reservoir fluid and injected fluid properties. But since thermodynamic properties are hard to predict in near critical region, then it may lead to different real value of MMP.

Due to drawbacks of experimental method, computational method for MMP estimation were developed. Computational method provides a fast and cheap alternative in MMP estimation. They are also indispensable tools in tuning equations of state to MMP for compositional simulations. There are three types of computational methods to estimate MMP: numerical simulation of slim-tube, analytical methods, and mixing cell (cell-to -cell) methods. In this study cell to cell computational and 1-D slimtube simulation method is used to estimate MMP.

7.1.4.1 Mixing Cell (Cell to Cell) Method (PVT/EoS Simulation Test)

The mixing cell method consists of one or a series of virtual PVT cells in which phase equilibrium calculations are performed. The basic idea in these single and multiple mixing cell methods is to mix (analytically) gas and oil in repeated contacts, resulting in new equilibrium compositions.

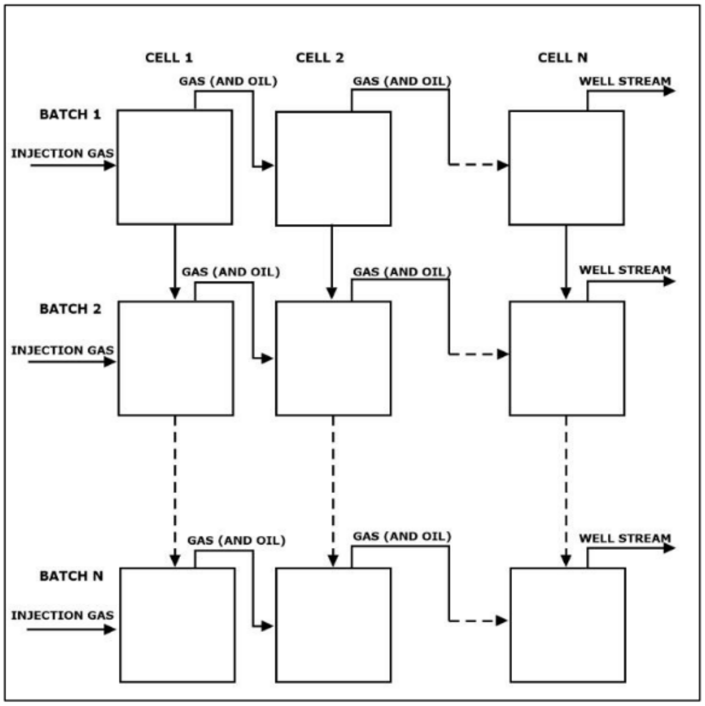

Figure 7-3. Basic principle of cell to cell calculation (Pederson, 1985)

Figure 3 shows the illustration of cell to cell method's basic principle. Number of cells of equal volume is kept constant and the temperature and pressure are all the same in each cell. All the cells contain initially the same fluid. A specified amount of gas is added to cell 1. It is assumed that perfect mixing takes place, and that thermodynamic phase equilibrium is reached. After mixing of the injected gas and the cell fluid, the gas plus liquid volumes will be larger than the assumed cell volume. The excess volume from cell 1 is transferred to cell 2. If two phases are present, gas and liquid, are moved according to their relative phase mobilities.

The excess volume from cell 2 is transferred to cell 3 and so on. When one batch calculation has been completed, a new injection into cell 1 can take place, and the cell to cell calculation is continued. The composition of the injected gas may be changed from batch to batch. (Pederson, et al., 1985).

7.1.4.2 1-D Slimtube Simulation Test

1-D slim-tube simulation is used in this study that provide more accurately, cost-effective, and quick in estimate the CO_2 MMP. Slim-tube is saturated with crude oil and the injection gas, then the miscibility conditions are determined by applying different injection pressures. Every single injection pressure corresponds to a recovery factor resulted by 1.2 Pore Volume (PV) of injected gas, where the displacement as miscible one near 1.2 PV of injected gas and correlated the crude oil color degradation from dark black to yellow to multi-contact miscibility development (Yellig and Metcalfe, 1980). The points must be taken from tests with the same reservoir fluid, injection gas, test temperature, and using the same injection pressure being the only variable. In the end, oil recovery vs pressure is plot and then interpretation is conducted to determine the MMP, in the other hand MMP can be defined as the break-over point on the plot of oil recovery to injection pressure. Fig. 1 shows plot of recovery factor against pressure, which emphasizes the value of MMP at the point where the break-over occurs.

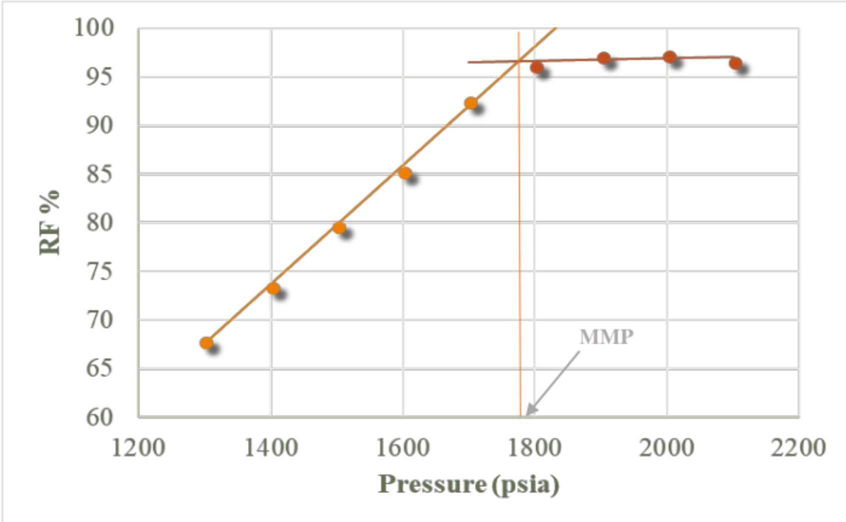

Figure 7-4. MMP determination using break-over point

7.2 MMP Results of Langgak Field

7.2.1 PVT/EoS Simulation

The simulation used oil composition from Langgak Field shown in **Table 1. Table 2** shows the reservoir current condition pressure and temperature, and oil density.

Table 7-1. Oil composition of Langgak Field

Component		Mole Percent
Hydrogen Sulfide	H_2S	0
Carbon Dioxide	CO_2	0.56
Nitrogen	N_2	0
Methane	C_1	0.67
Ethane	C_2	0.67
Propane	C_3	1.51
Iso-Butane	i-C_4	0.9
n-Butane	n-C_4	1.57
Iso-Pentane	i-C_5	1.56
n-Pentane	n-C_5	1.5
Hexanes	C_6	0.35

Heptanes Plus	C_{7+}	90.71
Total		**100**

Table 7-2. Additional reservoir data in Langgak Field

Pb	113	psig
Tres	136	F
API	30.8	deg

The calculation of MMP was obtained using Multiple Contact Miscibility Calculation tool in a commercial phase behavior and fluid property program, CMG Winprop. MMP may be determined based on the amount of solvent composition and range of pressure to be tested. The steps of building the EOS model is as follows:

a. Titles/EOS/Units: Choose the model basis included equation of state for the oil and gas phases (Peng-Robinson 1978), units (pressures in psia and temperatures in Fahrenheit degree), and feed (form composition is in moles, mole fractions, or mole percent).
b. Component Selection/Properties: Insert all the components; oil, CO_2, and additives. For components that are not available in Library Component, insert individually the properties of component included molecular weight, specific gravity, and boiling point. Correlations used for physical properties, critical properties, and acentric factor are respectively Twu, Twu, and Lee-Kesler as the default correlation.
c. Composition: Insert the composition of each component in mole percent. The oil composition is considered as primary composition while injected gas composition (CO_2 and additives) as secondary composition.
d. Saturation Pressure: Enter the reservoir temperature and saturation pressure.
e. Two-phase Envelope: For simulation that using cell-to-cell method, the pseudoization scheme needs to have a value of 1, 2 or 3 to group a given component into the first, second or third pseudo-component respectively. It is used to determine the post-processing step in ternary plots.

f. Multiple Contacts: Input the temperature condition of reservoir, solvent increment ratio (default = 0.01), and equilibrium gas/original oil mixing ratio (default value = 0.1). Solvent increment ratio is defined as the enhancement of solvent added to oil molar ratio for each mixture. Select starting pressure, amount of pressure step, and maximum number of pressure steps that indicates the number of cells. MMP/MME calculation method used is cell-to-cell simulation.

g. Run the simulation

This methodology has been applied and validated using the oil model of "M" Field from the previous study about Evaluation of Minimum Miscibility Pressure (Berylian, 2017).

CO_2 flooding simulation is conducted using oil composition data from Langgak Field. The depth of reservoir is 1100-1300 ft. It has more than 90% mole C_{7+} and the additional reservoir data used can be seen in **Table 1**. The MMP for 100% CO_2 injection at temperature 136^0 F equals to 3197 psia.

7.2.2 1-D Slimtube Simulation

1-D slim-tube simulation model has been performed to reproduce the slim-tube experiment condition as shown as Figure 5 below. Basic model will be the same as slim-tube experiment parameters, include porosity of 38.8%, permeability 700 mD, as shown in the **Table 3**. The oil composition used from Langgak Field shown in **Table 1**. Slim-tube characteristic and data adapted from the experiments in EOR Laboratory of Sejong University, South Korea (Muslim and Permadi, 2015). Those are injector well with constraint of BHF total reservoir fluid rate and producer well with bottom hole pressure constraint.

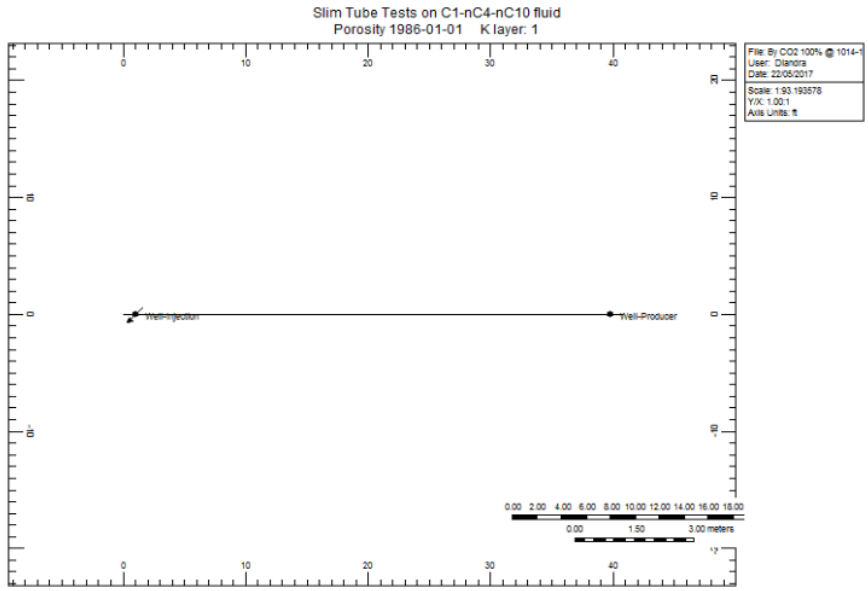

Figure 7-5. 1-D slimtube simulation model

Table 7-3. Slimtube characteristics

Characteristics	Value	Unit
Length	1242	cm
Inside Diameter	0.45	cm
Porosity	38.8	%
Permeability	700	mD

In general, miscible displacements were defined to have final recoveries at 1.2 PV of CO_2 injected; which were equal to or very near the maximum final recovery obtained in a series of tests. In order to determine the CO_2 MMP for a given test oil at a fixed temperature, CO_2 displacements test were conducted at various pressure levels. Final recoveries were then plotted as percent recovery vs test pressure (Yellig and Metcalfe, 1980). Wu and Batycky (1990) conclude that for the MMP criteria is 90+% oil recovery at 1.2 PV of solvent injection for indicative multiple-contact miscibility process. The MMP value is determined from the break-over point in percent recovery vs test pressure plot (Elsharkawy et al, 1992) as shown in Figure 6.

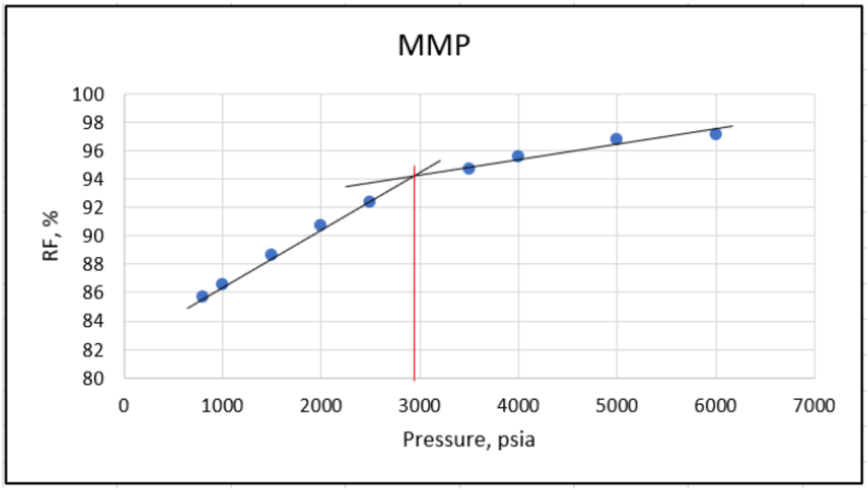

Figure 7-6. MMP of Langgak Field from 1-D simulation result

The above plot result denotes that MMP will be achieved at the pressure of 2935 psia with reservoir temperature 136^0 F.

CHAPTER VIII
CO_2 INJECTION PERFORMANCE: SINGLE WELL, COREFLOODING & 2-WELL SIMULATION

8.1 Introduction

CO_2 EOR method is one of promising EOR method lately. By injecting CO_2 into the reservoir to reach the miscibility with the oil within the advancement of technology and demand of petroleum industry to maximize the oil/gas recovery or profit gain, this enhanced oil recovery method has attracted more attention in the past few years. Many countries have historically applied this method in reservoir with medium to light gravity oils referring to which currently active in the United States in Colorado, Mississippi, New Mexico, etc. The result is promising to enhance oil recovery. There are two conditions in CO_2 injection EOR method; miscible and immiscible as following:

a. If the reservoir pressure/injection pressure is higher than the MMP between the crude oil and CO_2, the CO_2 injection is classified as a miscible solvent injection. Since, under miscible crude oil-CO_2 conditions, interfacial tension (IFT) and capillary pressure (P_c) tend to be zero or negligible, the residual oil saturation reduces to a low value in miscible CO_2 injection (Holm, 1986; Nobakht et al., 2008).
b. If the reservoir pressure is lower than the MMP between the crude oil and CO_2, the CO_2 injection is classified as an immiscible solvent injection.

Besides, there are several methods used in CO_2 injection. One of the most common method and to be focused in this study of CO_2 injection EOR method known as the huff and puff method, a slug of gas or solvent is injected into the reservoir either in miscible or immiscible condition (huff cycle). After injection, the well is shut-in for a "soak" period to allow for gas/solvent interaction with the formation oil to reach the equilibrium and then the production is resumed through the same well (puff cycle). The whole process of huff and puff can be seen in figure

VIII.2. This method has shown great potential for enhancing the oil recovery in light oil reservoirs (Thomas and Monger, 1990). CO_2 huff and puff does not require a high remaining oil saturation and is thus well-suited to fields exhibiting high water cuts (Thomas and Monger, 1990). It has been reported that oil swelling and viscosity reduction effects combining with changes in gas/oil relative permeabilities resulted in an increase of oil recovery obtained by CO_2 huff-and-puff process.

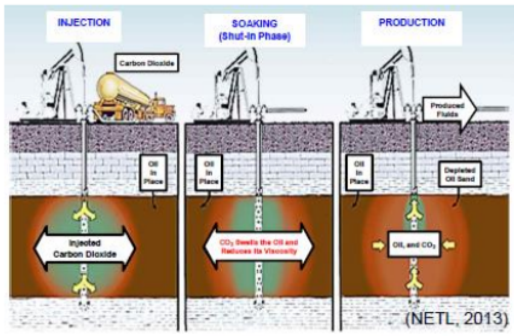

Figure 8-1. Huff anf puff method process
Source: National Energy Technology Laboratory, NETL

Injection method always related to MMP of which to determine the injection fluid condition with the reservoir fluid. The minimum miscibility pressure (MMP) of a crude oil–CO_2 system at a specified temperature is defined as the minimum pressure under which CO_2 can achieve miscibility with the crude oil (Dong et al., 2001). The MMP can be commonly categorized into first-contact miscibility (FCM) and multi-contact miscibility (MCM) pressures. In FCM conditions, the CO_2 is miscible with crude oil mixed in any proportions (Holm and Josendal, 1974; Holm, 1986). However, in practice, it is difficult to achieve FCM in crude oil– CO_2 systems, especially at high temperatures. Therefore, the term MCM or dynamic miscibility is more commonly used for multi-component systems wherein miscibility between the CO_2 and some of the lighter components of crude oil starts earlier than the others at certain pressures and temperatures.

Mechanisms contributing to increase oil recovery in cyclic solvent injection processes include oil viscosity reduction, oil swelling due to dissolution of gas in crude oil, solution gas drive aided by gravity drainage, vaporization of lighter components of oil, interfacial tension reduction, and relative permeability effects (Mohammed-Singh et al., 2006; Shi et al., 2008).

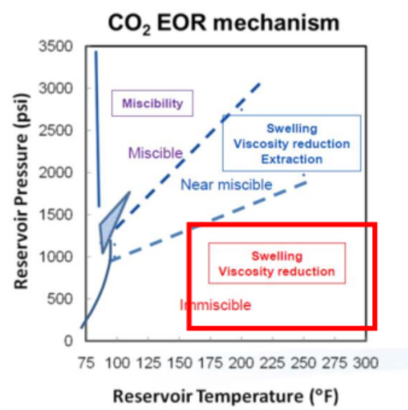

Figure 8-2. Driving mechanism in each CO2 injection condition (Klins, 1984)

Generally, CO_2 injection in miscible condition is better to enhance more oil recovery than the immiscible condition. These can be explained by discussing its driving mechanism shown in **Figure 7**. In near-miscible and miscible CO_2 injection processes in which the pressure is near and above MMP, the extraction of lighter components by CO_2 is the greatest governing mechanism. Generally, in most cases, FCM between crude oil and CO_2 cannot be achieved. However, CO_2 becomes miscible with the crude oil through two-way interfacial mass transfer between crude oil and CO_2 phases and produces dynamic miscibility or MCM (Holm and Josendal, 1974; Nobakht et al., 2008). At the specific pressure below the MMP, which is the so-called "extraction pressure", the interfacial tension reduces to a definite amount at which the significant level of mass transfer between crude oil and CO_2 occurs and the extraction and vaporization of lighter components is initiated. Reduction and elimination of interfacial tension decreases the capillary pressure and increases the capillary number, which, together, improve the recovery efficiency.

8.2 Single Well Simulation for CO_2 Huff and Puff Injection

8.2.1 Well Properties

Langgak-24 Well is proposed as CO_2 injection well. This well penetrates three sand zones (P,A and B Sand) and two perforations are opened in A-Sand.

Depth of perforations are in 1180 – 1186 ft MD and 1195 – 1201 ft MD. Well log interpretation and well configuration are shown in the following figure:

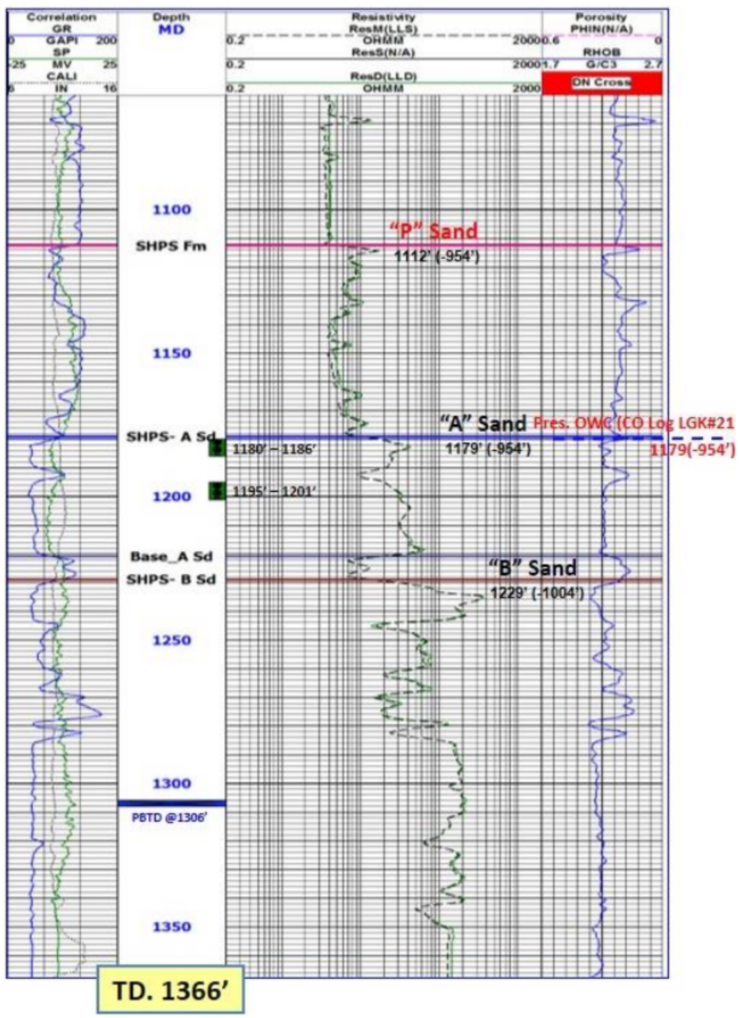

Figure 8-3. Well log interpretation and well configuration of LGK-24 Well

Single well 3-D model is built by using cylindrical grid distribution. The total grid of this model is built on 336 grid blocks that represents the reservoir model with 21-i (radial) divisions, 4-j (angular) divisions, and 40-k divisions with outer radius of outermost block equals to 1000 ft. The model represents the Langgak-24 well itself with only targeted injected layers which are P-Sand and A-Sand at reservoir depth 1100-1230 ft MD. The simplified model can be seen in Figure 9.

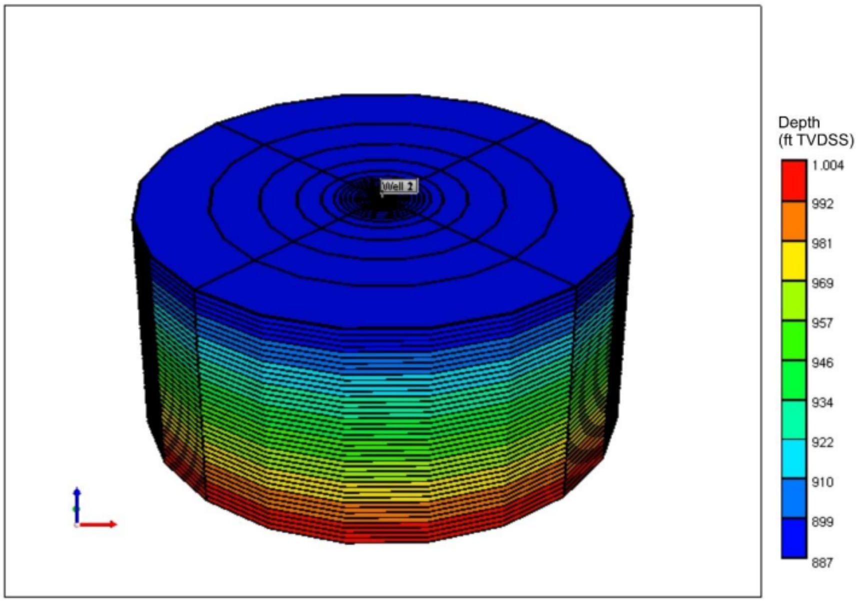

Figure 8-4. 3-D model of Langgak-24 well

The proposed injection mechanism was divided into several phases as following:

1. Production phase
2. Injection phase
3. Soaking phase

Injection mechanism of the trial study was divided into two phases. 1st phase is production which was in the condition where the injection had not been conducted which was the period in February 1st 1989 to June 30th 2018. The well was shut-in for the end of 1st production phase. As for the 2nd phase was in the condition where the injection had been conducted for several times. After that, the soaking period begin to be conducted. One cycle of injection is measured from the beginning period of injection phase to the end of soaking phase. This cycle parameter will be designed according to the success project conducted in Meruap

Field combining to the study from Rido (2018). The well will be converted again to be producer after the soaking time finished.

For preliminary forecasting, Injection scheduling uses the study from Rido (2018) in evaluating for CO_2 Huff and Puff Injection cunducting in Meruap Field. This study states that the optimum condition of CO_2 Huff and Puff Injection is the longest period of interaction between CO_2 and oil reservoir. Then decision of the design should consider the economic evaluation for further study. To compare the advantage of CO_2 Huff and Puff Injection to conventional production, assumed the supplies of CO_2 are excess. The best injection scheduling is obtained from sensitivity of injection and soaking time period.

8.2.2 Simulation Results

Two cases are developed to compare between the conventional production and CO_2 Huff and Puff Injection:

1. Case 1 : conventional production for 549 days
2. Case 2 : 7 days of preparation, 30 days of injection, 30 days of soaking and 482 days of production

The simulation forecasting begins on the 1st of July 2018 and will end on the 1st of January 2020. Simulation constraints set to 320 STBD of liquid rate and minimum BHP at 400 psi (according to simulation result of hypothetic model at latest time of production data). The results for these cases are shown in the following figure.

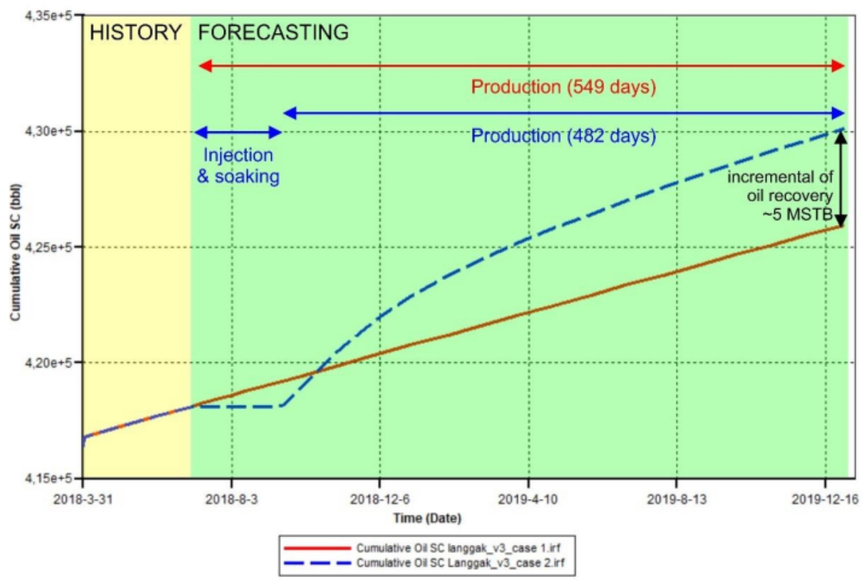

Figure 8-5. Cumulative oil production between conventional production and CO_2 Huff and Puff Injection

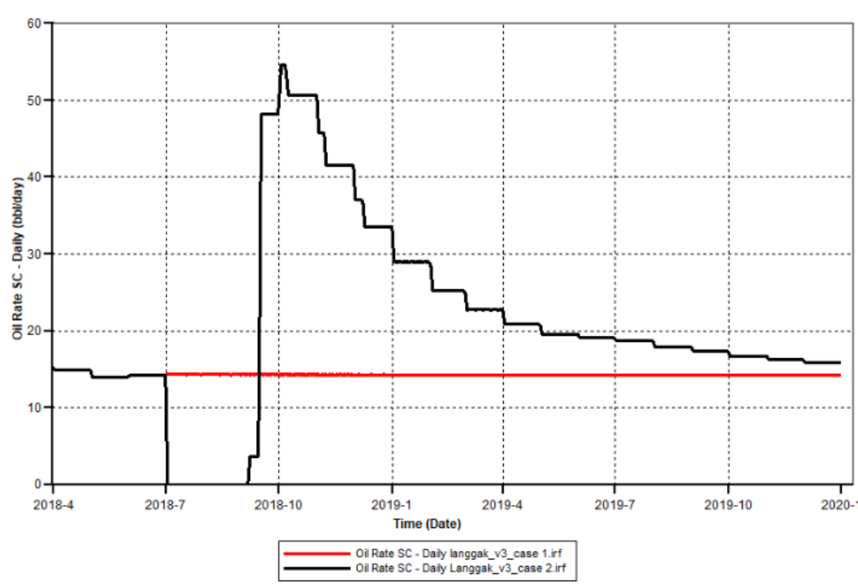

Figure 8-6. Oil rate between conventional production and CO_2 Huff and Puff Injection

The viscosity reduction is a part of effects on incremental recovery of CO_2 Huff and Puff Injection method. The viscosity of oil in the reservoir decreases until reach 2 times than initial beacause of interaction between CO_2 gas and oil reservoir. The distribution of oil viscosity within the reservoir is shown in the following figure.

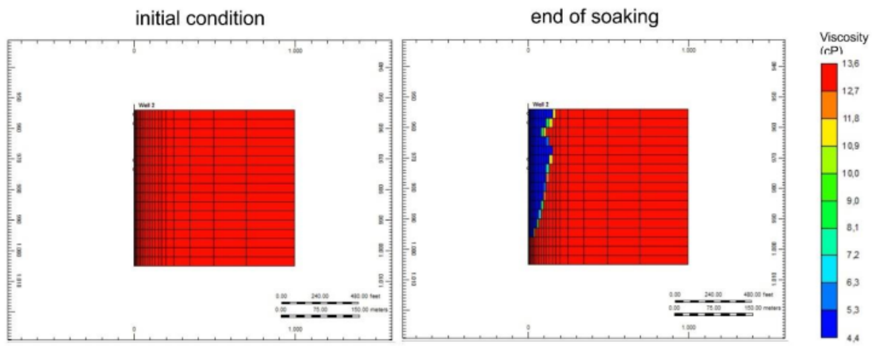

Figure 8-7. Viscosity reduction during injection CO_2 and soaking period

To determine the best injection and soaking period scheduling technically for Langgak Field, sensitivity analysis for these parameters are conducted. The detail of cases developed for sensitivity analysis are shown in the following table.

Table 8-1. Detail of cases for sensitivity analysis

	Case		Explanation
30 days of soaking time	3	45	days of injection
	4	55	days of injection
	5	75	days of injection
75 days of injection time	6	45	days of soaking
	7	60	days of soaking
	8	75	days of soaking
75 days injection – 30 days soaking	9	30	ton/day of injection rate
	10	50	ton/day of injection rate

The results for the sensitivity analysis are shown in the following figures:

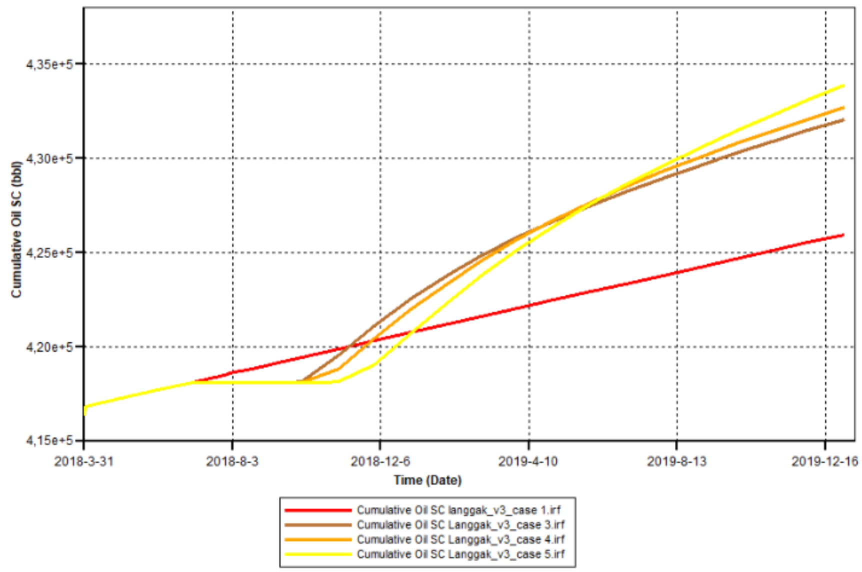

Figure 8-8. Cumulative oil production for injection time sensitivity [case 1 (no EOR), 3, 4, and 5]

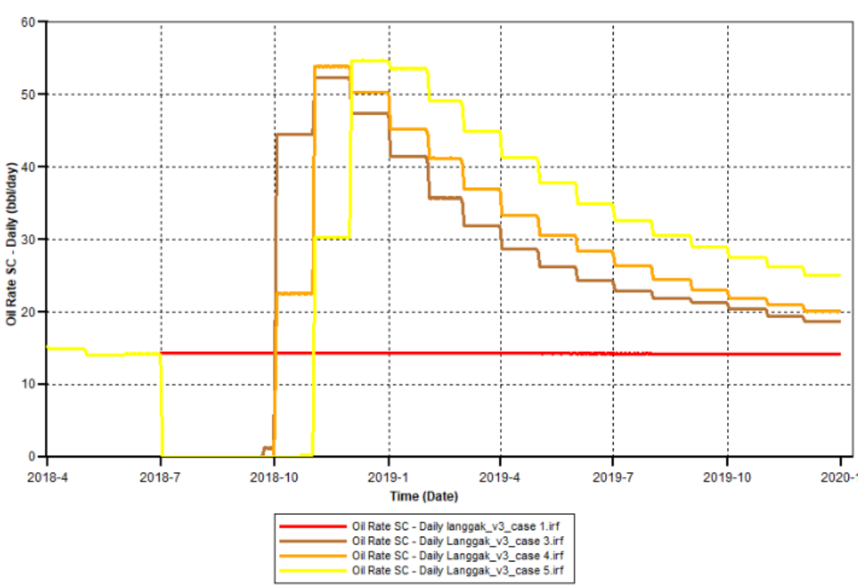

Figure 8-9. Oil rate for injection time sensitivity [case 1 (no EOR), 3, 4, and 5]

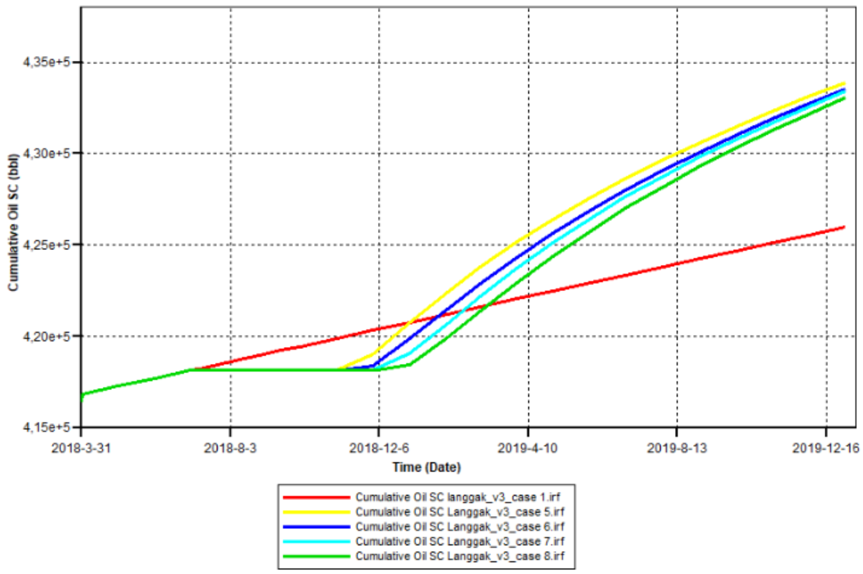

Figure 8-10. Cumulative oil production for soaking time sensitivity (case 1(no EOR), 5, 6, 7,and 8)

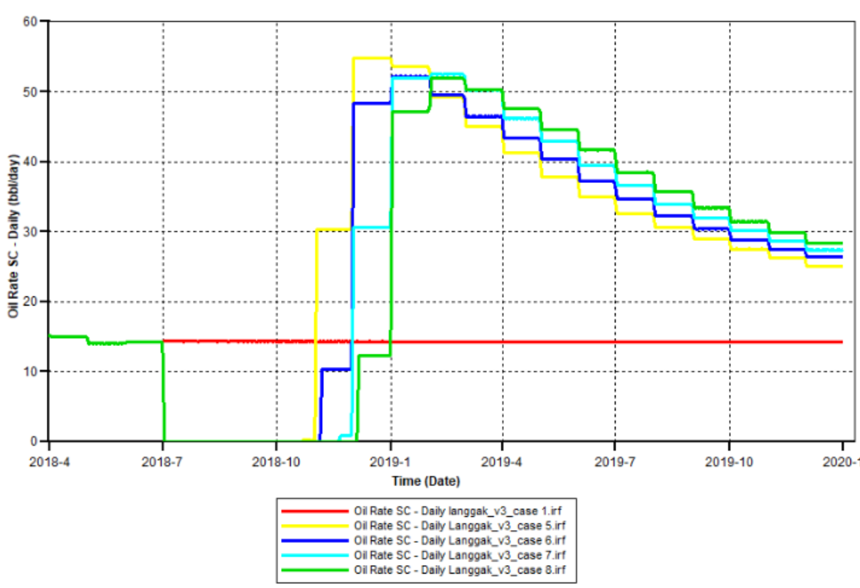

Figure 8-11 . Oil rate for soaking time sensitivity (case 1(no EOR), 5, 6, 7, and 8)

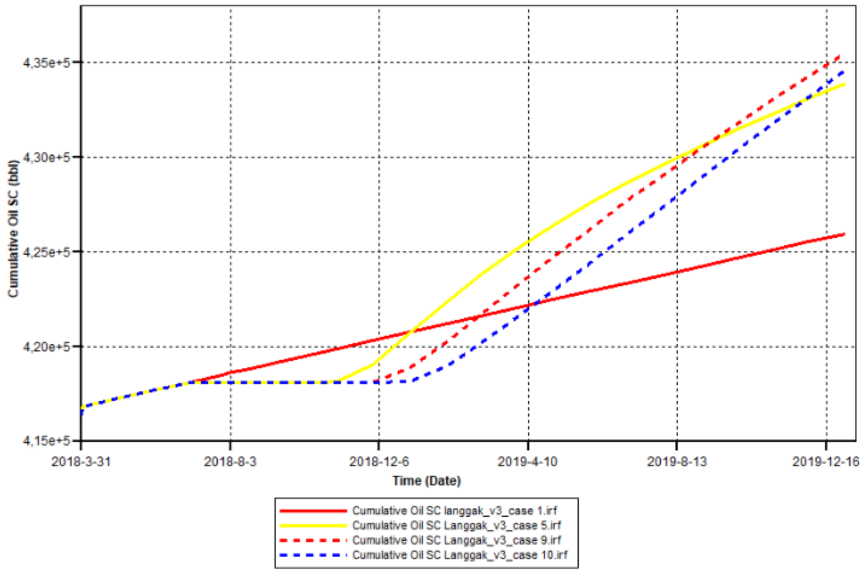

Figure 8-12. Cumulative oil production for injection rate sensitivity (case 1(no EOR), 9,and 10)

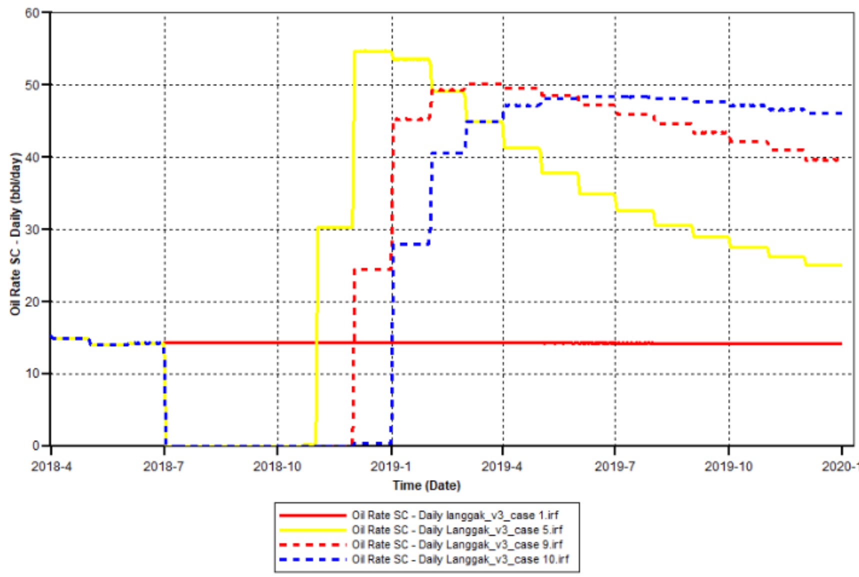

Figure 8-13. Oil rate for injection rate sensitivity (case 1(no EOR), 9,and 10)

According to Figure 8-8, the more time taking for injection, the more oil will recover as case 5 produces more oil than case 3 and 4. Oil rate declining (Figure 8-9) for case 5 is lower than other cases because more CO_2 are injected into the reservoir and more time is taken for CO_2 and oil interaction. Hence, the more oil volume will reduce in its viscosity.

On the other hand, the more duration taking for soaking time can not afford more oil recovery (Figure 8-10). Figure 8-11 shows the declining of oil rate for case 6, 7, and 8 are decreased respectively. However, the lower declining oil rate of case 8 can not afford the late time of beginning of its production phase.

According to Figure 8-12 and Figure 8-13, the more higher injection rate will create lower declining of oil rate. It is due to the more amount of CO_2 injected into reservoir. Another cause of higher injection rate is delaying oil production. CO_2 which is not miscible will produce first, then it makes 50 ton/day of injection rate doesn't give more oil recovered than 30 ton/day of injection rate.

The summary results of these sensitivity analysis are representated in the following table (for only 1.5 years of development scenario),

Table 8-2. Summary results of all cases

	Case	Explanation	Additional / Total Cumulative Oil Recovery (MSTB)	CO2 Injected (ton)
	1	Basecase	3.4/426	0
30 days of soaking time	2	30 days of injection	7.5/430.1	300
	3	45 days of injection	9.4/432	450
	4	55 days of injection	10.1/432.7	550
	5	75 days of injection	11.3/433.9	750
75 days of injection time	6	45 days of soaking	10.9/433.5	750
	7	60 days of soaking	10.8/433.4	750
	8	75 days of soaking	10.5/433.1	750
75 days injection – 30 days soaking	9	30 ton/day of injection rate	12.9/435.5	2250
	10	50 ton/day of injection rate	12/434.6	3750

8.3 Coreflood Simulation for CO_2 Huff & Puff Injection

As the limit of laboratory experiment tools and opportunity, coreflood simulation is conducted to forecast the performance of CO_2 injection to core sampel 3-D model of Langgak Field. Coreflood model is built homogeneous which means the permeability and porosity are equal for each grid. The model is shown in the following figure:

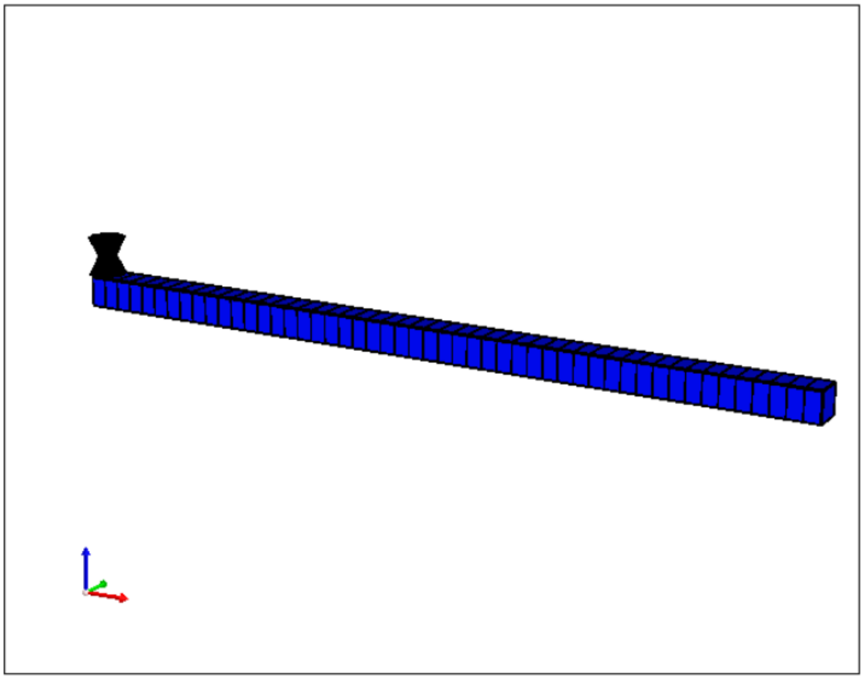

Figure 8-14. 3-D model for coreflood simulation

The properties of core model in simulation are adjusted to core sample data from SCAL to the sample. Model is initialized to reach similar paramaters to the real data such as: pore volume, fluids saturation, and initial oil in place.

The study of coreflood simulation for Huff & Puff method is proposed to identify the potential of injection cycle. Injection rate sets to the rate which creates bottom hole pressure equals to fracture pressure of reservoir (mostly 1000-1500 psi). To ensure the comparison, volume of CO_2 injected inside core, total duration of injection (3.6 hours) and total duration of soaking (1 day) are set similar.

Three cases are developed according to injection cycle:

1. 1 cycle (injection-soaking-production)
2. 2 cycle (injection-soaking-injection-soaking-production)
3. 3 cycle (injection-soaking-injection-soaking-injection-soaking-production)

8.3.1 Simulation Results

The results of simulation are represented by the following figure:

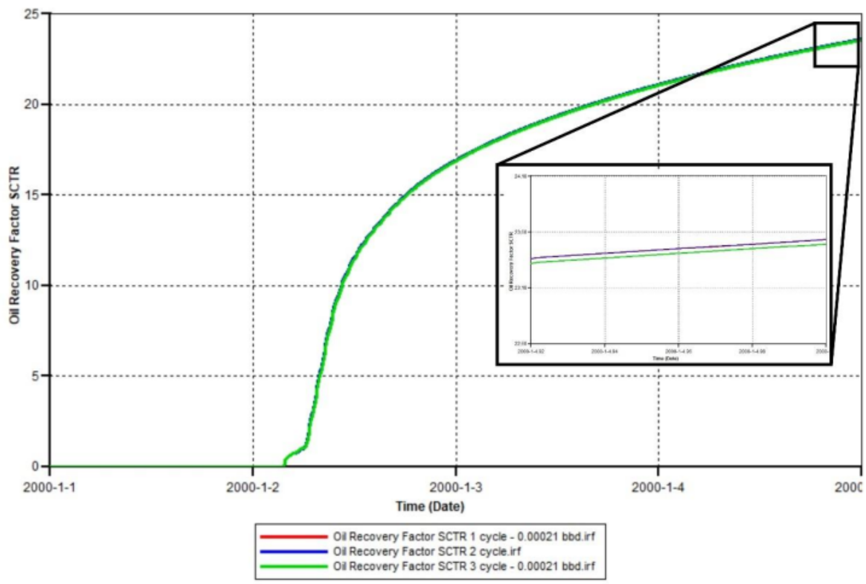

Figure 8-15. Oil recovery factor of CO_2 coreflod huff and puff injection

Core is injected by CO_2 using 1.4 cc/hr injection rate which gains 1500 psi core pressure after injection period. There is no significant different of oil recovery factor for all cases. Case 1 and case 2 gain 23.61% oil RF as case 3 gains lower with 23.57% oil RF.

The general method of coreflooding for CO_2 Huff & Puff injection is not available. Some problems found when running simulation. Pressure system of core drops significantly during production. The fluid (CO_2, oil and water connate) are avoided to interact with another fluid from outside, then there is no pressure support to maintain the pressure of coreflood. These conditions created small oil recovery factor for these experiments (less than 25%).

The pressure of core at everytime is shown in the following figure:

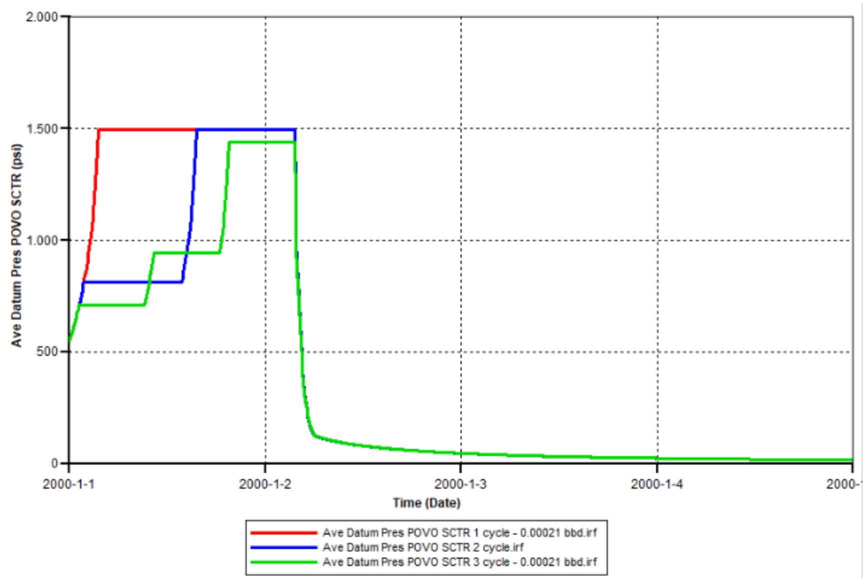

Figure 8-16. Pressure of core during experiment

The lower oil RF of case 3 is indicated by the lower pressure of core resulted at the end of injection and/ soaking period at final cycle than another cases. This phenomenon shows that interaction between CO_2 and oil are increased due to lower core pressure resulted. Volume of CO_2 which dissolved into oil for case 3 must be higher than other cases as the amount of CO_2 injected are set similar, on the other hand core pressure are lower.

8.4 Coreflood Simulation for CO_2 Continuous Injection

By using similar model with Coreflood Huff & Puff Injection, the core is reconstructed by adding injector well in the other side of core model. The simulation is proposed to identify the role of CO_2 interaction with Langgak Oil whether as displace component only or EOR.

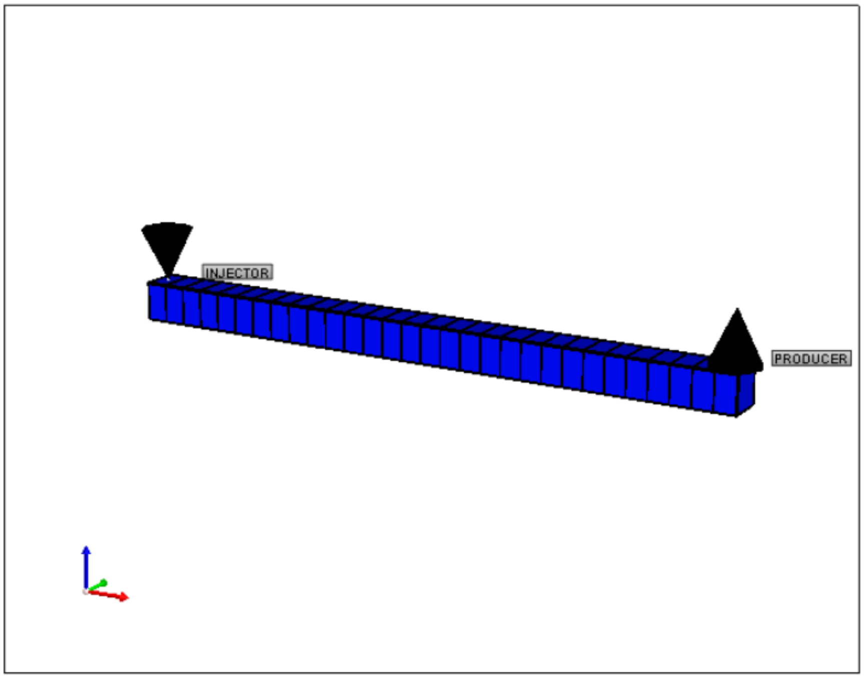

Figure 8-17. 3-D model for coreflood simulation (continuous injection)

Three cases of injection rate are developed for this simulation:

1. 10 cc CO_2/hr
2. 30 cc CO_2/hr
3. 50 cc CO_2/hr

Core is set in 0.2 water saturation as water connate saturation, then oil will be the only fluid displaced during injection of CO_2.

8.4.1 Simulation Results

Oil recovery factor results of CO_2 coreflood continuous injection for all cases are represented by the following figure:

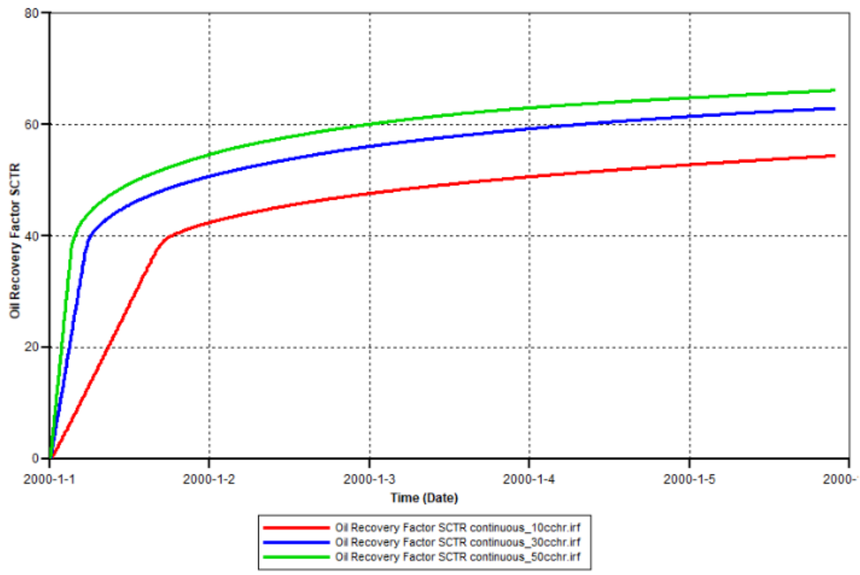

Figure 8-18. Oil recovery factor results of CO_2 continuous injection for coreflood simulation

Case 3 (50 cc CO_2/hr) has a highest oil recovery than other cases. Fingering phenomenon will not be identified due to homogenous model and single "z" (vertical) layer. High injection rate will increase the displacement and interaction between CO2 and oil beside its role as EOR.

The following figure will show the fraction of cumulative CO_2 injected and oil produced to pore volume:

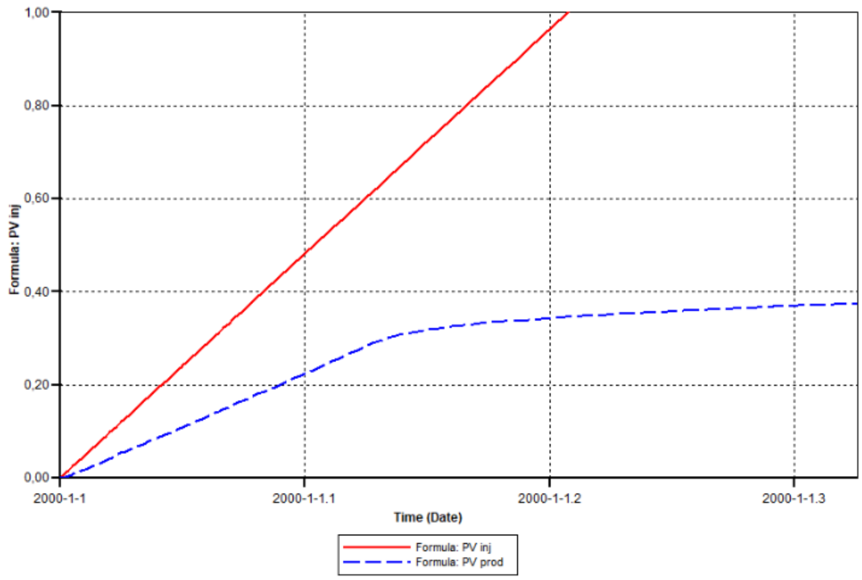

Figure 8-19. Fraction of cumulative CO_2 injected and oil produced volume to pore volume for case 3 (50 cc CO_2/hr)

According to the previous figure, the only displacement phenomenon doesn't happen because the injection fraction is higher than production fraction. It means some of CO_2 dissolved into oil phase and working as EOR method.

8.5 2-well Simulation for CO_2 Continuous Injection

To identify the potential of CO_2 Injection in the form of continuous method, the simulation of 2-well CO_2 continuous injection is conducted in the 3-D model of Langgak Field. LGK-24 well will be producer and LGK-15 well is converted to be injector. The following figure represents previous explanation:

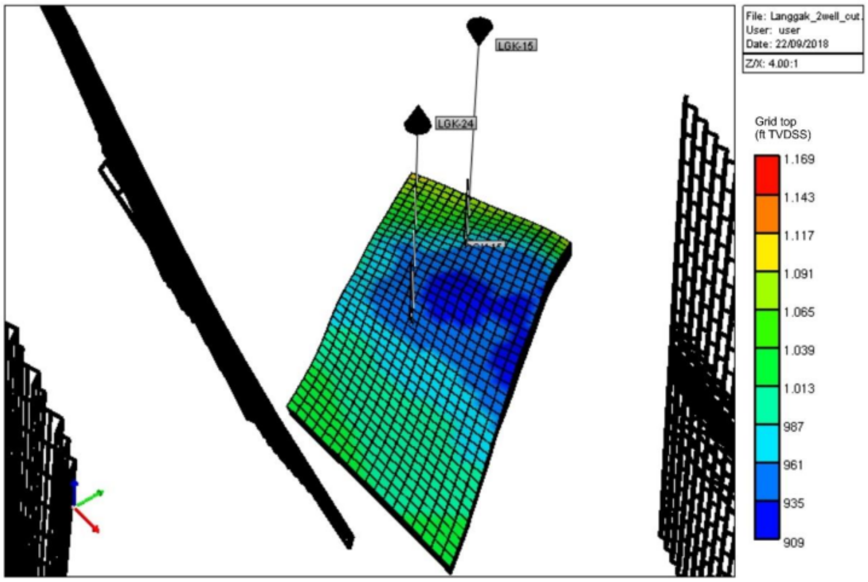

Figure 8-20. 3D model for 2-well simulation

Three cases are developed to see the potential of CO_2 Continuous Injection:

1. 10 ton CO_2/day injection rate
2. 30 ton CO_2/day injection rate
3. 50 ton CO_2/day injection rate

8.5.1 Simulation Results

Cumulative oil recovery and oil rate for each cases are represented by the following figures:

E

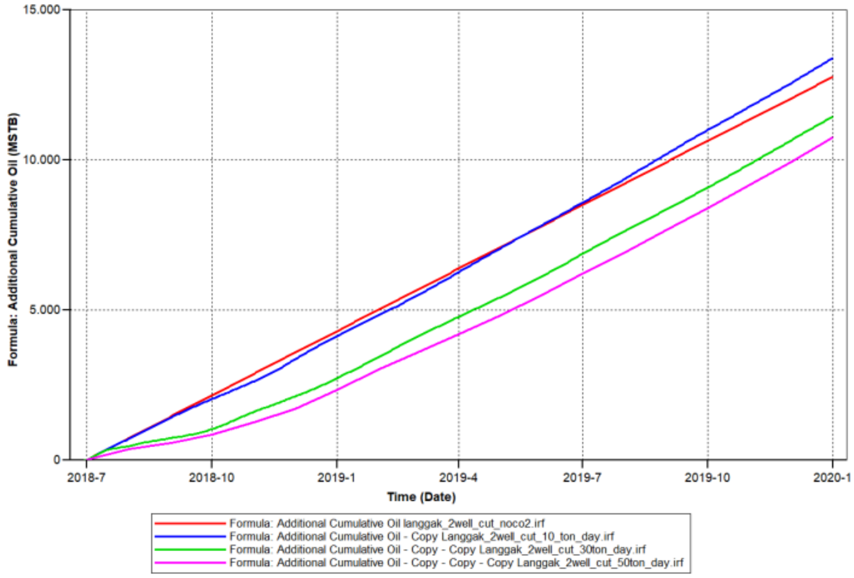

Figure 8-21. Additional cumulative oil for 3 cases of 2-wells CO_2 Continuous Injection

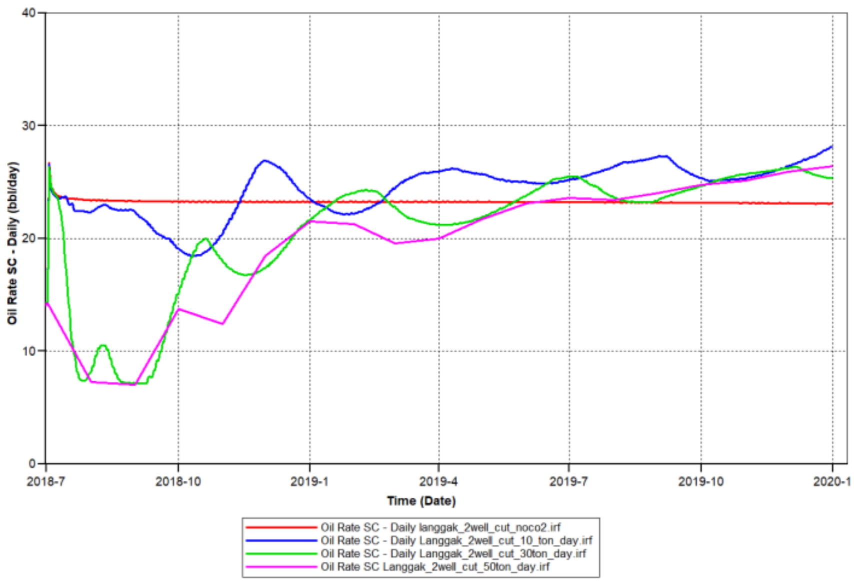

Figure 8-22. Oil rate for 3 cases of 2-wells CO_2 Continuous Injection

Table 8-3. Additional cumulative oil recovery results for 2-wells CO_2 Continuous Injection

Case	Explanation	Additional Cumulative Oil Recovery (MSTB)	CO2 Injected (ton)
Basecase (w/o CO2 injection)		12.07	0
1	10 ton CO2/day	13.04	5480
2	30 ton CO2/day	11.04	16440
3	50 ton CO2/day	10.08	27400

Case 2 and case 3 creates lower additional cumulative oil than no CO_2 injection time. In initial period of injection, oil rate of case 2 and case 3 are lower than no CO_2 injection case, but they can afford the oil rate in the middle of development (as EOR mechanism).

The initial time of injection period increases water cut then oil rate of case 1, 2 and 3 drop under the no CO_2 injection case. Case 3 (50 ton CO_2/day injection rate) creates the highest water cut. For these cases, as CO_2 injected is not miscible to oil, the role of CO_2 changes to be the displacement component is dominant than than EOR method, from well LGK-15. On the other hand, even the lower rate for these cases, 10 ton CO_2/day injection rate, basically creates more volume injecting into reservoir than production fluid out of reservoir. This condition is represented by the following figure:

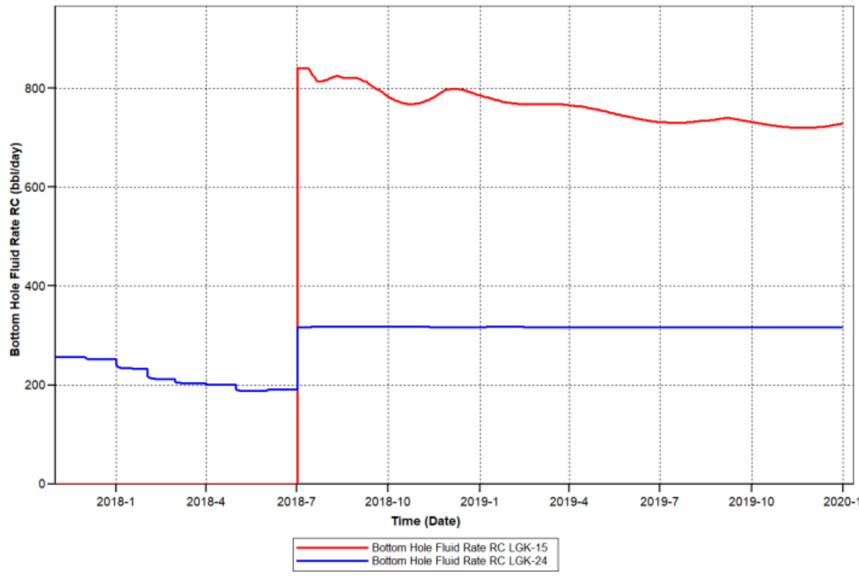

Figure 8-23. Bottom hole fluid rate of LGK-15 and LGK-24 wells for 10 ton CO_2/day injection rate

According to material balance, volume accumulation of reservoir will increase during injection period because of higher volume of inlet than outlet. It will increase reservoir pressure automatically. As a consequence, fracture pressure of formation must be considered to be the additional limit parameter in designing CO_2 continuous injection. The reservoir pressure results for three cases are represented by the following figure.

Figure 8-24. Reservoir pressure during injection period

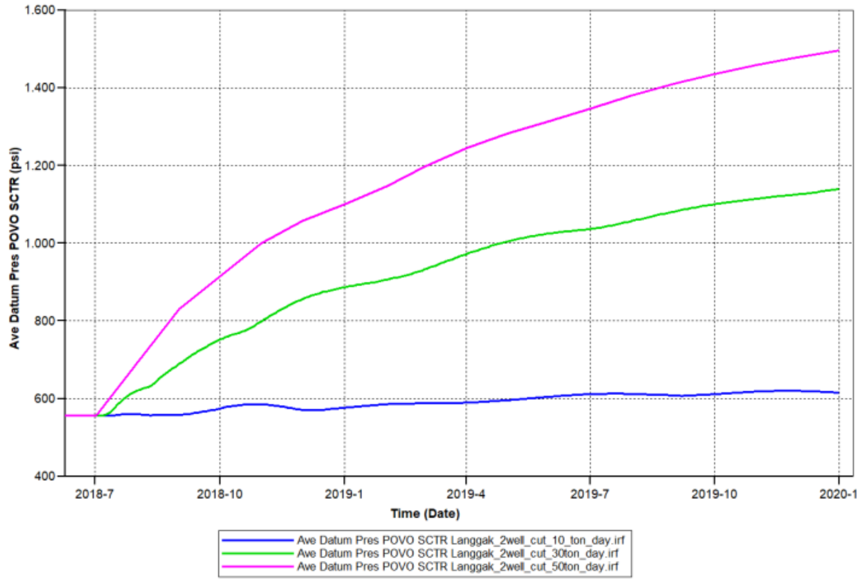
Ave Datum Pres POVO SCTR (psi)
1.600
1.400
1.200
1.000
800
600
400
2018-7
2018-10
2019-1
2019-4
2019-7
2019-10
2020-1
Time (Date)
Ave Datum Pres POVO SCTR Langgak_2well_cut_10_ton_day.irf
Ave Datum Pres POVO SCTR Langgak_2well_cut_30ton_day.irf
Ave Datum Pres POVO SCTR Langgak_2well_cut_50ton_day.irf

CONCLUSION

1. Proposed screening process for Langgak Field EOR are as follows:
   - Define objectives
   - Identify 'site-specific or time-specific' advantage or disadvantages
   - Define method of injection
2. Using Langgak Field's properties, EOR method that is the most suitable based on each reference (technical and economical consideration) are as follows:
   - Taber Meruap: CO_2 flooding
   - SPE 35385: CO_2 Immiscible injection
   - SPE 39234: CO_2 Immiscible injection
   - Based on SPE 10044, CO_2 Huff and Puff injection is very potential to be conducted in Langgak field.
3. Proposed EOR Method for Langgak field is CO_2 Immiscible Huff and Puff based on screening criteria and previous CO2 huff and puff injection projects as the reflection.
4. Study on laboratory yields Minimun Miscibility Pressure of CO_2 to reservoir fluid in Langgak Field is in range of 2400 – 2600 psia.
5. According to EoS and 1-D Slimtube simulation, MMP of Langgak Field are as follows:
   - EoS simulation : 3197 psia
   - 1-D Slimtube simulation : 2935 psia
6. Simulation study results on Single Well CO_2 Huff and Puff injection performance implementing to Langgak Field are represented by using single well simulation model can lift additional cumulative oil production about 12.99 MSTB for one well (LGK-24) in 547 days (7 days of preparation, 75 days of injection, 30 days of soaking, and /1.5 years of implemantation.
7. There is no significant different of oil recovery for 1,2, and 3 injection cycle according to simulation of Coreflooding CO_2 Huff & Puff Injection

8. The more higher injection rate of CO_2, the more oil is recovered according to coreflooding simulation of CO_2 Continuous Injection.
9. Injection rate becomes more critical and meaningless when productivity of producer well is not able to afford the amount of CO_2 injected. Too much CO_2 injected causes water cut increasing significantly due to the role of CO_2 is not enhancing oil recovery, but only displacement.

REFERENCES

1. Taber J.J, Martin, F.D., and Seright, R.S.: "EOR Screening Criteria Revisited: Part 1—Introduction to Screening Criteria and Enhanced Recovery Field Projects," SPERE (August 1997).
2. Taber J.J, Martin, F.D., and Seright, R.S.: "EOR Screening Criteria Revisited: Part 2—Application and Impact of Oil Prices Field Projects," SPERE (August 1997).
3. Moritis, G.: "EOR Dips in U.S. but Remains a Significant Factor," Oil & Gas J. (26 September 1994) 51.
4. Haynes, H.J. et al.: Enhanced Oil Recovery, Natl. Petroleum Council, Industry Advisory Council to the U.S. Dept. of the Interior (1976).
5. Bailey, R.E. et al.: Enhanced Oil Recovery, Natl. Petroleum Council, Industry
6. Committee to the U.S. Secretary of Energy, Washington, DC (1984).
7. J.J. Taber, F.D. Martin, and R.S. Seright: *EOR Screening Criteria Revisited – Part 1: Introduction to Screening Criteria and Enhanced Recovery Field Project,* SPE Reservoir Engineering (1997).
8. Alasadani, Ahmad: *Updated EOR Screening Criteria and Modeling the Impacts of Water Salinity Changes on Oil Recovery,* Geosciences and Geological and Petroleum Engineering of Missouri University of Science and Technology (2012).
9. Mohammed-Singh, L. J., Singhal, A. K., & Sim, S. S.-K. (2006, January 1). Screening Criteria for CO2 Huff 'n' Puff Operations. Society of Petroleum Engineers. doi:10.2118/100044-MS
10. Kumar, S., Awang, M., Abbas, G., Farouque, K., & Ahmed, S. (2014, March 25). Simulation Protocol for Core Flooding: Relative Permeability and Capillary Pressure Analysis. Offshore Technology Conference. doi:10.4043/24715-MS
11. Haskin, H. K. and Alston, R. B.: "An Evaluation of CO2 Huff 'n Puff Tests in Texas", JPT (Feb. 1989), 177-184.

12. Thomas, J. A. and Monger-McClure, T. G.: “Feasibility of Cyclic CO2 Injection for Light Oil Recovery”, SPERE (May 1991) 179-184.

13. Mohammed-Singh, L. and Singhal, A. K.: “Lessons from Trinidad/s CO2 Immiscible Pilot Projects 1973-2003”, SPERE, Oct. 2005, 397-403.

14. Monger, T. G. and Coma, J. M.: “A Laboratory and Field Evaluation of the CO2 Huff ‘n Puff Process for Light Oil Recovery”, SPERE (Nov. 1988), 1168-76.

15. Green, D.W., Willhite, G.P., 1998. Enhanced Oil Recovery, SPE Text Book Series, vol 6,92.

16. Guo, W.K., Cheng, J.C., Liao, G.Z., 2002. The current situation on EOR technique and development trend in Daqing. J. Pet. Geol. Oilfield Dev. Daqing 21 (3), 1-6.

17. Taber, J.J., Martin, F.D., Seright, R.S., 1997. EOR screen criteria revisited part 1: Introduction to screen criteria and enhanced recovery field projects. SPEREE 12 (3), 189-198.

18. Haynes, H.J. et al: *Enhanced Oil Recovery*, NPC, Industry Advisory ouncil to the U.S. Dept of the Interior, Washington DC (1976).

19. Bailey R.E. et al.:*Enhanced Oil Recovery*, NPC, Industry Advisory Committee to the U.S. Secretary of Energy, Washington DC (1984).

20. Parkinson, W.J. et al.: “An Expert System for Screening Enhanced Oil Recovery Methods”, Presented at 1990 AIChE Summer Meeting, San Diego, California, 19-22 August.

21. “CO2 Activity Picks up in W. Texas, New Mexico”, Oil and Gas J. (17 July 1995 26.

22. Taber, J.J.: “A Study of Technical Feasibility for the Utilization of CO2 for Enhanced Oil Recovery”, P.Reimer (ed.), IEA Greenhouse Gas R&D Programme, Cheltenham, England (19914) Appendix B, 134.

23. Heller, J.P. and Taber, J.J.:”Influence of Reservoir Depth on Enhanced Oil Recovery by CO2 flooding”, Paper SPE 15001 presented at the 1986 Permian Basin Oil and Gas Recovery conference, Midland, Texas, 13-14 March.

24. Yellig, W.F. and Metcalfe, R.S.:”Determination and Prediction of CO2 Minimum Miscibility Pressure”, JPT (January 1980) 160.

25. Abdassah, D., Siregar, S., and Kristanto, D. The Potential of Carbon Dioxide Gas Injection Application in Improving Oil Recovery . Society of Petroleum Engineers 64730-MS (2000)
26. Abedini, Ali., 2014. Thesis: Mechanisms of Oil Recovery During Cyclic CO2 Injection Process: Impact of Fluid Interactions, Operating Parameters, and Porous Medium. Petroleum Systems Engineering, Faculty of Engineering and Applied Science, University of Regina.
27. Abedini, Ali and Farshid Torabi, 2014. Oil Recovery Performance of Immiscible and Miscible CO2 Huff-and-Puff Processes. Petroleum Systems Engineering, Faculty of Engineering and Applied Science, University of Regina.
28. Ahmadi, Kaveh and T. John, Russels. Mutiple Mixing-Cell Method for MMP Calculations. SPE 116823 (2008)
29. Ahmed, T. Minimum Miscibility Pressure from EOS. Canadian International Petroleum Conference (2000)
30. Akbar, Fikri A., 2017. Thesis: Designing CO2 Immiscible Injection Using Huff 'n' Puff Method for Light-Oil Recovery in A High Temperature and Low Pressure Reservoir. Petroleum Engineering Department, Bandung Institute of Technology.
31. Bashir, et al. Addition of Branched Alcohols to Reduce The Minimum Miscibility Pressure Between CO2 and crude oil (2012)
32. Djabbarah, N.F.: Miscible Oil Recovery Process using Carbon Dioxide. Google Patents (1990).
33. Golkari, Abdolah and Masoud Riazi. Experimental Investigation of Miscibility Conditions of Dead and Live Asphaltenic Crude Oil. Shiraz University (2016)
34. Gondiken, S., 1987. Camurlu Field Immiscible CO2 Huff and Puff Pilot Project. SPE 15749. Turkish Petroleum Corp.
35. Green, W., Don and G. Paul Willhite: Enhance Oil Recovery. University of Adelaide (1998), pp 202-210.
36. Haskin, Helen K. and Robert B. Alston., 1989. An Evaluation of CO2 Huff 'n' Puff Tests in Texas. Journal of Petroleum Technology. Texaco Inc.

37. Holm, L.W. and Josendal, V.A. Mechanisms of Oil Displacement by Carbon Dioxide (1974).
38. Holm, L.W. Miscibility and Miscible Displacement. Jounal of Petroleum Technology (1986)
39. Huang, Tuo, et al. CO2 Flooding Strategy to Enhance Heavy Oil Recovery (2016)
40. Jeong, Moon Sik and Kun Sang Lee, 2015. Maximizing Oil Recovery for CO2 Huff and Puff Process in Pilot Scale Reservoir. Advances in Civil, Environmental, and Materials Research (ACEM15), Incheon, Korea.
41. Klins, M.A. Carbon Dioxide Flooding: Basic Mechanisms and Project Design (1984)
42. Lake, L.W.: Enhanced Oil Recovery, Prentice Hall, New Jersey (1989) 234.
43. Lee, John and Robert A. Wattenbarger., 1996. Gas Reservoir Engineering. SPE Textbook Series Volume 5, Texas A&M University, Richardson, Texas.
44. Martin, F. David and Taber, J.J. Carbon Dioxide Flooding (1992)
45. McKean, T. A. M. et al., 1999. Schrader Bluff EOR Evaluation. SPE 54619.
46. Menouar, Habib. Discussion on Carbon Dioxide Mininum Miscible Pressure Estimation: An Experimental Investigation. Texas tech University. SPE-165351 (2013).
47. Metcalfe, R.S. and Yarborough, L. The Effect of Phase Equilibrium on the CO2 Displacement Mechanism (1979)
48. Mohammadi, S. et al., 2011. Optimal Conditions for Immiscible Recycle Gas Injection Process: A Simulation Study for One of the Iranian Oil Reservoirs. Sharif University of Technology. Elsevier B. V.
49. Mohammed-Singh, Lorna J. and Ashok K. Singhal, 2004. Lessons from Trinidad's CO2 Immiscible Pilot Projects. SPE 89364.
50. Monger, T.G. and J.M. Coma, 1988. A Laboratory and Field Evaluation of the CO2 Huff 'n' Puff Process for Light-Oil Recovery. SPE. Louisiana State University.
51. Muslim, A. et al., 2013. Opportunities and Challenges of CO2 Flooding in Indonesia. SPE. Jakarta, Indonesia.

52. Muslim, A., et al. CO2 Sources and Future EOR Prospects in Sumatra Island-Indonesia. Advances in Civil, Environmental, and Materials Research (2015).
53. Muslim and A.K. Permadi: CO2 Gas Blending to Lower the Minimum Miscibility Pressure: A Case Study at AB-4 and AB-5 Layers of Air Benakat Formation, South Sumatera Basin, Jurnal Teknologi Minyak dan Gas Bumi (2016)
54. Pederson, et al. Studies of Gas Injection Into Oil Reservoirs by a Cell to Cell Simulation Model. SPE 15599 (1985)
55. Perera, M. S. A. et al., 2016. A Review of CO2-Enhanced Oil Recovery with A Stimulated Sensitivity Analysis. Monash University. Energies.
56. Rahmatabadi, K.A. Advances in Calculation of Minimum Miscibility Pressure. The University of Texas at Austin (2011, May)
57. Renke, et al. Reducing the Miscibility Pressure in Gas Injection Oil Recovery Processes. University of Stuttgart. SPE-183389-MS (2016)
58. Rommerskirchen, R. et al. Additives for CO2 EOR Applications. SPE-181304-MS (2016)
59. Salim et al., 2015. Design and Dynamic Simulation of a CO2 Injection System for CO2 Enhanced Oil Recovery. Advances in Civil, Environmental, and Materials Research (ACEM15). Konkuk University, Seoul.
60. Stalkup, F.I. Jr. Miscible Displacement Monograph Series (1983)
61. Teklu, et al. Minimum Miscibility Pressure Determination: Modified Multiple Mixing Cell Method. Colorado School of Mines. SPE-155454 (2012)
62. G.A, Thomas. And T. G., 1990. Monger-McCluire. Feasibility of Cyclic CO2 Injection for Light-Oil Recovery". SPE. Louisiana State University.
63. Voon, C.L. and Awang, M. Reduction of MMP Using Oleophilic Chemicals. International Journal of Chemical and Molecular Engineering Vol 8. (2014)
64. Yellig, W.F.; Metcalfe, R.S. Determination and Prediction of CO2 Minimum Miscibility Pressures. Journal of Petroleum Technology (1980, May)
65. Yoosook, Hutthapong et al., 2017. CO2 Utilization for Enhance Oil Recovery with Huff-N-Puff Process in Depleting Heterogeneous Reservoir. Elsevier Ltd. Chulalongkorn University, Bangkok.

CO2 Langgak

ORIGINALITY REPORT

16%	16%	12%	5%
SIMILARITY INDEX	INTERNET SOURCES	PUBLICATIONS	STUDENT PAPERS

PRIMARY SOURCES

1	scholarsmine.mst.edu Internet Source	9%
2	pustaka.pekanbaru.go.id Internet Source	7%

Exclude quotes	On	Exclude matches	< 3%
Exclude bibliography	Off		